Optimal Design of a Multi-Phase Pipeline

A THESIS SUBMITTED IN PARTIAL FULFILMENT OF THE REQUIREMENTS FOR THE DEGREE OF DOCTOR OF PHILOSOPHY AT THE UNIVERSITY OF HUDDERSFIELD

by

Hawre Hussein
B.Eng. Salahaddin University, Iraq, 2003
M.Sc. University of Huddersfield, UK, 2013

Director of Research: Prof. Rakesh Mishra
Leader of Energy, Emissions and the Environment Research Group

2019

In memory of Mr. Raouf Muhammed Amin (late).

You shan’t be forgotten

- **Abstract**

A slurry pipeline is one of the transportation modes used for transporting bulk materials for long distance using water or any other type of liquid as a carrier fluid [1-3]. Extensive research has been carried out on the improvement of this type of transportation in addition to the development of alternative ways for transpotation of solid materials. Although the use of fluid flow for transportation purposes has been practiced for more than a millennium, detailed information on the flow behaviour of such complex mixtures in pipelines is still the subject of active research today.

The optimal design of a slurry pipeline includes the selection of the correct pipe sizes, shapes and materials for optimum energy consumption, equipment sizing and reliable operation of the pipeline networks. The prediction of some parameters such as pressure loss, concentration distribution, velocity distribution and wear rate will help the designer to optimise the selection of the design parameters [3-5]. The experimental investigation was carried out to obtain an improved database for modelling the solid-liquid flow in horizontal pipelines. Tests are conducted using uni-sized plastic beads, 4.5 mm diameter and 1329.2 kg/m^3 density, as solid particles, and water as a carrier fluid. Frictional head loss is measured as a function of solid concentration and mean velocity. Transparent pipe section is used to study solids' deposition velocities and solids' bed. In addition to the experimental results, some other published experimental results are used to develop advanced modelling tools based on an SRC (Saskatchewan Research Council) two-layer model in order to predict and quantify the solid-liquid flow properties horizontally.

In order to improve the accuracy of the predicted data, this study includes improvement over the last previous version of Multi-Layer model for predicting flow properties across the cross-section of horizontal pipes transporting a solid-liquid mixture. The proposed model contains empirical correlations, which incorporate a wide range of experimental conditions. The model is applied for the prediction of concentration distribution of solid particles, velocity profile, and pressure drop. The predicted data are compared with the experimental results of different experimental works.

Furthermore, an optimisation model is developed in the current study based on the least cost principle. This model is designed based on the proposed multi-layer model to find the cost of energy for running any slurry system. In addition, the model has been used to find the optimal diameter of horizontal pipelines transporting slurries.

- **List of Publications**

- Hussein, H., & Mishra, R. (2019). An Improved Optimisation Model for Horizontal Pipelines Transporting Solid Liquid mixtures. International Journal of COMADEM, 22(2), 33-38.

The respondent is the first author of the above mentioned publication wherein he performed the numerical and the analytical modelling. The respondent implemented the analytical methodologies and analysed the results. Discussions were performed in collaboration with supervisor Prof. Mishra and the rest of the team. This work is reproduced in page numbers 123-137 of the thesis.

- **Declaration**

- The author of this thesis (including any appendices and/or schedules to this thesis) owns any copyright in it (the “Copyright”) and he has given The University of Huddersfield the right to use such Copyright for any administrative, promotional, educational and/or teaching purposes.

- Copies of this thesis, either in full or in extracts, may be made only in accordance with the regulations of the University Library. Details of these regulations may be obtained from the Librarian. This page must form part of any such copies made.

- The ownership of any patents, designs, trademarks and any and all other intellectual property rights except for the Copyright (the “Intellectual Property Rights”) and any reproductions of copyright works, for example graphs and tables (“Reproductions”), which may be described in this thesis, may not be owned by the author and may be owned by third parties. Such Intellectual Property Rights and Reproductions cannot and must not be made available for use without the prior written permission of the owner(s) of the relevant Intellectual Property Rights and/or Reproductions.

- **Acknowledgement**

It is a great pleasure to express my sincere appreciation to those who have directly or indirectly contributed to complete my amazing research journey. Most importantly, all praise and thanks are due to the Almighty Allah for his infinite blessings and grace and for giving me the ability to finish this work.

I would like to express a deepest gratitude to my supervisor Prof. Rakesh Mishra for his constant effort, encouragement and valuable guidance. He steered me in the right direction whenever he thought I needed it. His wisdom, immense knowledge and commitment to the highest standards inspired and motivated me.

I owe my sincere gratitude to my colleagues at the Energy, Emissions and Environment Research group at the University of Huddersfield for their support and friendship. I would also like to thank the School of Computing and Engineering at the University of Huddersfield for providing an excellent environment for research students. In addition to supportive courses, classes, seminars and workshops, references, materials and analysis software were always available. Furthermore, I would like to acknowledge the continuous support of the research admin staff at the School of computing and Engineering.

I am deeply indebted to my parent who have provided me through moral and emotional support in my life. I am also grateful to my other family members and friends who have supported me along the way.

Last but not least, I would like to thank my better half (Sara), my daughter (Bana) and my sons (Bawar & Blnd) for their patience and countless help and support. Without their support, love and constant encouragement, I wouldn't able to achieve this.

Contents

- **List of Figures**

- **List of Tables**

- **List of Symbols**

Nomenclature

A cross-sectional area of flow (m^2).

C concentration (v/v or w/w).

C_1 solid concentration in upper layer (equation 2.6).

C_2 solid concentration in lower layer (equation 2.7).

C_c contact load particles average concentration over the whole pipe.

C_D settling particle drag coefficient.

C_f fine particle concentration.

C_{lim} total concentration of coarse particles in the lower layer.

C_{max} particle maximum packing concentration.

C_r overall coarse particle concentration (equation 2.9).

C_t in-situ concentration (v/v or w/w).

C_v concentration by volume, (%).

C_w concentration by weight, (%).

d particle diameter (m).

d_{50} median particle diameter (m).

d_{cf} particle diameter used in equation (1.8), (m).

D pipe diameter, (m).

f fanning friction factor.

f_1 parameter used in equation (2.21 and 2.22).

g acceleration due to gravity (m/s^2).

k pipe wall equivalent roughness.

L length of pipe (m).

P pressure (Pa).

d_p particle diameter

Q volumetric flow rate, (m^3/s).

Q_s solid volumetric flow rate, (kg/s).

Q_L liquid volumetric flow rate, (m^3/s).

Re terminal rise velocity, (m/s).

Re_p particle Reynolds number.

S_p percentage finer

S_s ratio of solids to liquid density.

t time (s).

v local velocity, (m/s).

v_1 velocity in the first layer in two-layer model, (m/s).

v_2 velocity in the second layer in two-layer model, (m/s).

v_0 solid settling velocity, (m/s).

v_c solid deposition velocity, (m/s).

v_s mean solid velocity, (m/s).

v_L mean liquid velocity, (m/s).

v_∞ particle settling velocity infinite dilution, (m/s).

K flow consistency index equation (1.19 a)

Greek letters

β an angle defining the upper and lower layers area in two layer model (figure 2.2).

Δ deformation tensor rate.

Δp pressure differential, (pa).

$\Delta : \Delta$ 2nd invariant of the rate of deformation tensor.

$\emptyset$ actual slurry frictional headloss to the actual slurry frictional head loss i to the carrier fluid frictional headloss.

$\dot{\gamma}$ time rate of shear strain, shear rate, (s-1).

ς parameter used in equation (4.15).

η effective mixture viscosity, (Pa.s).

η_f fluid apparent viscosity, (Pa.s).

η_s coefficient of sliding friction.

μ Newtonian viscosity, (Pa-s).

μ_c Casson viscosity Pa-s, (Equation 1.19c)

μ_p Bingham plastic viscosity (Pa-s), (Equation 1.19b)

μ_0 mixture viscosity, (Pa-s).

ρ mixture density, (kg/m^3).

ρ_f density of carrier fluid, (kg/m^3).

ρ_L density of the liquid, (kg/m^3).

ρ_{2f} fluid density in lower layer, kg/m^3 (equation 2.15)

ρ_s solids density, (kg/m^3).

m mixture density, (kg/m^3).

τ shear stress, (pa).

τ_c Casson yield stress, pa (Equation 1.19c).

τ_y yield stress, (pa).

τ_{ij} shear stress tensor, (pa).

Ψ dimensionless grouping of the independent variables used in equation (1.15).

CHAPTER 1 Introduction

Pipelines play an important part in many engineering systems. Pipelines are used as a mode of transportation in various industries to move ores such as iron, coal, mining waste etc. over long distances. In order to analyse the complex flow phenomena in hydraulic pipelines transporting slurries, it is essential to understand the flow properties of solid-liquid pipelines. This chapter provides an introduction regarding the design of horizontal pipelines transporting slurries. In addition, this chapter provides detailed information about the flow parameters and the requirements of the design.

1.1 Introduction

A slurry pipeline is one of the transportation modes used for solid materials transportation by using a carrier fluid such as water or any other liquid. The carrier fluid transfers the necessary energy from the pump to the solid particles to keep in suspension and to move along with the flow [3, 4]. This mode of transportation is appropriate for long distance bulk materials haulage, such as transporting raw materials to processing plants, coal to thermal power plants, and for the disposal of waste material like fly ash, etc. [6, 7].

In this chapter, a brief background of solid-liquid flow modelling and its evolution over the years is presented. A detailed information are needed regarding flow properties such as head loss, critical velocity, regimes of flow prior to the design of the pipeline and the pump station [3]. In this chapter, the meaning and implications of design parameters in slurry flow modelling, motivation, and the scope of the present thesis are presented. In addition, a route map is given regarding the whole thesis.

Many chemical processing industries involve the transport or handling of some type of slurry or liquid-solid mixture. As a result of the development of chemical technology, since the turn of the last century the behaviour of liquid-solid mixtures flowing through pipelines has become the subject of continuous investigation. In the middle of the last century, many research studies were done in different countries, causing considerable technical progression. For example, in the United Kingdom, experimental works on the handling of coarse coal slurries were carried out by the well-known firm “British Hydraulic Research Association (BHRA)” in

cooperation with “the National Coal Board, UK”. A large amount of work has been carried out by Durand and Condolios [8] on the hydraulic transport of aggregates. Several advantages of using slurry pipelines have been highlighted, such as tremendous economy of scale, high degree of efficiency and reliability, simplicity of installation, ease of operation and automation, and ease of crossing both natural and artificial obstacles, etc. [3, 4].

Contrary to the aforementioned advantages, there are some disadvantages of the use of this mode of transportation. The required initial capital cost is high for building a new pipeline, large volumes of carrier fluid are required which may not be easily available, quality control is stringent, and the system is solely dedicated to the transportation of solids or multiphase mixtures [3, 4].

1.2 Hydraulic Design Considerations for the Slurry Pipeline

For the design of the solid-liquid pipeline, a large number of variables must be considered. These parameters can be classified as “hydraulic parameters, parameters affecting corrosion-erosion characteristics, and parameters affecting the operational stability of the system” [4].

1.2.1 Hydraulic Parameters

- Carrier fluid Selection: This depends on its availability and the solid materials used.
- Optimum particle size: Coarse slurry needs high transportation velocity and this leads to high pressure drop and wear rate. Extremely fine slurries also lead to high pressure drop.

- Optimum concentration of solids: It should be high enough to satisfy the required throughput and less than static settling concentration of 10% to 20%.
- Minimum system operation velocity: Depends on the concentration level and pipe diameter. On the other hand, the operation velocity should be higher than solid deposition velocity by 0.5 to 1 m/s.
- Pipe diameter should be designed as per the required solid throughput at optimum concentration and velocity.
- Pressure drop should be minimized.
- Additives may be required for flow improvement.
- Attrition of particles due to pumping should be minimised which is usually negligible except in a very long pipeline.

1.2.2 Parameters of Corrosion-Erosion

- Pipeline life expectation should be as long as possible (20 to 50 years).
- Corrosion additives should be used to control pH and dissolved oxygen.
- Selection of metal allowance.

1.2.3 Parameters of Operational Stability

- Shutdown start-up requirement.

Start-up of a slurry flow system, with either single pumps or several pumps in series, may create significant problems for the pump and pipeline. This may cause

damage to the motor or pipeline as a result of starting the pump using a "synchronous electric motor against an open valve" [3]. In addition, other difficulties can occur if there are any large changes in the mixture level in the pipeline. In the case of system shutdown, the "local high spots" are liable to "sub-atmospheric" pressure and might cause vaporisation. Subsequently, this vapour could cause undesirable hydraulic transients during start-up procedures. The mentioned problems can be avoided either by using Vacuum relief valves at high points of the pipeline or by draining the pipeline after each shutdown [3].

- Maximum allowance slope

The pipe inclination has significant effects on flow velocity, deposition limit and friction loss. The solid particle size and concentration are important factors in estimating the maximum allowance slop of the pipeline [3, 11].

1.3 Definitions

In principle, the solid-liquid flow can be defined as the process of transporting solid particles at a volumetric flow rate Q_S and carrier fluid at a volumetric flow rate Q_L. The quantities of each phase are considered an important parameter to be fixed in any design suggestion.

The operational velocity V is an important design parameter and it must be higher than the slurry deposition velocity for a given pipe diameter D. For a circular pipe cross section area $A = \frac{\pi}{4} D^2$, the operational (mean) velocity can be calculated as follows [12-15]:

$$v = {(Q_S + Q_L)}/{A} \tag{1.1}$$

Newitt et al [16] defined three regimes of flow which are flow with “homogeneous suspension”, flow with “heterogeneous suspension” and flow with a “sliding bed” which occurs in the lower part of the slurry pipe. The minimum operating velocity for slurry pipelines should ensure stable suspension of solid particles in the pipeline. The operating velocity normally chosen is slightly over the deposition velocity. In the case of turbulent flow and operating the system at a velocity higher than the deposition velocity, higher frictional head loss is expected along the pipeline [4, 17].

The solid fraction of the mixture can be simply related to both solid and liquid volume flow rate as follows:

$$C_v = {Q_S}/{(Q_S + Q_L)} \tag{1.2}$$

Experimentally, in a circular cross-sectional pipeline loop, the total in situ concentration is fixed, as a known amount of solids is placed in the pipeline. Therefore, the mean in situ concentration C_t remains unchanged at any time during the operation but the concentration of the delivered solids may vary as a result of any changes in flow rates.

$$C_t = \frac{1}{A}\int c\, dA \tag{1.3}$$

The mean solid velocity v_S can be related as follows:

$$v_S = {Q_s}/{AC_t} \tag{1.4}$$

Similarly, the mean velocity of carrier fluid v_L can be determined as follows:

$$v_L = {Q_L}/{A(1 - C_t)} \tag{1.5}$$

For coarse particle slurry flow, any variations in solid or carrier fluid velocity may cause a significant change in volume at each phase. By considering the density of each phase of carrier liquid and delivered solid (ρ_s and ρ_L), the solid mass fraction (efflux concentration by weight) can be calculated as follows:

$$C_w = {\rho_s Q_s}\Big/{(\rho_s Q_s + \rho_L Q_L)} \tag{1.6}$$

For a given solid concentration c, the density of the mixture is:

$$\rho_m = \rho_s c + \rho_f (1 - c) \tag{1.7}$$

1.4 Characterizing Slurries

The solid-liquid mixture can be classified into “fine-particle” and “coarse-particle” slurries. In fine-particle slurries, also called non-settling slurries, the particles are fully suspended or slowly settling along the pipeline in a quiescent state of flow. The mixture flows are either laminar or turbulent and the particle distribution appears homogeneous along the non-settling slurry pipeline [5, 15].

The second category of slurries, which are called settling or coarse-particle slurries, contain coarse particles which are too large and heavy to be completely suspended by the carrier fluid during normal operation of the pipeline. The flows are usually turbulent and the particles’ distribution is less uniform in normal operation [1].

In non-settling slurries, the turbulence does not affect particle suspension in the case of rapid particle settling. The immersed weight of the particles is transmitted to the pipe wall due to particle-to-particle interaction. The process of fluid-like friction consumes energy during the pipeline flow [9, 12]. On the other hand, as a

result of particle to pipe wall interactions, a considerably larger amount of energy is consumed. Therefore, the single-phase fluid models are not applicable for the prediction of the flow properties of coarse particle slurries [18].

If the slurry contains ultra-fine-particles, “it is assumed that these particles combine with the carrier fluid to form a new carrier fluid” with a different density and viscosity [1]. Mishra [4] proposed that all the particles smaller than a diameter d_{cf}which corresponds to a particle settling Reynolds number equal to 0.1, will be treated as ultra-fine. Particle settling Reynolds number is usually denoted by Re_p which represents the nature of surrounding flow and the fall velocity for a particle moving in a fluid. d_{cf} depends on solid specific gravity and can be calculated from the expression:

$$d_{cf} = \left((1.8 \left({}^{\mu_1}/_{\rho_1} \right)^2 / (g(S_s - 1) \right)^{1/3} \tag{1.8}$$

Where S_s is the ratio of solids to liquid density.

1.5 Head loss for Non-settling Slurry Flows

The flow of fine particle slurries are considersd as homogeneous flow in pipelines. Usually a suitable fluid flow model for fine particle slurries is determined by conducting laminar flow experiments. In 1902, Einstein [9] presented a theoretical equation of the relative viscosity of the mixture μ_r according to the solids volume fraction c for very dilute suspension.

$$\mu_r = 1 + 2.5c \tag{1.9}$$

D. G. Thomas [19] suggested an empirical equation to modify Einstein's equation to higher concentrations depending on the outcomes of some experimental works with “deflocculated” mono-sized spheres.

$$\mu_r = 1 + 2.5c + 10.05c^2 + 0.00273\exp(16.6c) \quad (1.10)$$

Churchill [20] modified a correlation of the Moody diagram which spanned the entire range of laminar, transient and turbulent flow in pipes. The correlation consists of the following expression:

$$f = 2\left[\left(8/Re\right) + \left(1/(A+B)^{3/2}\right)\right]^{1/12} \quad (1.11)$$

$$A = \left\{-2.457ln\left[\left(7/Re_p\right)^{0.9} + 0.27k/D\right]\right\}^{16} \quad (1.12)$$

Where D_h is the hydraulic diameter and k is pipe wall equivalent roughness.

$$B = \left(37530/Re_p\right)^{16} \quad (1.13)$$

For a Newtonian fluid, Churchill’s equation may be used to predict the head losses for turbulent flows. The shear strain rate and the shear history can be used for a non-Newtonian fluid mixture.

For scaling the data of laminar pipe flow to pipes with large diameter, the Metzner and Reed [21, 22] method can be applied. Several methods are proposed by Dodge and Metzner [23], Wilson and Thomas [24] and others for predicting turbulent flow head losses for laminar flow of non-Newtonian slurries.

The Durand-Condolios correlation introduced in 1952 contains two important dimensionless factors for predicting pressure drop, an excess head loss Φ and a

dimensionless factor Ψ which depends on the independent variables. The factor Φ is the ration of the actual slurry frictional head loss i to the carrier fluid frictional head loss for a given pipe diameter and mean velocity i_L.

$$\Phi = {\mathrm{i} - i_L}/{C_V i_L} \tag{1.14}$$

A widely used version of the Durand-Condolios correlation is [25]:

$$\Phi = 81\Psi^{-3/2} \tag{1.15}$$

$$\Psi = {\mathrm{V}^2\sqrt{C_D}}\Big/{gD(S_S - 1)}$$

Charles [26] proposed the following modification:

$$\Phi = 120\Psi^{-3/2} + (S_s - 1) \tag{1.16}$$

S_s is the ratio of solids to liquid density

Accoring to Wasp et al [27], solid-liquid mixture contains both "homogeneous" and "heterogeneous" portions. The homogeneous portion contains solidsthat assumed to increase the density and the viscosity of the slurry loop. Several modifications have been made to the Durand-Condolios equation. Based on this method, the solids contains several size intervals. An empirical equation has been developed to estimate the fraction of the homogeneous parts of each size interval. According to Shook et al [28], the pressure drop results for coarse particle solid-liquid flow in large pipes by using the Durand-Condolios method are overestimated.

Mechanistically based models are gradually replacing the mentioned correlations for the prediction of pressure drop in a coarse particle solid-liquid flow pipeline. Macroscopic and microscopic approaches are the two common modelling approaches, which are explained in detail in the next chapter. The mechanistic

two-layer model has been originally developed by Wilson [29] and then improved by Shook and Roco [25], Gillies et al [30] and Shook et al [31]. These works were based on extensive experimental data and derived from powerful empirical equations and correlations. Microscopic modelling is the basis of Computational Fluid Dynamics (CFD). The model depends on the solution of the governing differential equations that are derived based on the flow problems [12]. This type of modelling has benefitted as a result of the b of high-performance computers which include several techniques to make fast and efficient simulations [32].

1.6 Homogeneous Fluid Model

A fluid can be defined as a substance with continuous displacement as a result of applying shear force [12, 31]. In a Newtonian fluid, the shear stress (τ) is directly proportional to the time rate of shear strain $(\dot{\gamma})$ in a moving fluid and fluid viscosity as shown in equation 1.17.

$$\tau = \mu\dot{\gamma} \tag{1.17}$$

For a Newtonian fluid, dynamic viscosity as a scalar parameter can be used to define the linear relation between the stress and the shear strain. A homogeneous fluid has rheological behaviour and can be described as:

$$\tau = \eta\dot{\gamma} \tag{1.18}$$

Equation 1.18 shows the basic relationship between the applied shear stress and the rate of deformation of the fluid. η is the apparent viscosity of the fluid depending on multiple rheological parameters (τ) and $(\dot{\gamma})$.

For a Newtonian fluid, η has the same value of normal fluid viscosity and different parameters are required to derive the equation of shear stress as a function of the applied rate of shear strain as shown in equations 1.19 [25].

$$\tau = K\dot{\gamma}^n \quad \text{Power Low} \quad (1.19a)$$

$$\tau = \tau_y + \mu_p\dot{\gamma} \quad \text{Bingham} \quad (1.19b)$$

$$\tau^{0.5} = \tau_c^{0.5} + (\mu_c\dot{\gamma})^{0.5} \quad \text{Casson} \quad (1.19c)$$

$$\tau = \tau_y + K\dot{\gamma}^n \quad \text{Herchel-Bulkey} \quad (1.19d)$$

In Power Low and Herchel-Bulkey [25], K is the consistency index, $\dot{\gamma}$ is the shear rate and n is “the flow behaviour index”. In Bingham-type behaviour of fluid,τ_y is the yield stress and μ_p is plastic viscosity. In equation 1.19c, τ_c is Casson yield stress, μ_c is “Casson viscosity” (Pa-s).

The Bingham model is considered to be the simplest of the rheological models as it represents a linear relationship between the shear stress and the shear strain rate. The flow of fluid happens when applied shear stress exceeds the yield stress [13, 33].

1.7 Bingham Fluid Model

The rheological behaviour of a fluid can be expressed by the mathematical equation between applied shear stress and the shear rate. The general tensor notation is:

$$\tau = -\eta\Delta \quad (1.20)$$

Where τ is the viscous stress tensor, η is the effective viscosity and Δ is deformation tensor rate. For a Bingham fluid, the effective viscosity can be expressed as follows [14]:

$$\eta = \infty \qquad when\ \tau \leq \tau_y \tag{1.21a}$$

$$\eta = \mu_0 + {}^{\tau_0}/_{\dot{\gamma}} \qquad when\ \tau \geq \tau_y \tag{1.21b}$$

$$\tau = \sqrt{1/2(\Delta{:}\,\Delta)} \tag{1.21c}$$

τ_y is the yield stress which the flow generates in any stresses higher than this amount. μ_0 is a parameter with the unit of viscosity. $(\Delta{:}\,\Delta)$ is the second invariant of the rate of deformation tensor.

The equation can be rearranged to relate an apparent viscosity with the rheological parameters and the shear rate:

$$\eta = \mu_p + {}^{\tau_y}\Big/_{\left|\sqrt{1/2(\Delta{:}\,\Delta)}\right|} \tag{1.22}$$

For one-dimensional problem, equation 1.21b can be used. Both the yield stress and the plastic viscosity have been shown as a function of the fine particle volumetric fraction [34]. It can be thus concluded that the Bingham fluid model has more in common with laminar flow than turbulent flow [35].

1.8 Motivation

Many long multi-phase pipelines have been built and are operating throughout the world. Many interdependent flow parameters need to be taken into consideration for the design of multi-phase pipelines transporting solid particles. Accurate information is needed regarding pressure drop, concentration of each phase, critical velocity, flow regimes etc. at the early stage of the design. Several methods

and techniques have been introduced to predict the behaviour of solid-liquid flow inside pipelines. Most of these correlations are empirical in nature and they have different degrees of accuracy due to the complexity of the interdependent hydraulic parameters. These reasons motivated the author of this study to conduct a detailed research study in this field.

The majority of the slurry pipelines built around the world consist of horizontal pipes and bends. Therefore, analysing the solid-liquid flow in horizontal pipes is fundamental. Generally, the design parameters are set by referring to the flow properties of the mixture. Head loss is one of the primary parameters that has to be predicted. Mechanistically based models give an estimation of flow properties such as head loss, velocity and solid particle distribution according to flow field and geometric variables. These models can be directly used for the design optimisation of a solid-liquid flow pipeline [36].

A slurry pipeline contains solid particles, which are usually heterogeneously distributed across the pipeline cross-section. The collision between particles and the pipe wall, and between particles, leads to an additional pressure drop in the pipe. Furthermore, the carrier fluid works as a lubricant in the flow system. Therefore, to accurately design the solid-liquid pipeline, modifications in the main parameters of friction factor and pressure drop are essential.

The accuracy of the predicted data is based on the accuracy of the model that has been used. In order to improve the prediction power, the model limitations should be removed. Hence, there is a need for a more coherent and realistic prediction model. Any proposed model needs to be validated with accurate experimental

data. Conducting experimental works to analyse slurry flow in horizontal pipelines is quite important. In addition, using more than one experimental result will decrease the uncertainties in the measurement results.

Analysing the flow structure and the concentration profile are very important as usually a slurry pipeline is working in a turbulent mode with non-homogeneous distribution of the solid phase. Furthermore, for the commercial validity of slurry pipelines, it is obvious that these pipelines must be designed acceptably and optimally according to the standards of widespread use in industry. The designers are in need of a mechanistic model which covers as many as possible of the hydraulic and mechanical parameters to design the slurry pipeline in various projects with acceptable accuracy and minimum cost.

1.9 Research Aim

The specific research aims, listed below, were formulated based on the motivation for this study:

- To develop experimental based flow diagnostics of solid-liquid flow.
- To develop numerical based flow diagnostic and design of horizontal pipelines transporting slurries.
- To develop an Analytical Model for the optimum design of pipelines transporting slurries.

The objectives for this research will be presented in the last section of the next chapter.

1.10 Organization of this Report

This report presents the work that has been carried out so far for the current research study.

Chapter 1 consists of an overview of solid-liquid two-phase flow through horizontal pipelines. The hydraulic design and important hydraulic parameters have been discussed for designing a slurry pipeline. From this overview, the motivation for carrying out this work is illustrated and the key areas to be reviewed in the literature are identified.

Chapter 2 contains a detailed review of the works that have been done in solid-liquid flow area. Furthermore, the scope and the individual objectives of the research are explained.

Chapter 3 highlights the experimental and numerical setups. These included flow loop setup, measurement devices, calibration of the used machines and the experimental procedure. In addition, a detailed discussion regarding the used materials and the used computer-based codes is presented.

Chapter 4 describes in detail the proposed equation for sliding friction between solid particles and the pipe wall. In addition, this equation has been used to develop a two-layer model for predicting pressure drops in horizontal pipelines transporting slurries.

Chapter 5 presents the proposed multi-layer model for predicting solid-liquid flow properties in horizontal pipes. This model has been applied for the prediction of concentration distribution, velocity profile and pressure drop. Details about the

steps of the model development, and the base equations, have also been highlighted.

Chapter 6 sheds light on the optimisation model for the design of a horizontal pipeline transporting slurries. The proposed model is based on least cost principles. In addition, the proposed multi-layer model has been used to predict the cost of power for operating the flow system.

Chapter 7 concludes the proposed equations, models and the findings of this study. In addition, the achievements and the additions to existing knowledge have been clearly presented and explained. Furthermore, recommendations for future research have also been presented.

CHAPTER 2 Literature Review

In the previous chapter, detailed information regarding the parameters involved in the design of horizontal slurry pipelines have been discussed. In this chapter, a detailed literature review is presented in order to highlight the knowledge gaps in the existing literature. The presented published works focus on topics related to pressure drop prediction models, concentration distribution prediction models, velocity profile prediction models and the optimisation methodologies of the design of horizontal slurry pipeline transporting slurries. Furthermore, the scope of this study has been specified and the research objectives have been explained as per the knowledge gaps concluded in the literature review.

2.1 Introduction

Solid-liquid flow is an important aspect of many applications in diffirent engineering fields such as chemical process plants. The applications of this mode of transport encouraged many of the researchers to conduct new experimental and theoretical investigations to fulfil the industry's requirements. Various models have been introduced by researchers to predict the flow properties of solid-liquid flow.

2.2 Pressure Drop in Horizontal Slurry Pipelines

The flow of solid-liquid in pipelines is associated with consumption of required energy to overcome the impedances that resist the flow. This resistance is called pressure drop [37]. An improved analysis which is called the force-balance model was used to estimate the limit of stationary deposition and pressure drop for a dense-phase flow [3]. Two-layer model has been developed by using force balance model in order to predict the flow behaviour for more dilute coarse-particle mixtures [3, 38]. The early version of the two-layer model is depicted in figure 2.1.

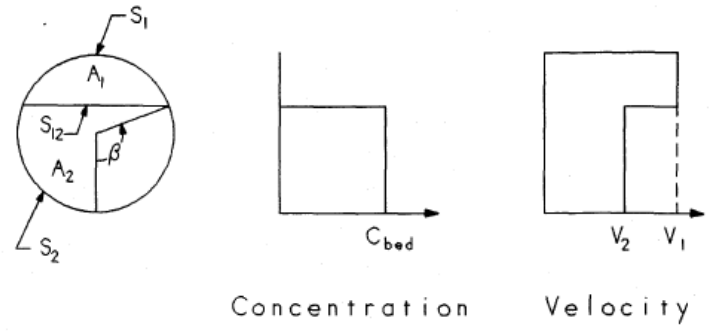

Figure 2-1. Two-Layer Model [9]

Gillies et al [30] proposed the modified two-layer model which divides the solids into two groups corresponding to fine and coarse particles in a model called the SRC Two-layer Model.

Gillies et al [39] proposed a version of the two-layer model for slurry with negligible quantities of fine and slowly settling particles. As most industrial slurries contain fine particles, that version of the two-layer model is modified to consider fine particles [30].

The terminal settling velocity can be related to the physical properties of a single particle and a fluid as follows:

$$V_{\infty} = \sqrt{4gd(\rho_s - \rho_f) \Big/ 3\rho_f C_D} \tag{2.1}$$

Where:

g: Local acceleration due to gravity

d: particle diameter

ρ_s: Solid density

ρ_f: Fluid density

C_D: Drag Force

The interfacial particle drag force F_D can be calculated as follows:

$$F_D = 0.5 C_D A_P \rho_L (V_L - V_S)|V_L - V_S| \tag{2.2}$$

The total in-situ solid concentration C_t can be determined by adding the fractions of both fine particles C_f and coarse particles C_r

$$C_t = C_f + C_r \tag{2.3}$$

The new carrier fluid density ρ_f can be determined as follows:

$$\rho_f = \left[\rho_l\,(1 - C_t) + \rho_s\,C_f\right] / \left[1 - C_t + C_f\right] \tag{2.4}$$

The viscosity of the new carrier fluid can be measured or calculated mathematically as proposed by Thomas [19] as below:

$$\mu_f = \mu_l \left(1 + 1.25\, C_f + 10.5\, {C_f}^2 + 0.00273 \exp\left(16.7\, C_f\right)\right) \quad (2.5)$$

Coarse particles with a diameter greater than d_{cf} are assumed to create two composition layers as depicted in figure 2.2. The suspended particles by "fluid forces" are distributed uniformly with C_1 concentration. The second layer is formed in the lower part of the pipe, which contains particles with concentration C_2 whose immersed weight is transmitted to the pipe wall due to particle-particle interaction as a contact load. The contact load particles average concentration over the whole pipe is assumed to be C_c, thus the overall coarse particle concentration C_r can be defined as follows [4]:

$$C_r = C_c + C_1 \quad (2.6)$$

C_c and C_2 can be related considering the cross-sectional area of the whole pipe and the lower layers.

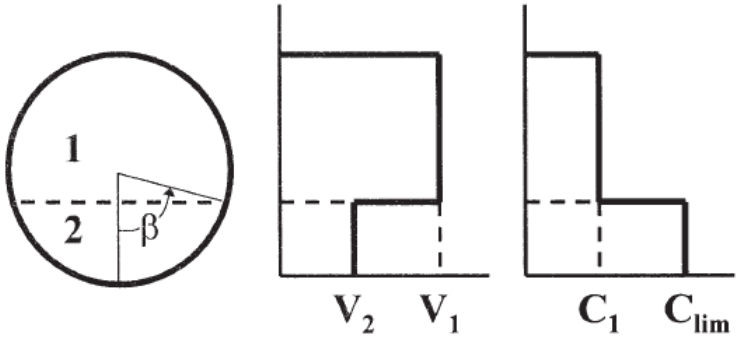

Figure 2-2. Idealised velocity and concentration profile used in SRC Two-Layer Model [30]

$$C_2\ A_2 = C_c\ A \tag{2.7}$$

The total concentration of coarse particles in the lower layer C_{lim} is given by:

$$C_{lim} = C_1 + C_2 \tag{2.8}$$

The contact load fraction C_c/C_r is proposed by Gillies [30]:

$$C_c/C_r = \exp\left(-0.0184\ V/V_\infty\right) \tag{2.9}$$

Gillies and Shook [40] observed that the contact load fraction is a function of the ratio of (V/v_∞) and the Reynolds number of the flow.

$$C_C/C_r = exp\left(-0.001013\ Re^{0.25}\ V/V_\infty\right) \tag{2.10}$$

For coarse particle slurries, the ratio of the mean velocity to the deposition velocity is a function of Froude number.

$$F_r = V/[g\ D\ (S_S - 1)]^{0.5} \tag{2.11}$$

Based on equation (2.11), an empirical correlation has been suggested by [18] to modify equation (2.10) as below:

$$C_C/C_r = exp\left[-0.0097\ Re^{0.193}\ \left(V/V_\infty\right)^{0.864}\ F_r^{-0.292}\right] \tag{2.12}$$

V_∞ is the terminal settling velocity at an infinite dilution, and can be determined by equation (2.1). Gillies et al. [30] proposed the following empirical equation:

$$(C_{max} - C_{lim})/(C_{max} - C_r) = 0.074\left(V/V_\infty\right)^{0.44}(1 - C_r)^{0.189} \tag{2.13}$$

Here C_{lim} is the mean concentration for the whole lower layer, and C_{max} is a property of the solid-liquid suspension known as the static settling concentration.

Gillies and Shook [41] proposed another semi-empirical approach for determining C_{lim}. Their approach depends on solid concentration distribution,

which is predicted by considering the solid turbulent diffusion. The concentration at the position of y/D=0.15 relative to the bottom of the pipe is assumed to be the predicted concentration of C_{lim}. The assigned C_{lim} with the contact-load fraction is determined in equation (2.12) and (2.13). Thus, by using equations (2.7), (2.8) and (2.9), C_1 and C_2 can be calculated.

The mixture density in the upper and lower layers is ρ_1 and ρ_{2f} respectively, which can be determined as follows:

$$\rho_1 = \rho_f(1 - C_1) + \rho_s\, C_1 \tag{2.14}$$

$$\rho_{2f} = \left[\rho_f\,(1 - C_{lim}) + \rho_s\, C_1\right]/[1 - C_{lim} + C_1] \tag{2.15}$$

By neglecting the slip between the phases, the volumetric balance for mixtures and solid particles is as follows:

$$A\,V = A_1\,V_1 + A_2\,V_2 \tag{2.16}$$

The momentum for the upper layer, lower layer and entire pipe is expressed in the equations (2.17), (2.18) and (2.19) respectively.

$$-\,d(P + \rho_1\, g\, h)/_{dz} = {}^{\tau_1\, S_{1+}\, \tau_{12}\, S_{12}}/_{A_1} \tag{2.17}$$

$$-\,d(P + \rho_2\, g\, h)/_{dz} = {}^{-\tau_{12}S_{12} + \tau_2 S_2}/_{A_2} \tag{2.18}$$

$$-\,d(P + \rho_m\, g\, h)/_{dz} = {}^{\tau_1 S_1 + \tau_2 S_2}/_{A} \tag{2.19}$$

The average mixture density can be expressed as:

$$\rho_m = \rho_s\, C_r + \rho_f\,(1 - C_r) \tag{2.20}$$

The shear stress along the upper pipe boundary τ_1 is presented in forms of the "Fanning friction factor" [4, 9, 12] as:

$$\tau_1 = {f_1 V_1 |V_1| \rho_1}/{2} \quad (2.21)$$

f_1 is a function of the bulk flow "Reynolds number" and pipe roughness k and can be determined as:

$$f_1 = f_1\left[\left({D V \rho_1}/{\mu_f}\right), \left({k}/{D}\right)\right] \quad (2.22)$$

The force per unit length $\tau_2 S_s$ is produced as a result of fluid-like resistance to the flow of a mixture with ρ_{2f} density.

$$\tau_2 S_2 = 0.5\, f_1\, V_2\, |V_2|\, \rho_{2f}\, S_2 + {0.5\left(\rho_s - \rho_f\right) C_2 (1 - C_{lim})(sin\beta - \beta\, cos\beta)\, \eta_s}\Big/{1 - C_2} \quad (2.23)$$

η_s is "the coefficient of friction between solid particles and the pipe wall", and the angle β is depicted in figure 2.2. Many researchers assumed the value of η_s as a constant, such as [30]. In addition, this factor has also been reported as a variable [42, 43]. This can be considered as a significant gap in this area. In the next chapter of this work, an extensive analysis will be carried out in order to derive a new empirical equation for predicting overall friction factor in the slurry.

τ_{12}, is the shear force at the interface between the two layers, and can be expressed as:

$$\tau_{12} = 0.5 f_{12}(V_1 - V_2)\, |V_1 - V_2|\, \rho_1 \quad (2.24)$$

f_{12} is a modified Colebrook friction factor and can be expressed as:

$$f_{12} = (1 + 2Y)/[(4\, log_{10}\, (D/d_{12}) + 3.36]^2 \quad (2.25)$$

Where [13]

$$Y = 0 \qquad for\ \frac{d_{12}}{D} < 0.0015 \quad (2.26a)$$

$$Y = 4 + 1.42\, log_{10}\left({d_{12}}/{D}\right) \qquad for\ 0.0015 < \frac{d_{12}}{D} < 0.15 \qquad (2.26b)$$

Where d_{12} is the particle diameter at the hypothetical interface.

The flux of fine particles (-d_{cf}) can be calculated as:

$$F_f = C_f[(1 - C_1)\, A_1\, V_1 + (1 - C_{lim}) A_2\, V_2]/(1 - C_r) \qquad (2.27)$$

The total delivered flow rate of the solids is calculated as:

$$C_v\, A\, V = C_1\, A\, V + C_2\, A_2\, V_2 + F_f \qquad (2.28)$$

In order to validate the proposed SRC two-layer model, Gillies [9] conducted a practical test using sand and coal slurries in industrial pipelines. Pressure drop, transferred solids concentrations, particle concentration distributions and velocity profile were found as functions of “in situ solids concentration” and the mean velocity of system operation. By using transparent pipe sections, the deposition velocities of Solids were estimated visually [9]. The main gaps of the two-layer model can be listed as below:

- The model considers any particles < 74 micron as fine particles for any slurry flow.
- Generally, the model was built based on the assumption that the solid concentration at Y/D=0.15 is equal to the average concentration of lower layer C_{lim}.
- An empirical equation was used for calculating C_{lim} for both uni-sized and multi-sized slurries. Two different modifications of the C_{lim} equation have been made since the introduction of the modified two-layer model in 1991.
- No equation has been suggested for calculating C_{max} and the effect of multi-sized mixture is not taken into consideration.

- The sliding friction coefficient between solid particles and pipe wall has been considered as a constant value, 0.5 for sand slurry and 0.4 for coal slurry.

Mishra [4] designed a software called ‘PRES2PHASE’ using FORTRAN language to predict pressure drops, solid distribution and mixture velocity distribution for a steady, turbulent solid-liquid flow through circular pipes. The features of the programme include prediction of the parameters like pressure drops in both homogeneous and heterogeneous regimes of flow. The applicability of the programme varies from very dilute flows to extremely dense flows [4].

Hill [13] made experimental measurements using coarse particles (1.7 mm and 4.4 mm) in a 52 mm diameter pipe line to investigate the effect of fluid yield stresses. The results have been applied to evaluate two proposed numerical models for laminar and turbulent flows. The finite element method is used in the first numerical model to predict the velocity distribution, and then the concentration profile. A two-layer model principle has been considered in the second model and the effect of fluid yield stress on the model predictions was considered. The author concluded his work by mentioning that the two-layer model gives satisfactory predictions in turbulent flow and reasonably good predictions for laminar flow.

Kaushal and Tomita [44] predicted the pressure drop by summing head-loss due to homogeneously and heterogeneously distributed of multisized particles [45]. According to Kaushal and Tomita [44], the differences between the predicted and measured values of head-loss as “a percentage of the mean of measured values” are: for the Wasp et al [46] model: “5.0–21.8%; for the Gillies et al” [30] model:

6.0–9.2%; for the old version of the Kaushal and Tomita [45] model: 1.7–3.5%; and for their proposed model: 1.6–2.0%.

Kumar et al [1] used an integral flow model for predicting the pressure drop and solids distribution under various conditions. A transparent observation chamber was used to visually observe the particle movement near the bottom of the pipe. The research concluded that mixture with fine and coarse particles requires less energy for flowing than the energy needed for fine particles mixture. In addition, the required energy is even less for slurries with optimum particle size distribution. The results show that the slurry particle size has significant effects on head-loss and deposition velocity. The sold-liquid flow head loss and concentration distribution have been predicted by using the modified two-layer model and the modified Karabelas model respectively.

Spelay [12] developed a numerical model to estimate the laminar flow behaviour of coarse solid particles in open channel for non-Newtonian flows. In addition, the theory of shear-induced particle diffusion by Phillips et al [47] was used to formulate a set of relationships to define the diffusive flux of coarse particles within the flow. This study concluded that just before achieving a balance situation in the particle fluxes, particles form a settled bed near the bottom wall of the pipe. The limitation of this model is the incapability of distinguishing between coarse particles and carrier fluid while solving the momentum equation due to the use of mixture viscosity. The mentioned limitation is clearly evident in the packed bed region when the mixture velocity becomes zero.

Gillies et al [18] proposed a new correlation for the friction coefficient which shows that pipeline friction is lower than the expected values at high velocities for sand slurries. Laboratory experiments were done for 0.09 mm and 0.27 mm median particle diameters. The results show that the particle-wall friction reduced when the particles were small in comparison with the viscous sub layer thickness δ. The viscous sub-layer thickness can be defined as follows:

$$\delta = {5\mu_f}\Big/{\rho_f v\left(f_f/2\right)^{0.5}} \tag{2.29}$$

$$\eta_s = \eta_{s0}\varsigma \tag{2.30}$$

Where $\eta_{s0} = 0.5$ is the estimated value for sand slurries in steel pipes. The value constraint ς, is between 0 and 1, and can be determined as follows:

$$\varsigma = 2\left(1 - {\delta}/{d}\right) \tag{2.31}$$

Wilson et al [48] studied the support of slurry particles by fluid lift that is found in the near-wall zone of the pipe. This force assumed to be horizontal. The propossed model explains the effect of the ratio of particle size to the thickness of the viscous sub-layer on the lift coefficient. In addition, the effects of the shear Reynolds number of the particle and particle concentration have been taken into consideration.

Vlasak et al [49] conducted an experiment on the flow visualisation of coarse slurry, modelled in a closed loop smooth stainless steel pipeline using water, glass balls and washed graded pebble gravel. The study revealed that the Durand model accurately predicted the flow behaviour of coarse-grained particle-water mixtures for moderate and higher flow velocities. Furthermore, the study demonstrated that

the SRC two-layer model significantly underestimates the mixture pressure drop. The author explained this as probably due to higher energy consumption and particle saltation movement as a result of an extremely high value of pipe/particle diameter ratio, which caused amplified particle/particle and particle/pipe wall interactions.

Kumar A. [50] performed an experimental investigation to predict the flow characteristics of bi-modal sand slurries through horizontal pipelines. The work concluded that the head loss is directly proportional with the percentage of fine particles in the mixture and operational velocity. Kumar A. [50] performed a CFD simulation for the flow of silica sand-water slurries through horizontal pipes and bends using the Euleian and K-epsilon models. The paper concluded that the head loss will increase when increasing the operational velocity. Singh et al [51] modified the wasp model by replacing Durand's empirical equation with a modified Karabelas concentration ratio equation. The results show better prediction of pressure drop.

2.2.1 Summary of Literature Regarding Pressure Drops in Horizontal Pipelines

Based on the literature review presented in the previous sections, for the pressure drop in horizontal slurry pipelines, it can be summarised that different models, that rely on some empirical equations, have been used in order to get an accurate prediction of the values of pressure drop. Prediction of the coefficient of sliding friction between solid particles and pipe wall is a research area with knowledge gap in the existing literature. Based on the results of the published literature as

covered in the previous section, this area still needs more scientific investigations in order to build up an adequate database for pressure drop in horizontal pipelines transporting slurries.

2.3 Concentration Distribution in Horizontal Slurry Pipelines

The prediction of solid concentration and particle size distribution across the pipe cross-section can be considered as a complicated process because it involves a large number of parameters such as pipe diameter, flow velocity and density etc. Information about these is very important in the process of optimal design of the slurry pipelines [52].

A simple diffusion model for concentration distribution prediction of solid particles in turbulent streams was the first work in this field. The model was first proposed by O'Brien [53] and Rouse [54] and then modified by Ismail [55] by introducing a new correlation for the mass transfer coefficient to shear stress/velocity gradient. This correlation was derived from von Karman's universal velocity profile and validated based on the measured data of an experimental work using a rectangular channel. The work proved that the von Karman constant is inversely proportional to solid concentration. In addition, the work demonstrated that the concentration could be expressed in terms of exponential function. Wasp et al [56] modified the Ismail's equation by using the value of 0.35 as von Karman's constant. This modification led to a reasonable predicted concentration profile with respect to the experimental data. Subsequently, both results of Ismail [55] and Wasp et al [56] have been analysed by Wasp et al [57].

In addition to Wasp's work [56], Shook and Daniel [58] and Shook et al [59] were conducted extensive research about solid-liquid flow in pipelines. These works confirmed that the equation suggested by O'Brien [53] and Rouse [54] does not take the normal dispersive forces into consideration. Karabelas [60] proposed an analytical model to estimate the vertical composite concentration and particle distributions depending on Hunt's [61] model for slurry flow. He shown the applicability the developed expression by comparing the model results with experimental data. To estimate the overall concentration profile and particle size distribution, Seshadri et al [62] applied the equation developed by Wasp et al [57]. At the top half of the pipe, the results show good agreement with the experimental results. However, significant differences between model and experimental results were noticed at the bottom half of the pipe. Efforts are still ongoing to develop a more appropriate model for the prediction of concentration profile in pipes.

Kaushal and Tomita [45] introduced the Kaushal and Tomita model for solids' concentration profiles and particle size distribution. They modified the model based on extensive analysis of experimental data by taking the effect of efflux concentration and size of particles on diffusivity of particles into consideration [44]. In this work, the ratio of the homogeneously and heterogeneously distributed fraction of each particle size has been determined. Seshadri et al [63] modified the Karabelas model for solid concentration and particle size distribution for the flow of multi-size particulate slurries through open channels and 2-D duct. They used different experimental data in order to establish the limitations of the Karabelas

model in addition to taking the effects of solid concentration on particle settling and turbulent diffusivity into consideration.

Kumar et al [50, 64] conducted a CFD based simulation to study the behaviour of solid particles in horizontal planes of slurry pipelines. The work investigated a significant change in the concentration profile while the overall solid concentration, horizontal plane solid concentration and flow velocity are constant. This is a clear indication for having a sliding bed regime.

Gopaliya and Kaushal [65] presented a three-dimensional CFD analysis of sand-water slurry flow through horizontal pipelines. A mathematical model has been designed to determine the growth of the skin friction factor of each phase along the pipeline for different particulate size slurries. The work considered the concentration distribution as the only factor involved in estimating the friction factor. More experiments and mathematical analysis is needed in order to explain the effects of various factors on the friction factor such as particle shape and size, density and flow velocity.

Singh et al [51] proposed a new correlation to calculate the change of dimensionless particle diffusivity with respect to particle size and solid concentration across the slurry pipe cross section. The correlation was then used to modify Karabelas model. Sigh et al [66] designed a CFD based computational model for the flow of fine silica sand and fly ash. The purpose of the study is to find a solution for the problem of damping of coal ash in thermal plants in India. This work concentrated on different velocities of different phases of the flow and

concluded that the fine particles of fly ash in coarser sand particles distribute the particles and reduce the effect of sedimentation.

2.3.1 Summary of Literature Regarding Concentration Distribution in Horizontal Slurry Pipelines

Based on the literature review presented in the previous sections, for the study of concentration distribution in horizontal pipelines transporting slurries, it can be summarised that various models, based on either analytical or empirical equations, have been used in order to get an accurate prediction of the values of solid concentration and particle size distribution. Many parameters are involved in this prediction process which make it very complicated. The knowledge gaps in the literature review can be identified by taking a number of parameters into consideration and neglecting other parameters in the building of the prediction models. For building more accurate prediction models, more extensive studies are required to identify all the factors affecting the solid concentration profile and to remove the existing limitations. Based on the results of the published literature covered in the previous section, this area still needs more accurate experimental investigations in order to build up an adequate database for concentration profile in horizontal pipelines transporting slurries.

2.4 Velocity Distribution in Horizontal Slurry Pipelines

Velocity field at a cross-section of a slurry pipeline is an important parameter for the design of a slurry pipeline. A complete knowledge about the velocity field is essential for understanding the complex interrelation between various parameters that are involved in this field, such as pipe diameter, pressure drop, solid

concentration and particle size distribution, operating velocity and mixture density. This can be done by conducting extensive experimental investigations. In the third decade of 20th century, O'Brien [53] and Rouse [54] proposed a simple diffusion model based on experimental investigations for dilute slurry flow in an open channel. Then, many researches were performed for the study of different parameters including velocity profile, such as Wasp et.al [57], Doron et.al [67], Mishra [4], Sundqvist et. al [68], Hill [13], Mishra et.al [6], Gillies et al [69], Ghanta and Purohit [70], Wilson et.al [71], and Kaushal et al [72], [73].

Vlasak et al [49] conducted an experimental investigation and flow visualisation of coarse grained particles-water flow in a closed pipe loop. The work concluded that the velocity profile is independent of the mean operational velocity and the particle distance from the pipe invert. The above findings are based on experimental investigations only, and are not supported by mathematical expressions.

Nabil et.al [74] conducted a CFD simulation for the flow of sand-water slurries in a horizontal pipe to predict different flow parameters such as concentration distribution and velocity profile. The results of velocity profile show good agreement with the experimental data for up to 30% solid concentration and 5 m/s operational velocity. The work concluded that for a given velocity, the concentration of solid particles is inversely proportional with asymmetry due to the enhanced interference between solid particles especially in lower velocities.

Messa et. al [75] described a mathematical model for the simulation of fully-suspended slurry flows in horizontal pipeline using the Eulerian–Eulerian approach in addition to applying the Inter-Phase Slip Algorithm (IPSA). The turbulent

dispersion of particles has been taken into consideration by introducing phase diffusion fluxes in all conservation equations. The method of mixture viscosity is used to account for the effect of the presence of multiple particles on interfacial momentum transfer. The model predicted the pressure gradient, solid fraction distribution by volume, and velocity profile, and the performance of the model was checked by comparison with experimental data.

Gopaliya and Kaushal [65] applied the Eulerian model with RNG based K-epsilon model using CFD simulation of sand-water mixture flow through horizontal pipes. Both pressure drop and velocity distribution have been studied and compared with the experimental data.

2.4.1 Summary of Literature Regarding Velocity Distribution in Horizontal Slurry Pipelines

Based on the literature review presented above, for the velocity distribution in horizontal slurry pipelines, it can be summarised that the works are very limited in this area. Different models have been used in order to get an accurate prediction of the values of velocity profile. The knowledge gaps in the literature can be identified as disagreements between the experimental and the model data, and as considering some parameters as independent of the velocity profile without mathematically-based justifications. As illustrated in the previous section, the results are far from reality and require improved models. In addition, this area still needs more accurate experimental investigations in order to build up an adequate database for velocity profile in horizontal pipelines transporting slurries.

2.5 Design Optimisation of Horizontal Slurry Pipelines

Akintola and Solomon [76] used a least cost approach to find the optimal design of a pipeline transporting a non-viscous fluid. A computer-aided code was developed based on C++ program. The work concluded that the optimal pipe diameter is directly proportional with fluid compressibility in turbulent flow. The main limitation of this optimisation model is the applicability for single phase flow only.

Asim et al [77] used the least-cost principle to design an optimization model for the design of pipeline transporting slurries. The paper clearly demonstrated the steps of model operation and includes design case studies. The main strong point of this paper is that it takes a wide range of design parameters into consideration. Furthermore, the limitation of this model is in using Durand's equation for the estimation of pressure drop instead of head loss prediction models that were developed recently with higher prediction accuracy in the flow of solid-liquid mixture.

Laszlo et al [78] developed a life-cycle cost analysis model to study the effects of solid particle size distribution on the optimal sizing and lifetime of pipeline. According to the proposed model, the lifetime of the pipe corresponding to the least annual total cost per pipe unit length will be determined. In addition, by determining the optimal pipe diameter, the total cost of unit pipe per unit volume of transported mixture will be minimum. The work concluded that the lifetime decreases by increasing the particle size and the annual total cost throughout the optimum lifetime is minimum for midsize solids (100-200 μm). The main gap in this

work is way that used in finding pressure loss, In addition, the model did not validated by using different particle densities.

Ihle [79] implemented an optimisation study to find the best operation conditions for a long distance ore pipeline. In addition to the economical point of view, the study focused on some subjective factors such as possibilities of water scarcity and energy instabilities. Different scenarios of high and low water cost and fuel cost were applied in order to be applicable for various situations. The main gap of this research is considering the diameter of the pipeline as a constant factor. Applying the same method using the optimal value of pipe diameter might produce better results.

Yildiz et al [80] used a genetic algorithm as an optimisation method for pipelines transporting slurries. The pipe cost has been defined as a function of pipe diameter and the cost of system operation. The proposed algorithm was designed using C language to solve non-linear programming functions. Furthermore, this optimisation model has the following limitations:

- It uses an old approximation equation for head loss proposed by Thomas [81] which is applicable for iron ore slurries with a particle diameter of 40 micron.
- Limited parameters for the model analysis.
- The factors that produce pressure drop in the slurry pipeline have not been taken into consideration.

2.5.1 Summary of the Literature Regarding the Design Optimisation of Horizontal Slurry Pipelines

The methods of optimisation presented in the previous section are based on various factors for the design of slurry pipelines. It can be summarised that accurate prediction models for the calculation of pressure drop in slurry pipelines are essential for optimally designing such pipelines. It is necessary to include the prediction models of pressure drop in a slurry pipeline in order to get more accurate results. Furthermore, the technique of the model is also an important factor in order to be user-friendly and flexible for different purposes.

2.6 Scope of the Research

Most of the published literature regarding solid-liquid flow within pipelines is based on experimental findings. Hence, it becomes very difficult to monitor and analyse the slurry flow variables without a wider range of investigations in this area. With the advent of modern computational software, it is now possible to develop sophisticated systems to model and simulate the complex fluid flow structure within pipelines.

The key areas of research for solid-liquid flow systems have been found based on the literature review. The first main area of the present study is the diagnostics and analysis of slurry flow through horizontal pipelines. Furthermore, the effect of different hydraulic design parameters on the solid-liquid flow needs to be analysed. The most important slurry flow properties to predict are pressure drop, concentration distribution and velocity profile. For this purpose, developed prediction models are needed. Furthermore, the effects of flow parameters,

discussed in Chapter 1, on the slurry flow in horizontal pipelines need to be analysed. Based on the literature, and due to high root-mean-square differences between the predicted and measured values of solid-liquid flow parameters through horizontal pipeline, further improvements or more accurate models are needed in this area [44].

The optimisation of the horizontal pipelines transporting slurries is the third key area of research for this study. This area will be based on the findings of the first and second key areas mentioned above. The optimisation in the design is essential, as nowadays the commercial validity of such pipelines is a concern.

2.7 Individual Objectives of the Research

Based on the aims of this research presented in the previous chapter, and the detailed literature review presented in the previous sections, the following objectives have been formulated:

1- To develop a robust prediction model for predicting the pressure drop of multi-sized particulate slurry flow in horizontal pipes.

2- To determine the effects of the solid-liquid mixture properties, operational velocity, and pipe diameter on the pressure drop within the pipelines.

3- To develop of a semi-empirical equation for the coefficient of friction in the solid-liquid flow system.

4- To develop a Multi-Layer model for predicting the solid concentration distribution of a multi-sized particulate slurry flow across a cross-section of horizontal pipes.

5- To develop a Multi-Layer model for predicting the velocity profile of a multi-sized particulate slurry flow across a cross-section of horizontal pipes.
6- To determine the effects of the solid-liquid mixture properties, operational velocity and pipe diameter on the velocity profile within the pipelines.
7- To develop a Multi-Layer model for predicting the pressure drop of multi-sized particulate slurry flow across a cross-section of horizontal pipes.
8- To develop a robust optimisation model for a solid-liquid flow system based on the least-cost principle.

In order to justify the mentioned research objectives, the following steps were taken in this study:

1- Laboratory based experiments on the flow of slurry in horizontal pipelines were conducted. A transparent observation pipe has been used in the pipeline to visually observe the particle behaviour in different concentrations and different operating velocities. The next chapter presents the slurry flow experiments conducted in this study.
2- MATLAB program was used in order to first run the available prediction models and then develop the numerical model using the proposed equations in this study. Chapter 4 presents the proposed equations in this study to be used to develop the prediction models.

CHAPTER 3 Solid-liquid Multiphase Flow Experimental Apparatus and Procedure

Based on the research objectives identified in the previous chapter, the multiphase flow loop facility was extended to have horizontal flow experiments. This chapter presents the flow loop setup and the measurement instruments used in this study.

3.1 Flow Loop Setup

The purpose of this study is the development of a prediction model for solid-liquid flow in horizontal pipelines. The available multiphase flow loop facility, which was previously used to diagnose the flow properties of slurry through vertical and inclined pipes, has been developed. A new 90mm pipeline was installed and used to collect the experimental data as shown in figures 3.1 and 3.2.

The system is capable of providing either liquid flow via operating the water pump only, or solid-liquid flows via operating the solid pump or both pumps at the same time. The discharge and the volume fractions of solids and water can be controlled by either adjusting Valve 1 as shown in figure 3.1 or adjusting the speed of the solid pump. For solid phase, spherical plastic beads of 4.5mm diameter with density of 1329.2 kg m^3 were used. In order to obtain a homogeneous solid-liquid mixture, a mixing system that is mounted above the solids and water reservoir was used before being pumped to the working-section. The delivered solid-liquid mixture passes through the separator, which consists of a small inclined tank. The separator has a rectangular cross-section chute of stainless-steel mesh, which separates the liquid phase from the solid phase by the action of gravity. Baffles are positioned along the separator to impede the mixture movement and to accelerate the phase separation process as shown in figure 3.3. The separated phases then pass into two individual conical stainless-steel hoppers.

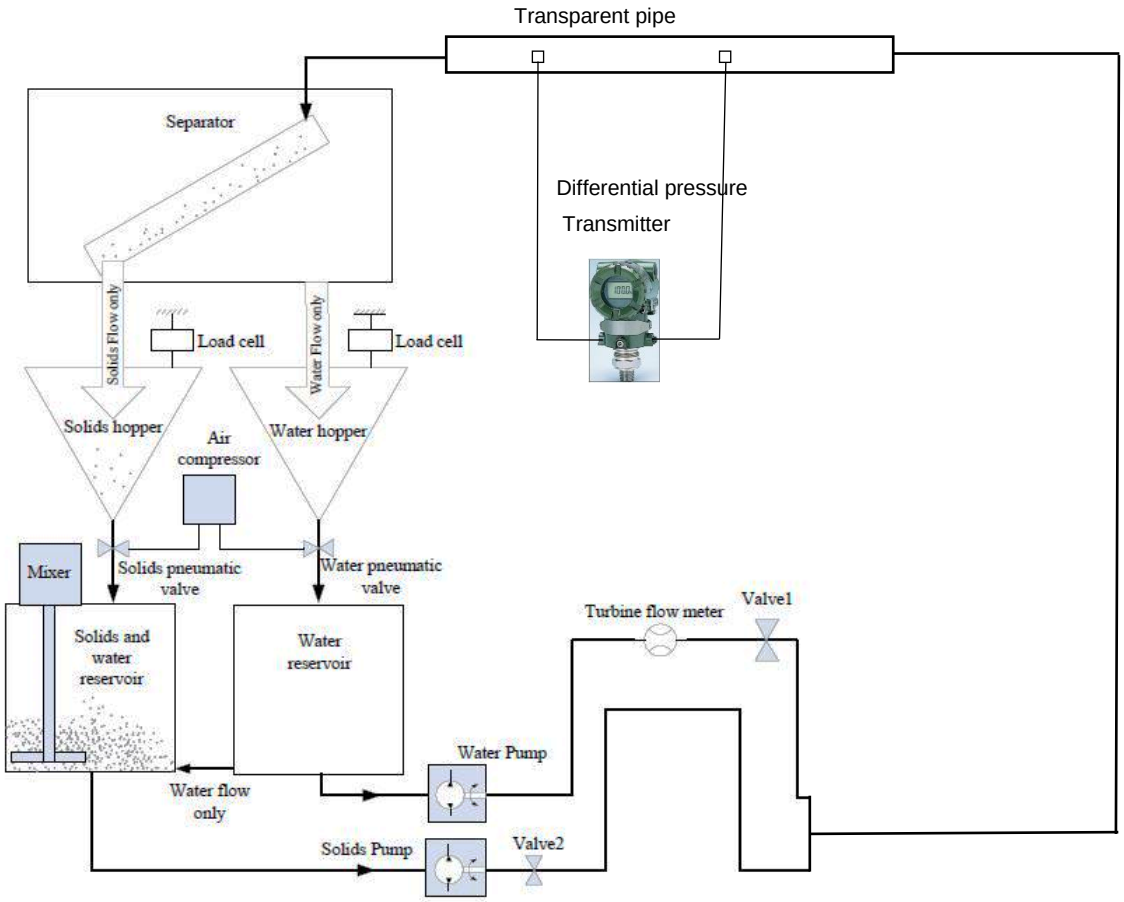

Figure 3-1. Schematic diagram of multiphase flow loop in the University of Huddersfield

The hoppers are suspended on two separate load cells to measure the mass of each phase as a function of time. Pneumatic ball valves were installed at the base of each hopper which are automatically controlled. Two pressure taps, 1m distance between them, were installed on the horizontal transparent pipe. The pressure taps were connected with the pressure transmitter to measure the horizontal solid-liquid flow pressure drop as shown in figure 3.1.

Figure 3-2. A photograph of the multiphase flow loop in the University of Huddersfield

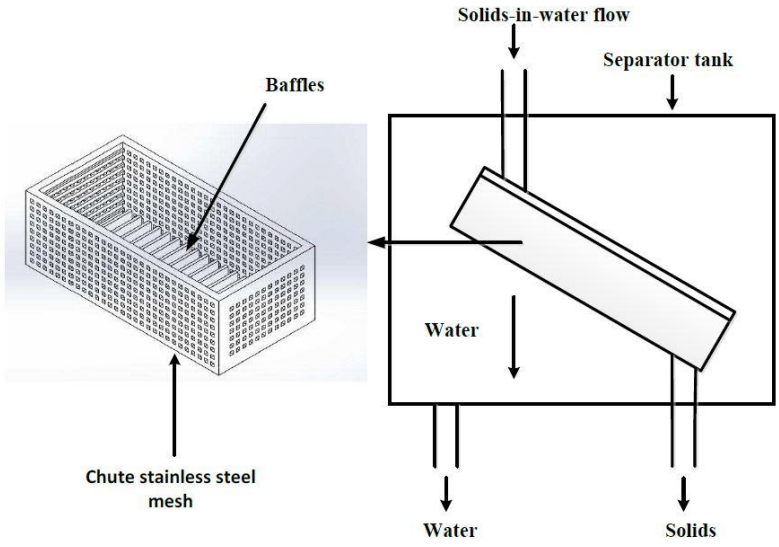

Figure 3-3. schematic diagram of stainless-steel mesh separator

3.2 Solid Particle Density

Plastic beads were used as the solid and water as a carrier fluid. The density of the solid was measured in the lab by measuring the volume of known mass of the solid particles. The test was repeated twice using different solid weights. As shown in table (3-1), two average values of solid densities were found 1329.4 kg/m^3 and 1329 kg/m^3 respectively. In this experiment, the density of 1329.2 kg/m^3 has been considered as the mean value between both results.

Table 3-1 measuring the density of solid particles

Weigh Kg	Volume M^3 x1E^{-3}	Density Kg/m3	Volume M3 x1E^{-3}	Density Kg/m^3
	Test 1		Test 2	
1	0.7519	1329.964091	0.7519	1329.964091
1.2	0.908	1321.585903	0.902	1330.37694
1.4	1.0615	1318.888366	1.0561	1325.632042
1.6	1.196	1337.792642	1.186	1349.072513
1.8	1.332	1351.351351	1.361	1322.556943
2	1.51	1324.503311	1.515	1320.132013
2.2	1.652	1331.719128	1.658	1326.899879
2.4	1.819	1319.406267	1.808	1327.433628
Average	1329.4 kg/m^3		1329 kg/m^3	

3.3 Reference Measurement Devices

3.3.1 Gravimetric Flow Measurement System

3.3.1.1 Hopper Load Cell System

The mass flow rate of both phases of liquid and solid can be obtained by using gravimetric systems after the process of separation of the phases. In the current investigations, two stainless steel hopper load cells were used for measuring the volumetric flow rate for water and solid particles (fine plastic beads) as shown in figure 3.1. A pneumatic ball valve was installed at the base of each hopper. The load cells and the pneumatic valves were interfaced to a computer. The mass flow rate for each phase can be calculated by considering the recorded time after closing the valves and the recorded mass flow rate of each hopper. By taking the density of each phase into consideration, the volumetric flow rate of each phase can be calculated.

$$Q = \dot{M}/\rho \tag{3.1}$$

Where $\dot{M}$ is the mass flow rate, ρ is density, and Q is the volume flow rate.

The phase separation process using the stainless-steel mesh separator is not 100% efficient. In order to calculate the amount of water that flows into the solid hopper, the weight ratio between dry solids and wet solids was calculated and the calibration equation was applied to all readings.

3.3.1.2 Calibration of Hopper Load Cell

The load cells of both the water and solid hoppers were calibrated. To calibrate the hoppers, known masses of water were added gradually to each hopper and the

output voltage signal from the hopper load cells was recorded. As shown in figures 3.4 and 3.5, the calibration curves for both hoppers show a good linear relationship between the added masses and the output voltage for the load cells.

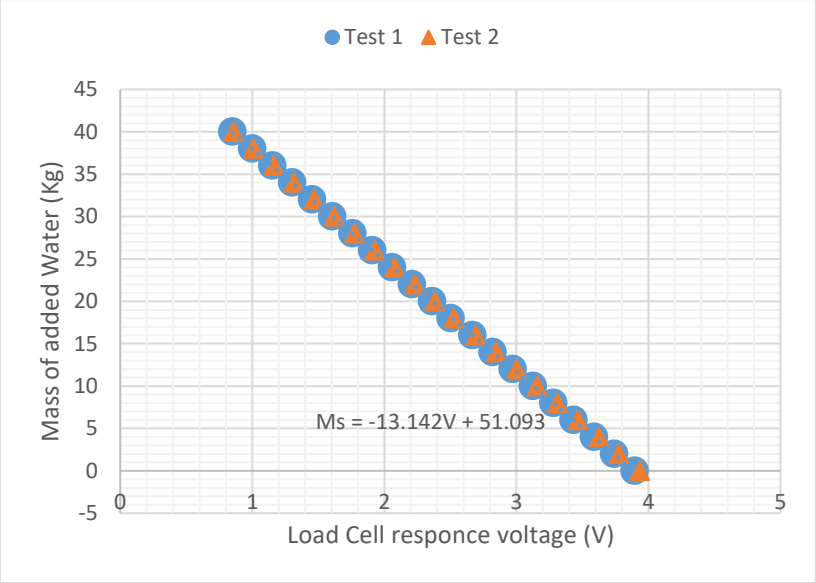

Figure 3-4. Calibration curve of solids hopper load cell

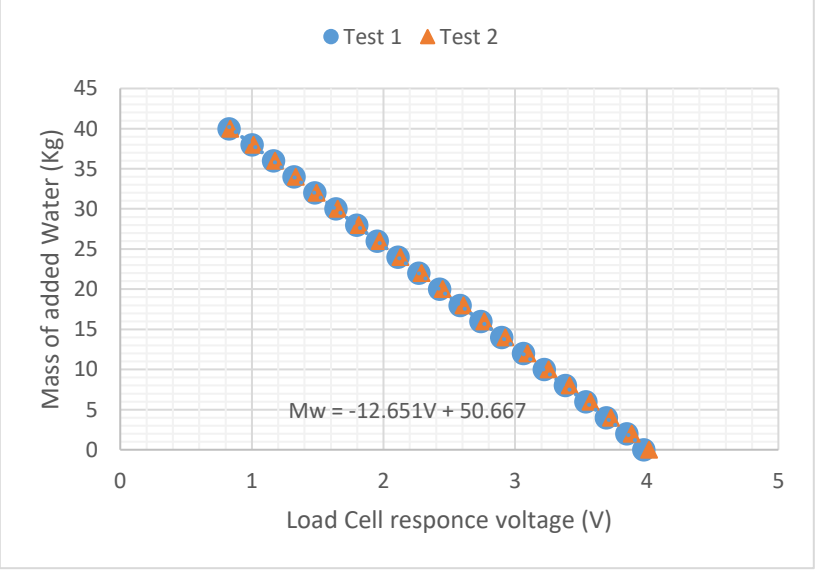

Figure 3-5. Calibration curve of water hopper load cell

By using the linear regression approach, the linear relationship between the reference masses and hopper's output voltages are as follows:

$$M_{SR} = 51.889 - 13.343\, V_S \tag{3.2}$$

$$M_{lR} = 48.78 - 12.5\, V_l \tag{3.3}$$

Where M_S and M_l are masses for solids and liquid respectively, V_S and V_l are hoppers' output voltage for the solids hopper and liquid hopper respectively.

3.3.1.3 Correction Methodology for the Solids Volumetric Flow Rate

In this study, a stainless-steel mesh separator was used to separate the solids from the water. The efficiency of this separation method must be known in order to calculate the amount of liquid that adheres to the surface of the solid particles and is carried into the solid hopper. Therefore, the amount of the actual masses of solids M_S and actual liquid masses M_l needs to be corrected according to the mass of excess water into the solid hopper M_{ex}.

$$M_S = M_{SR} - M_{ex} \tag{3.4}$$

$$M_l = M_{lR} + M_{ex} \tag{3.5}$$

The excess mean fraction by weight of the water inside the solids hopper C_{ex} can be calculated experimentally as:

$$C_{ex} = {M_{SR} - M_{dry}}\Big/{M_{SR}} \tag{3.6}$$

Where M_{SR} is the weight of a sample amount of wet solids in the hopper and M_{dry} is the weight of same amount of dry solids. The mass of excess water in the solid hopper can be defined as:

$$M_{ex} = C_{Wex}\, M_{SR} \tag{3.7}$$

The actual masses of solids M_S and liquids M_l can be defined as:

$$M_S = (1 - C_{ex})M_{SR} \tag{3.8}$$

$$M_l = M_{lR} + M_{ex} \tag{3.9}$$

The actual volume flow rates of the solids Q_S and liquids Q_l can be defined as:

$$Q_S = {}^{\Delta M_S}/_{\Delta t_S\, \rho_s} \tag{3.10}$$

$$Q_l = {}^{\Delta M_l}/_{\Delta t_l\, \rho_l} \tag{3.11}$$

Where Δt_S and Δt_l are the duration between two times taken by the solid hopper and liquid hopper respectively.

3.3.2 Differential Pressure Transmitter

In this investigation, a Yokogawa EJA 110A differential pressure transmitter has been used to measure the pressure drop (DP). As shown in figure 3.1, the DP has been installed on the flow loop to measure differential pressure along a one metre length of the working-section. The output of the Yokogawa DP cell output signal (4 mA to 20 mA) is converted to range of (1 V to 5V) for the differential pressure range 0–1 metre water gauge by using a current-to-voltage convertor. As depicted in figure 3.6, the circuit consists of (250 Ω) Ω, ±1% high precision resistor (Rref1). The voltage drop across the resistor is fed into two buffer amplifiers and the output from the buffers is connected to the input of a unity gain differential amplifier.

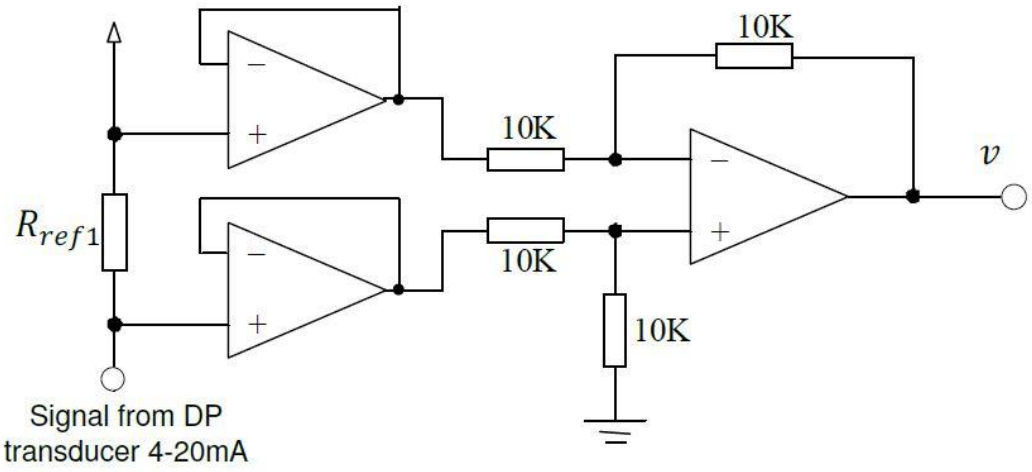

Figure 3-6. Schematic of current to voltage converter circuit

3.3.2.1 Calibration of Differential Pressure Transmitter

The Yokogawa EJA 110A DP was calibrated using a column of water as a physical source to provide different values of pressure loads. As shown in figure 3.7, both ends of the DP cell were connected with the upper and lower point of the pipe at level 0 and 1m respectively. The first reading is the 1m pressure head reading when water level was at reference point 0m. Then the pressure head readings of 0.8m, 0.6m, 0.4m, 0.2m and 0m when the water level was at levels 0.2, 0.4, 0.6, 0.8 and 1 respectively. The test has been done twice and similar readings have been recorded as shown in figure 3.8.

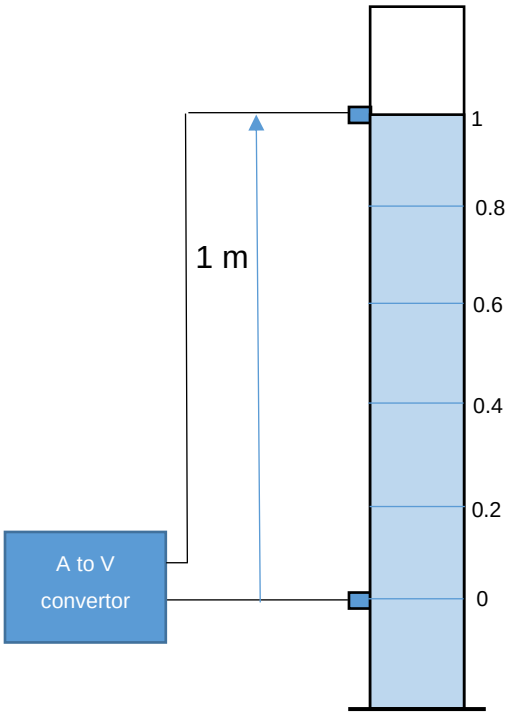

Figure 3-7. Calibration of DP cell

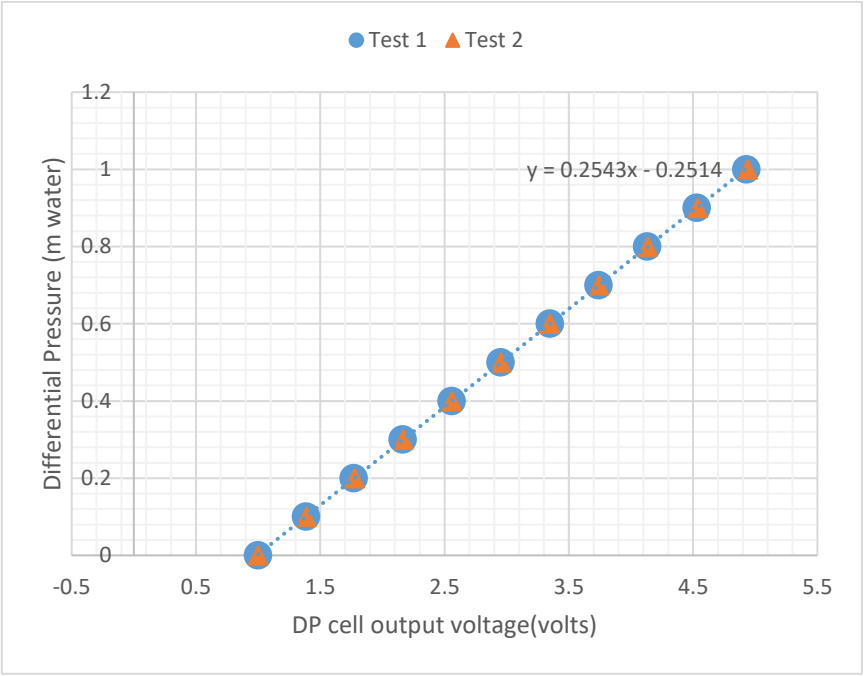

Figure 3-8. DP Transducer Calibration Curve

3.4 Experimental Procedure

The following steps are considered to collect the experimental data:

- Fill up the reservoirs using the available water tap and the water hose.
- Fill the nylon hoses at both ends of the transducer using the water tap.
- Turn on the main electric switch and sub switches.
- Turn on the water pump to operate the flow loop in a single phase flow until the steady state condition is reached. Make sure Valve 2 is closed and Valve 1 is opened figure 3.1.
- Turn on the mixer.
- Turn on the solid pump at different speeds to produce various solid-liquid flow conditions and open Valve 2.
- Turn on the air compressor and adjust it at 3.6 bar. The compressed air supply is used to operate the solid and water pneumatic valves as shown in figure 3.1.
- For each flow condition, the pressure drop, liquid hopper flow rate and solid hopper flow rate readings are collected around three minutes after setting the new flow condition.
- Turn on the computer and the load cell.
- Take readings from the load cells and record them and record the pressure drop data at the same time.
- The operation velocity is calculated from the total flow rate of the delivered mixture and considering the pipe diameter.

- Different flow velocity and solid concentration can be created by partially closing Valve 1 or/and Valve 2 as shown in figure 3.1.
- After the experimental data have been collected, turn off the mixer, the water pump and the solid pump.
- Close Valve 2 and turn off the air compressor.
- Close the program and turn off the PC.
- Drain the reservoirs by turning on the installed single phase submersible pump.

Special care needs to be taken while running the loop as three (3-phase) motors are operating. The main hazard is receiving an electric shock from the cable or pump body. This hazard can be minimised by checking the pump. In addition, the pipe-loop should be checked for leakage at low operational velocity. If any leakages are noticed, the loop should be turned off immediately. Another hazard is hot parts on the pump motor. This hazard can also be minimised by preventing touching the motors while the loop is running and by the use of safety gloves.

Uncertainty in taking the readings can be minimised by using the following steps:

- Calibration:

  The calibration of the hopper load cells and the pressure transducer should be done very accurately and several times before starting the test.

- Repeatability data:

  Repeatability data allow the researcher to analyse and observe variabilities in the measurement results. This can be accomplished by performing the same

process over and over again [82]. In the current study, the repeatability data process was taken into consideration.

- Reproducibility data:

Reproducibility data allow the researcher to analyse and observe the variability in the measurement process. This can be done by changing the common elements in the experimental process such as environmental conditions, operators, water temperature, time and measurement devices [82]. In the current study, the reproducibility data process was taken into consideration.

3.5 Other Experimental Data

In this investigation, in order to verify the proposed model, different experimental results were used. In addition to the current experimental works that were carried out, other published experimental results were employed such as [30], [4], [45], [83] and [84].

3.6 Summary of the Chapter

The multiphase flow loop at the University of Huddersfield was developed to carry out the experimental works. A transparent horizontal pipeline was added to the flow loop in order to conduct investigations about solid-liquid flow in a horizontal pipeline. Plastic beads were used as the solid and water was used as the carrier fluid. Two hopper load cells were used and calibrated in order to measure the flow rate of each phase. A Yokogawa EJA 110A differential pressure transmitter (DP) was used and calibrated in order to produce a pressure drop in the solid-liquid flow in a horizontal pipe. In order to meet the objectives outlined in the previous chapter, a transparent horizontal pipe was used to visually observe the particle behaviour

in different concentrations and different operating velocities. In addition, the data of various flow conditions were recorded to be used in the next chapter as raw material to derive the empirical equations and to design the prediction models.

CHAPTER 4 Novel Pressure Drop Model for Horizontal Pipeline Flow with Enhanced Friction Factor

The experimental results discussed in the previous chapter and the results from the literature regarding the pressure drop in horizontal pipelines transporting slurries, are analysed here. A detailed analysis was carried out in order to understand the complex flow structure of the horizontal slurry pipelines. In addition, a detailed study was made to identify the effects of various parameters on a pressure drop. Furthermore, semi-empirical equations, for the flow of solid-liquid mixture in horizontal pipelines, were developed.

4.1 Introduction

An estimation of head loss is one of the most important points for the designer to be able to compute the actual power requirement under various operating conditions, and to select the pump size. Several correlations are presented in the literature, most of which are derived empirically [4, 12, 27, 30]. In commercial solid-liquid pipelines, the flow is generally turbulent and the particles distributed heterogeneously across the pipeline cross-section. Hence, the prediction of pressure drop becomes very complex, as many parameters are involved in the correlations. As reported in several articles, the SRC Two-Layer Model that was first proposed by Gillies et al. [30] can be considered as a valuable macroscopic model for predicting the flow parameters in slurry containing multi-sized particulate solids [4, 12, 13, 85]. As the original model is based on some simplified assumptions, this work can also contribute to further improvement of the model.

For a heterogeneous slurry pipeline, several parameters are known to affect the pressure drop or energy consumption. These parameters include flow velocity, solid concentration, particle size distribution, shape and size of the solid particles, and carrier fluid viscosity. The coefficient of friction between the solid particles and the pipe wall is another parameter whose effects on pressure drop are reported to be significant, but whose magnitudes have often been taken into less consideration by the researchers [9, 86, 87].

In a closed slurry flow system, the particles are transported by forces that result in a balance between the pressure gradient and frictional resistance of the solid particles on the pipe wall (Coulombic friction). However, the value of Coulombic

friction can be related to the minimum pressure gradient required to transport particles [9].

$$-{}^{dP}/_{dz} = 2\eta_s \phi_{max} g(\rho_s - \rho_f)\varphi \quad (4.1)$$

Where ϕ_{max} is maximum packing concentration by volume of the settled bed and φ is the geometric function which depends on the height of the sliding bed.

Modelling the solid-liquid flow macroscopically has been used since the middle of the last century [87]. This type of slurry flow modelling applies conservation equations to a large control volume of the solid-liquid mixture flow [49, 87]. An improved analysis, and the force-balance model, was used to estimate the limit of stationary deposition [88] and pressure drop for dense-phase flow [89]. The force balance model led to the development of a two-layer model to describe the flows of more dilute coarse-particle mixtures [90].

For heavy particles slurry, such as a slurry that contains gravels, the fluid force is unable to carry the submerged weight. Therefore, the immersed weight is transmitted by particle-particle interaction and carried by inter-granular contacts with the pipe wall. The mechanical forces of sliding friction resistance at the pipe wall increases as a result of increasing the normal force that arises from the immersed weight.

The focus of the present work is on reducing the uncertainty in this model and on the need for modification whilst improving the new definition of the coefficient of sliding friction between solid particles and pipe wall η_s. Based on an extensive analysis of experimental data, reported by Gillies [9], Mishra [4], Ming et al [83] and Fusheng et al [84], the original two-layer model has been modified. The

uncertainty of the original model was identified and modifications incorporated to take into account the effect of the coefficient of sliding friction between solid particles and the pipe wall η_s. The predictions of the modified model are in good agreement with the experimental results.

4.2 Two-Layer Model

Gillies et al [39] proposed a version of the two-layer model for slurry with negligible quantities of fine and slowly settling particles. The Saskatchewan research council (SRC) two-layer model, which divides the solids into two groups of fine and coarse particles, was originally proposed by Gillies et al. [30]. The model was successfully verified against experimental data with reasonable accuracy by Gillies and Shook [41]. Furthermore, the model has undergone a number of refinements such as extension to a higher solid volume fraction by Gillies et al [91] and higher velocities by Gillies et al [18]. Basically, the model considers two types of friction, which are kinematic, and sliding bed friction. Kinematic friction, also called velocity-dependent friction, depends on the carrier fluid's velocity and another component resulting from the particle dispersive stress [43, 92]. The Coulombic or sliding bed friction is produced by the action of the solid particles that are not suspended by the fluid turbulence and sliding against the pipe wall. The normal stress resulting from the immersed weight of the contact load particles is related to the shear stress required to move the sliding bed according to Coulomb's law of friction [42, 43]. The suspended particles contribute in producing velocity dependent kinematic friction while the contact load particles contribute in producing Coulomb friction through contact with the pipe wall [9, 25, 31, 42, 90].

As most industrial slurries contain fine particles, that version of the two-layer model is modified to consider fine particles.

The values of $V, C_v, D, C_{max}, \mu_l, \rho_s, \rho_l \; and \; A_k$ should be specified before using the model. In addition, the particle size distribution, viscosity and particle drag coefficient are important input parameters for the model. In order to calculate C_v, the following steps have to be followed:

1- C_f and d are determined from C_t using equation (2.3) and (2.4).

2- d_{cf} is calculated using equation (1.8).

3- Particle terminal velocity V_∞ is calculated using equation (2.1).

The new carrier fluid density ρ_f can be determined as follows:

$$\rho_f = \left[\rho_l \, (1 - C_t) + \rho_s \, C_f\right] / \left[1 - C_t + C_f\right] \tag{4.2}$$

The viscosity of the new carrier fluid can be measured or calculated mathematically as proposed by Thomas (1965) [19] as below:

$$\mu_f = \mu_l \left(1 + 1.25 \, C_f + 10.5 \, {C_f}^2 + 0.00273 \exp\left(16.7 \, C_f\right)\right) \tag{4.3}$$

The coarse particles with a diameter greater than d_{cf} are assumed to create two layers of composition as depicted in figure 2.2. The suspended particles by fluid forces are distributed uniformly with C_1 concentration. The second layer is formed in the lower part of the pipe, which contains particles with concentration C_2 whose immersed weight is transmitted to the pipe wall due to particle-particle interaction as a contact load. The contact load particles average concentration over the whole pipe is assumed to be C_c, thus the overall coarse particle concentration C_r can be defined as follows [4]:

$$C_r = C_c + C_1 \tag{4.4}$$

C_c and C_2 can be related considering the cross-sectional area of the whole pipe and the lower layers.

$$C_2 \, A_2 = C_c \, A \tag{4.5}$$

The total concentration of coarse particles in the lower layer C_{lim} is given by:

$$C_{lim} = C_1 + C_2 \quad (4.6)$$

The contact load fraction C_c/C_r is proposed by Gillies (1991):

$$C_c/C_r = \exp\left(-0.0184 \left(V/V_\infty\right)\right) \quad (4.7)$$

$$\mathrm{C_C}/\mathrm{C_r} = \exp\left(-0.001013\ \mathrm{Re}^{0.25}\ \mathrm{V}/\mathrm{V_\infty}\right)\ \text{Gillies and Shook (2000)}$$

V_∞ is the terminal settling velocity at an infinite dilution, and can be determined from equation (2.1). Gillies (1991) [30] proposed the following empirical equation:

$$(C_{max} - C_{lim})/(C_{max} - C_r) = 0.074(V/V_\infty)^{0.44}(1 - C_r)^{0.189} \quad (4.8)$$

Here C_{lim} is the mean concentration for the whole lower layer, and C_{max} is a property of the solid-liquid suspension known as the static settling concentration. Gillies and Shook (1994) proposed another semi-empirical approach for determining C_{lim}.Their approach depends on solid concentration distribution which is predicted by considering the solid turbulent diffusion. The concentration at the position of y/D=0.15 relative to the bottom of the pipe assumed to be the predicted concentration of C_{lim}.

Gillies and Shook [41] proposed a semi-empirical approach for determining C_{lim} which is used in two-layer models. Their approach depends on solid concentration distribution which is predicted by considering the solid turbulent diffusion. The concentration C_{lim} at the position of y/D=0.15 relative to the bottom of the pipe is assumed to be the predicted concentration of C_{lim}.

The main gaps in the two-layer model are listed as below:

1- Considering the coefficient of friction as a constant value.

2- Considering the value of C_{lim} as the concentration at the position of y/D=0.15.

3- Considering the value of C_{max} as a constant.

In the current study, two empirical equations are proposed for calculating C_{lim} for both uni-sized particles and multi-sized particles. Several assumptions have been applied for deriving the equations. The following steps were taken in order to derive the equation of C_{lim}:

1- A MATLAB code was designed to find the optimal C_{lim} for any experimental data. The experimental values of C_{lim} have been used as an input of the program.

2- Karabelas' model [60] was used to find the optimal $y/D$for the obtained C_{lim}.The optimal values of C_{lim} have been found at different positions of y/D.

For uni-sized particles, the best assumption was considered and the value of C_{lim} assumed to be dependent on the ratio of volume fraction to maximum packed concentration of solid particles C/C_{max}, the ratio of particle diameter to the diameter of ultrafine particles d/d_{cf}, and Reynolds number. The regression result shows the following equation:

$$C_{lim} = {27.53\ (C/C_{max})^{0.96}\left(d/d_{cf}\right)^{0.4}}\Big/{Re^{0.33}} \tag{4.9}$$

In addition, a new equation is proposed to calculate C_{lim} for multi-sized particles. Instead of d/d_{cf}, the ratios of median diameter of (+50%) coarser particles to the diameter of ultrafine particles ${d+50}/{d_{cf}}$ and the ratios of the median diameter of (-50%) finer particles to the diameter of ultrafine particles $d-50/d_{cf}$ are considered as below:

$$C_{lim} = 0.488\,(C/C_{max})^{0.33}\left(d_{+50}/d_{cf}\right)^{0.11} \Big/ Re^{0.0042}\left(d_{-50}/d_{cf}\right)^{0.025} \quad (4.10)$$

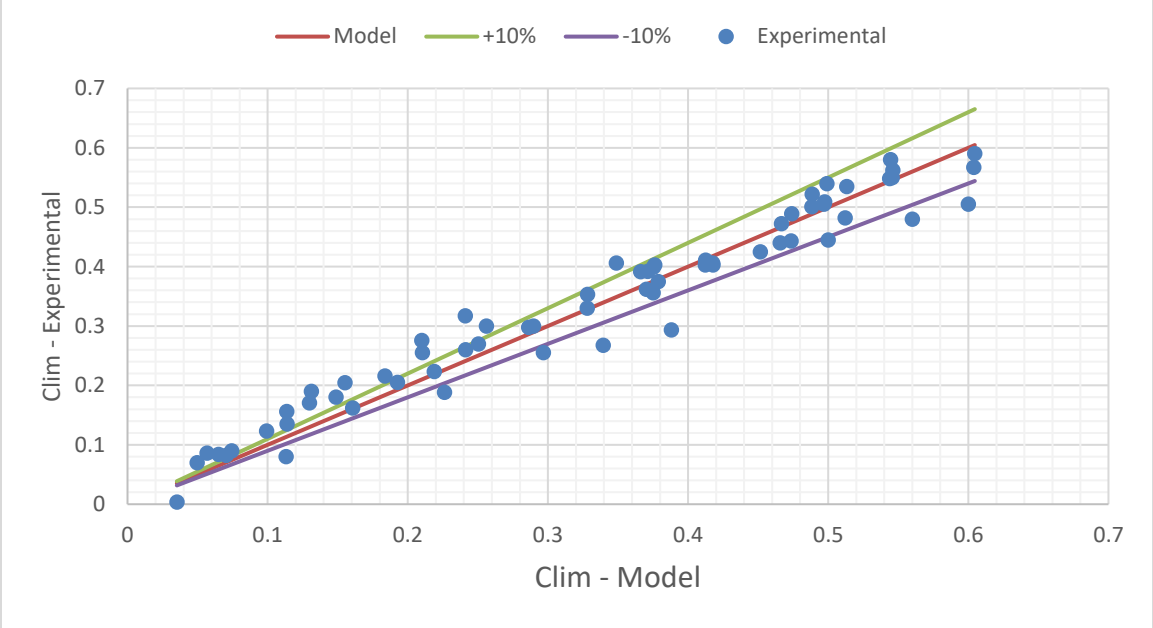

Figure 4-1. The experimental and model data of C_{lim}

As shown in figure 4-1, the model results of C_{lim} The predicted results have good agreement with the experimental data. Most of the experimental data are located between inside the two line $(C_{lim} + 0.05)$ and $(C_{lim} - 0.05)$.

For calculating the maximum packed concentration of solid particles C_{max}, two equations are proposed for uni-sized and multi-sized particles. For uni-sized spherical particles, the ratio of 1 unit diameter sphere volume to 1 unit length of cube volume was considered as below:

$$C_{max} = 0.167\pi + e \quad (4.11)$$

For C_{max} of multi-sized particles, the following empirical equation was proposed:

$$C_{max} = 0.167\pi + e\left(dC/_{dF}\right)^{1.1847} \quad (4.12)$$

e is the experimental coefficient and was found to be 0.009. dC and dF are the mean diameters of d_{+50} and d_{-50} particles respectively. d_{+50} include all the size fraction particles above percentage finer of 0.5 ($S_P > 0.5$) and d_{-50} include all the size fraction particles below a percentage finer of 0.5 ($S_P < 0.5$). If a percentage finer ($S_P = 0.5$) is not available, a linear interpolation might be used between two percentage finers data just under and above 0.5.

In the above equation, when the value of dC/dF approaches unity, the equation will be equal to (4.4) which is true for representing uni-sized particles. For a high value of dC/dF, the value of C_{max} will increase as the void fraction of coarse particles decreases and is filled out by partially fine particles.

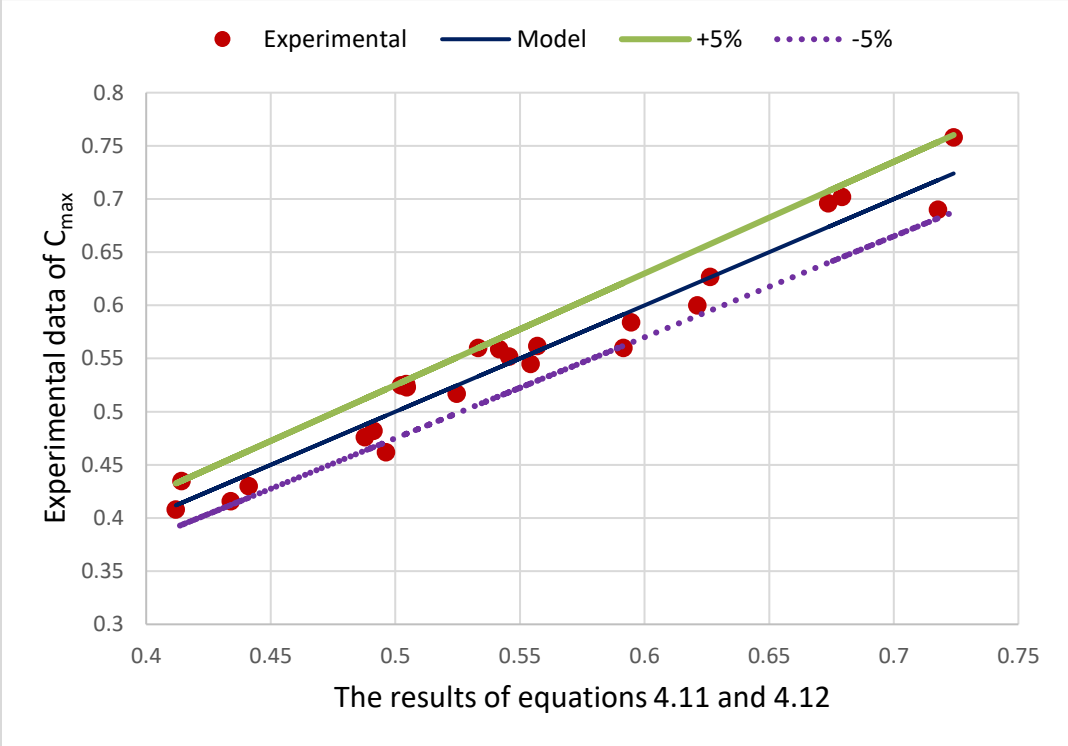

Figure 4-2. The experimental and model data of C_{max}

4.3 The Novel Equation of Coefficient of Friction in Solid-Liquid Flow

As presented in the literature, many works have been carried out on liquid-solid two-phase flow, including the two-layer model, considering the coefficient of friction between solid particles and pipe wall η_s as constant.

Wilson et al [3] suggested that η_s can be determined using a tilting tube test in the lab. Shook et al [28] experimentally determined that the average wall-particle coefficient of friction η_s is 0.5 for sand and gravel slurries and 0.4 for coal slurries. Gillies [9] reported that η_s is reduced when particles are moving parallel to the pipe wall due to the lubrication effect of the carrier fluid. However, η_s is independent of operational velocity as the lubrication force is small.

Wilson et al [93] predicted that the coefficient of friction will decrease as a result of increasing the generated lift force which repels the solid particles from the pipe wall. This argument is supported experimentally by Gillies et al [18]. As the generated lift force is directly proportional to the operational velocity, the coefficient of friction is dependent of the operational velocity. According to Gillies and Shook [40], the friction coefficient increases rapidly at low velocities as a result of increasing solid concentration up to 30% - 35%. This idea was also supported by Krampa [94] in his research with the Saskatchewan Research Council. Furthermore, the ANSYS simulation results of Eesa [95] concluded that the particle-wall coefficient of friction decreases by increasing the solid particle diameter whilst keeping the solid phase volume fraction unchanged.

A MATLAB program code was designed for predicting flow parameters in horizontal slurry pipelines, based on the Modified Two-Layer Model by Gillies et al [30]. The coefficient of friction between sand particles and the pipe wall was assumed to be 0.5 [9, 30]. In order to perform the work with high accuracy, different reliable and high quality experimental data were selected rather than a single experimental result, to perform the reproducibility data requirement as explained in the previous chapter (section 3-4). The model pressure drop results were compared with the chosen practical data reported by Gillies [9], Mishra [4], Kaushal et al [72], Ming et al [83], Fusheng, et al [84], and Mali et al [96] and the comparisons showed that the values of model pressure drop are generally higher than the used experimental readings as illustrated in figure 4.3. The value of η_s was reduced gradually and the experimental and model data were compared as shown in figure 4.4.

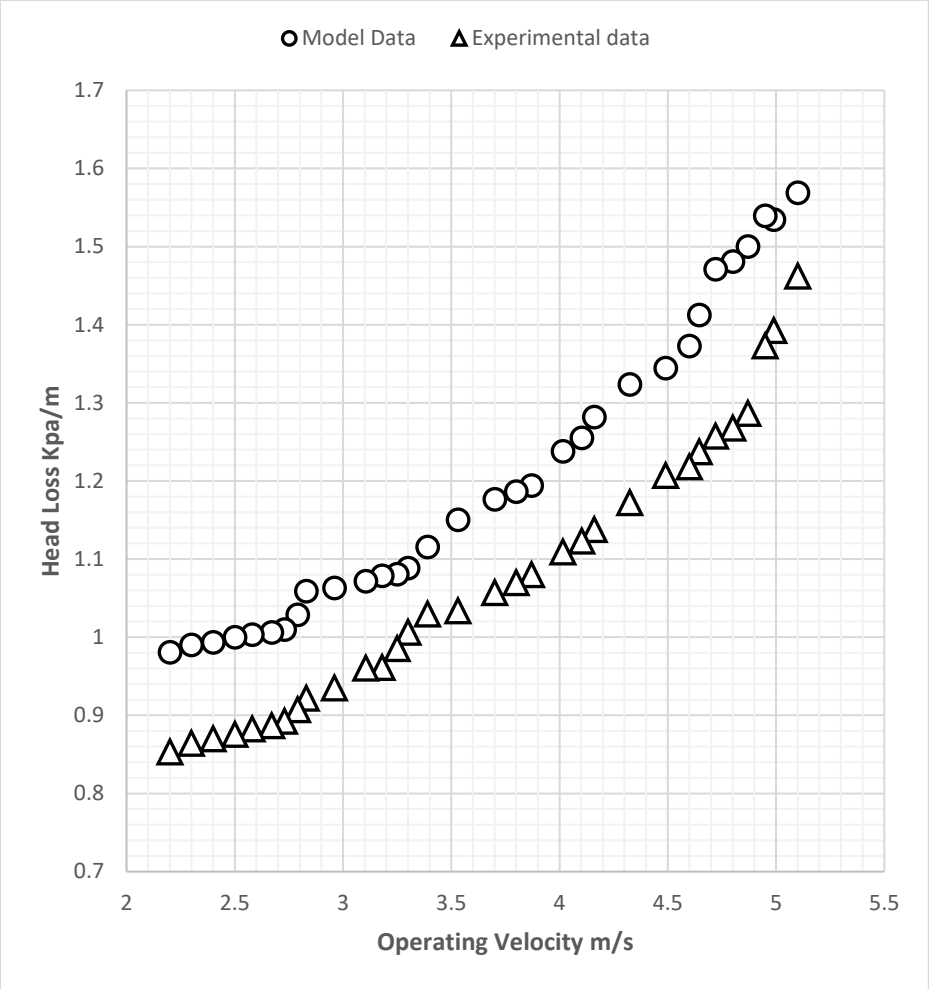

Figure 4-3. Experimental data and model data when $\eta_s = 0.5$, $D = 0.2631m$, $d_{50} = 0.45mm$, CV=13% [9]

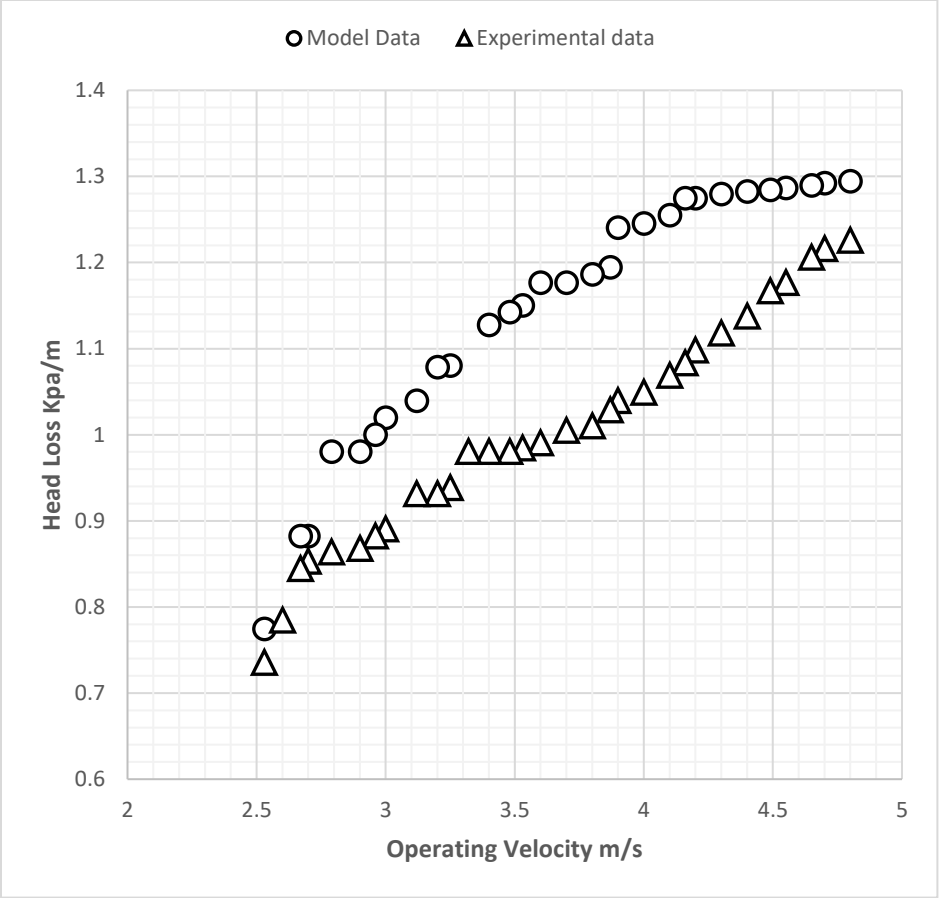

Figure 4-4. Experimental data and model data when $\eta_s = 0.2$, $D = 0.2631m$, $d_{50} = 0.45mm$, CV=22 % [9]

A second MATLAB code was designed to calculate the predicted value of the friction coefficient in order to equalise the experimental data on pressure drops with the model's result as depicted in figure 4.6. For this purpose, different MATLAB functions were prepared, which interact with the main program. It is mandatory for the user to enter and update the input data file (Excel file) which should have data on the physical properties of the solid and liquid each in the correct cells that are provided. As the code was designed based on the closed loop system, any predicted value of pressure drop is compared with the provided value

of the experimental result pressure drop and the error is calculated. As at the beginning, we start with a high value of η_s and the predicted value of pressure drop is expected to be higher than the experimental value, the program increases the value of η_s until the predicted value of the pressure drop equals the experimental result. The program prints the equivalent value of η_s.

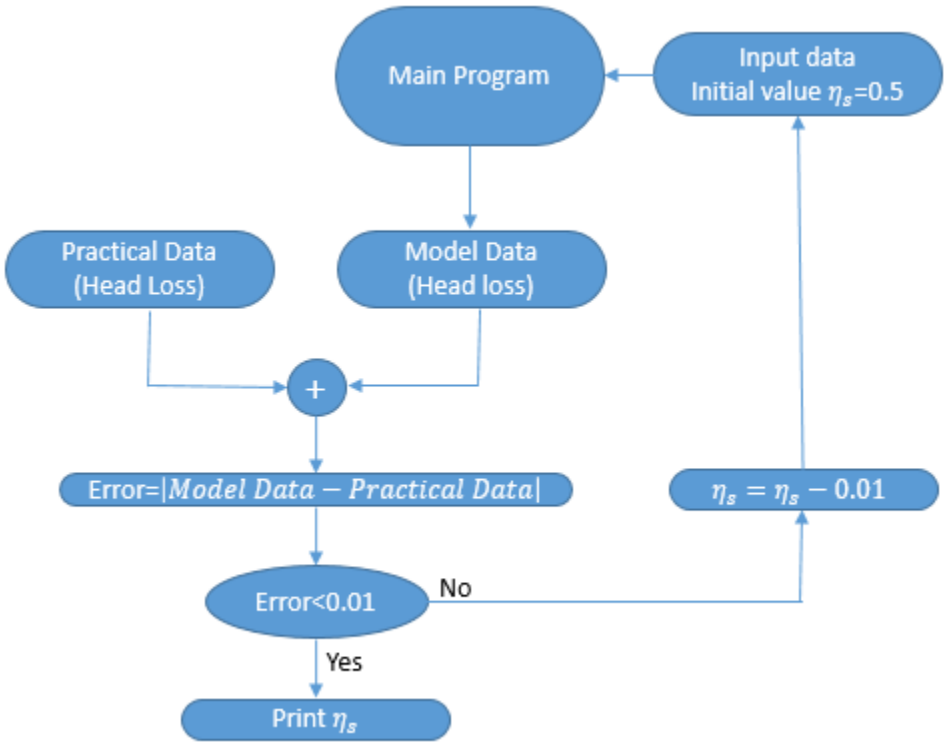

Figure 4-5. The program flow chart

The new predicted coefficient of friction data was recorded for each experimental case, see the two samples of data illustrated in figures 4.6 and 4.7 for both dilute and dense slurries respectively. As shown, the optimum value of the friction coefficient is small at low and high velocities.

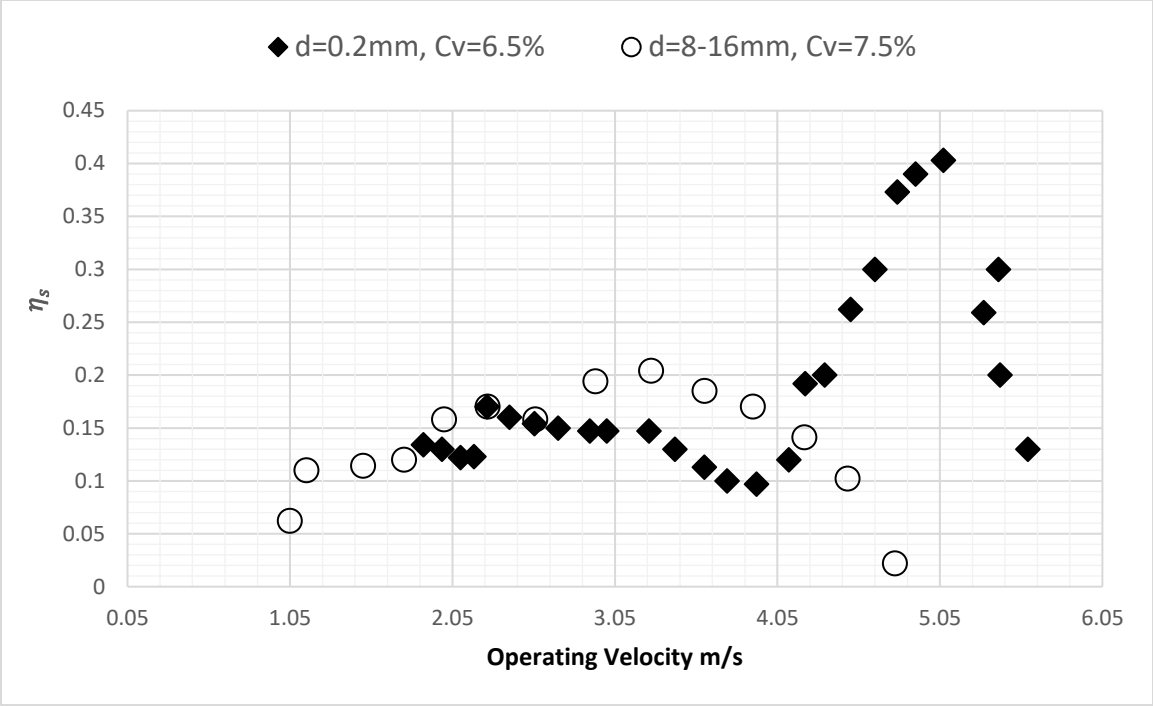

Figure 4-6. Optimum values of η_s for solid particle in dilute slurries [4, 9, 83, 84]

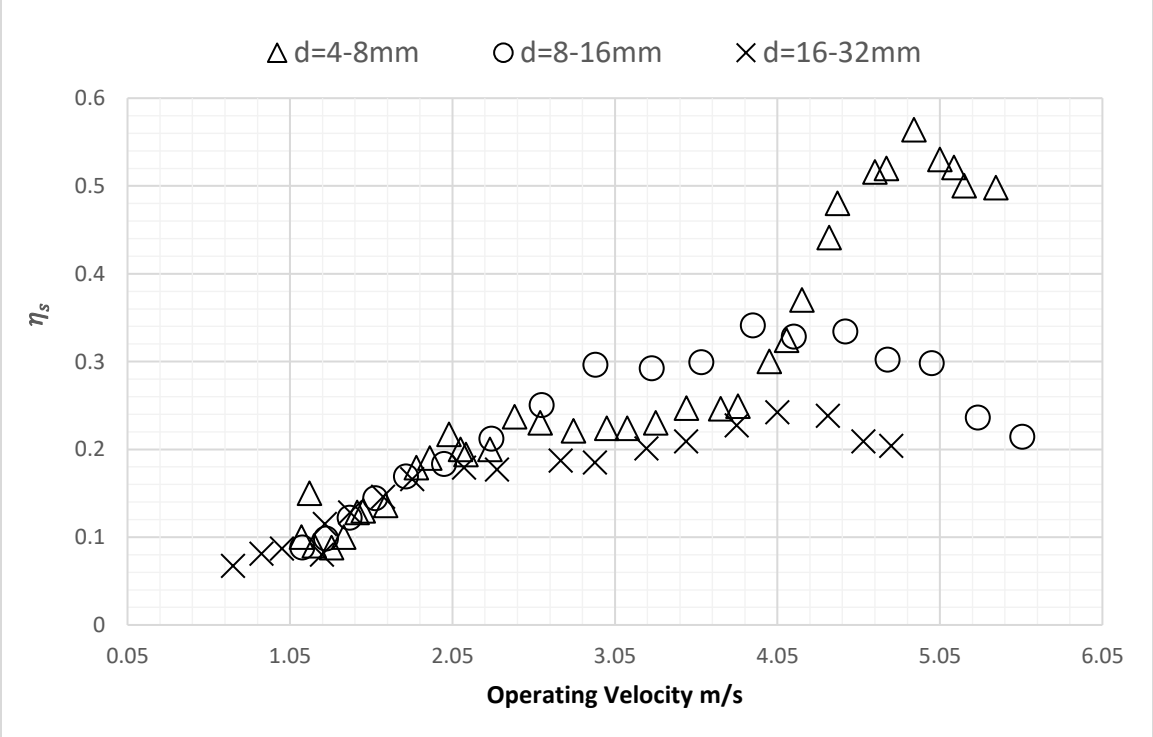

Figure 4-7. Optimum values of η_s for solid particle in slurries with c_v=11% [4, 9, 72, 84]

To derive the equation of the coefficient of sliding friction, many parameters were used to test the rate of dependency of η_s on each parameter. According to the test result, six parameters were considered based on the regression analysis results. The parameters were then converted to three dimensionless ratio values to guarantee that the output result would also be dimensionless. For considering the velocity factor, (v_2/v_C) is used. (V2) is the velocity in the lower layer and (Vc) is the deposition velocity. For solid concentrations, $(C_2/1-C_2)$ is used as a ratio of solid concentration in the lower level, to the liquid concentration at the same level. The third parameter being used is $((d_{50}-A_k)/A_k)$, where d50 is the mass median particle diameter and A_k is the roughness of the pipe. An empirical equation was created to predict the coefficient of friction in a coarse slurry pipeline based on the experimental data. Different regression analyses models were applied. The polynomial model, which is a special case of the multiple regression model, was chosen as it gives a best fit curve with the data. The regression statistics are presented in Appendix (1). The equation below shows the fifth order polynomial equation for the range of the data.

$$\eta_s = a + bX + cY + dZ + eX^2 + fY^2 + gz^2 + hX^3 + iY^3 + jz^3 + kX^4 + lY^4 + mz^4 + nX^5 + oY^5 + pz^5 \quad (4.13)$$

Where:

$$X = {}^{v_2}/_{v_c}\,,\ Y = {}^{c_2}/_{(1-c_2)}\,,\ Z = {}^{(d_{50}-A_k)}\Big/_{A_k} \quad (4.14)$$

Table 4-1 the values of the polynomial equation parameters

a	8.245407	i	-2361.55
b	0.431439	j	0.002401
c	-138.095	k	0.618793
d	0.240657	l	3219.703
e	0.562985	m	-5.60E-05
f	827.9651	n	-0.09727
g	-0.03893	o	-1686.33
h	-1.22816	p	4.08E-07

The contribution of the parameters (g,j,m and p) in the polynomial equation are very small and can be neglected. This indicates that the effects of Z is very small on the value of coefficient of sliding friction. As shown in figure 4.8, most data points are located inside the (-10%) and (+10%) error lines.

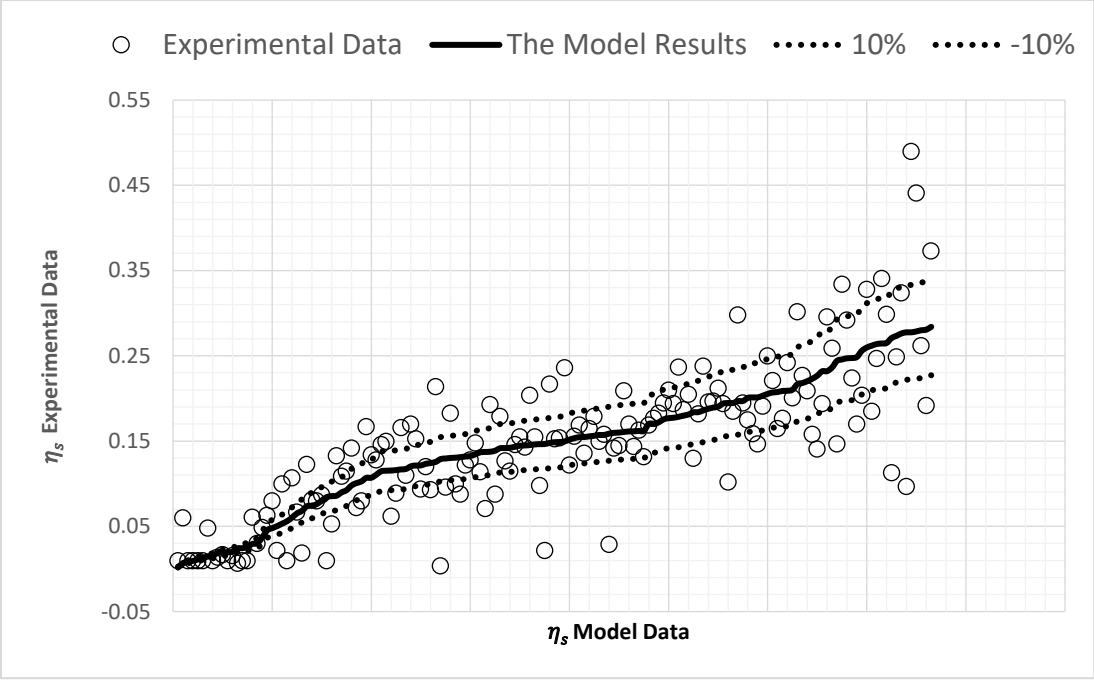

Figure 4-8. The modified model value of coefficient of sliding friction

4.4 Validation of the Proposed Model

The new values of the coefficient of sliding friction are shown in figure 4.9. The new equation was applied to the SRC Two-Layer Model. The results show better predictions of pressure drops in comparison to the experimental data. Most practical data for the pressure drops are near to the model line by less than +/- 10%. If the modified model results, as shown in figure 4.9, are compared with the original two-layer model results, as shown in figures 4.3 and 4.4, a significant improvement will be noticed. Considering the value of the coefficient of friction as 0.5 for sand and gravel slurries will generate higher pressure drops than the experimental data. Using the optimal value for the coefficient of sliding friction will move the model data series closer to the practical data series.

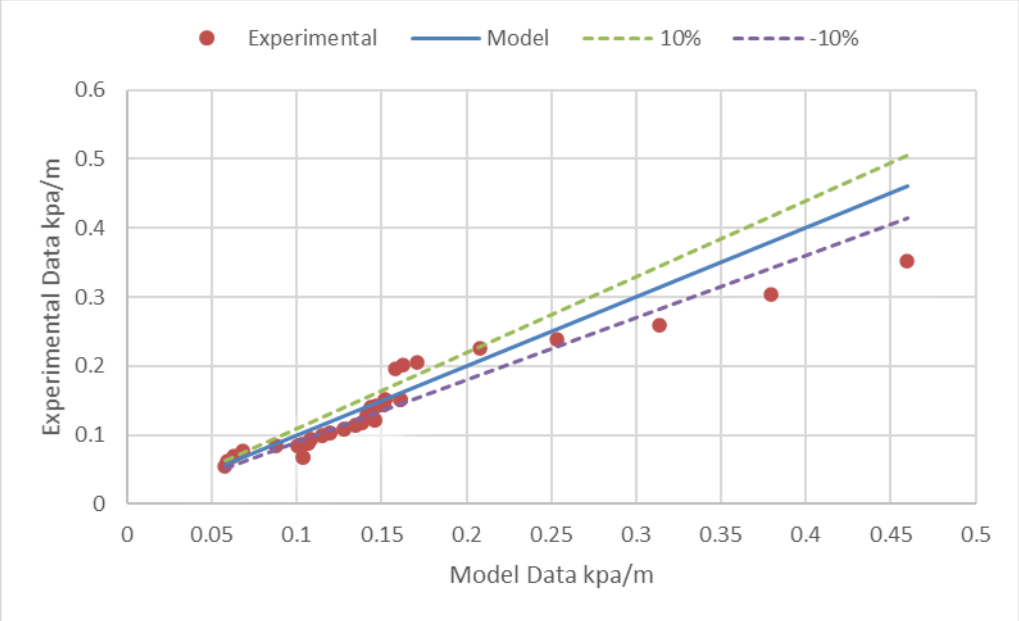

Figure 4-9. The modified model results

4.5 Factors Influencing the Pressure Drop

The predicted coefficient of friction data were recorded for each experimental case using sand and gravel with a particle density of 2650 kg/m^3. The effects of operational velocity, solid particle diameters and solid concentration on η_s have been studied separately.

4.5.1 The Effects of Operating Velocity on the Coefficient of Sliding Friction

To understand the effect of operational velocity on η_s, experimental values of operational velocity were considered for the same values of particle sizes and concentration. As shown in Figure 4.10, the value of η_s that ensures a good matching between the experimental and predicted data shows a mixed trend. It increases with increasing flow velocity before falling down to initial levels. The lower values of η_s at low velocities might be due to a stationary or relatively low movement of the solid bed at the bottom of the pipe. In addition, the value of η_s reaches the maximum when the generated lift force is slightly less than required to carry the contact load particles, and the generated motive force is high enough to move such particles along the flow. Furthermore, decreasing the value of η_s at relatively higher velocities might be due to the generation of enough lift force to keep the solid particles away from the pipe wall.

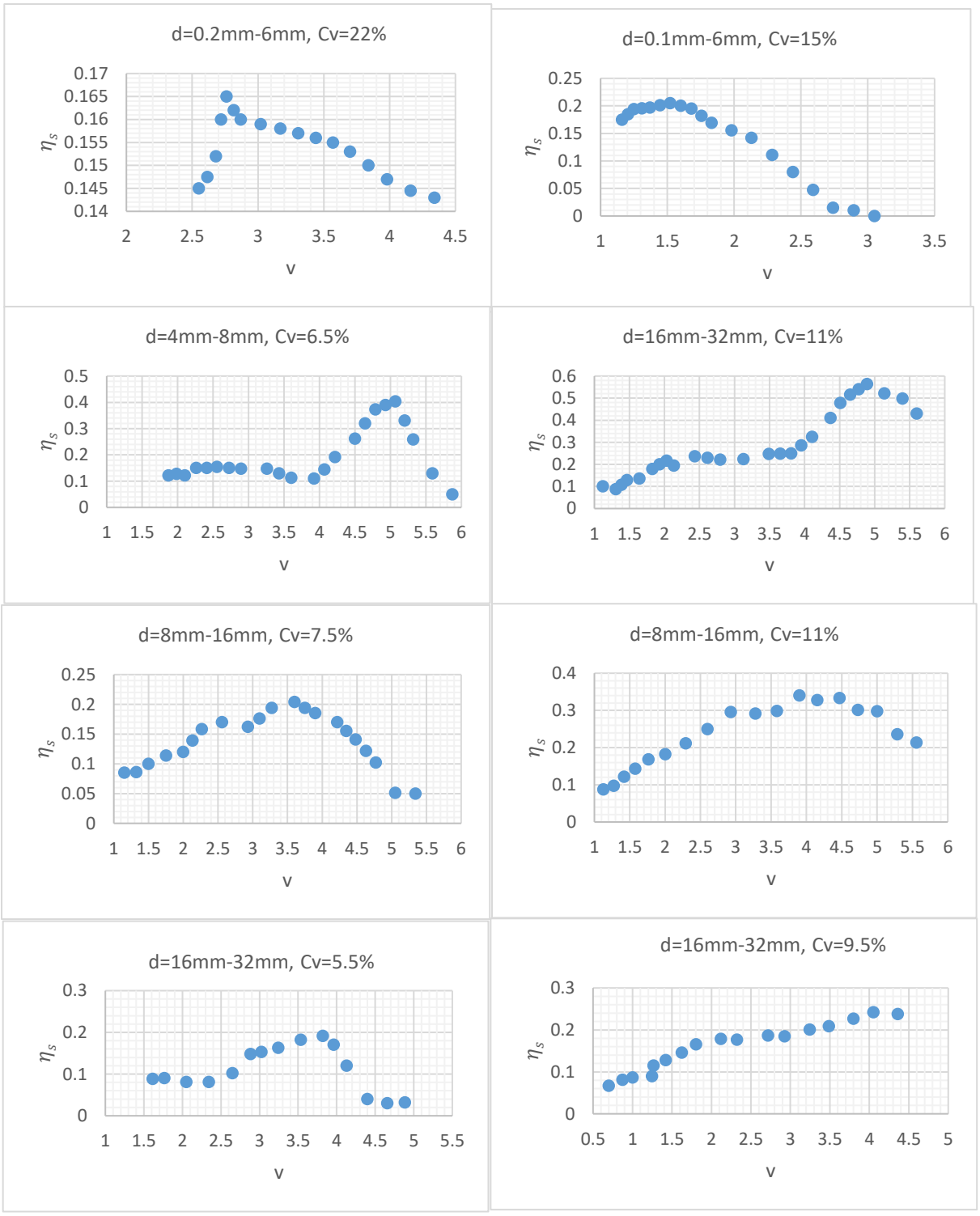

Figure 4-10. The effect of operational velocity on η_s

4.5.2 The effects of Solid Throughput on the Coefficient of Sliding Friction

The next step of this analysis is studying the effect of solid particle volume friction on the solids-wall coefficient of sliding friction. Experimental values of used solid concentration by volume were considered for the same values of operational velocity and the same range of particle sizes. As shown in figure 4.11, the value of η_s is directly proportional to the solid concentration.

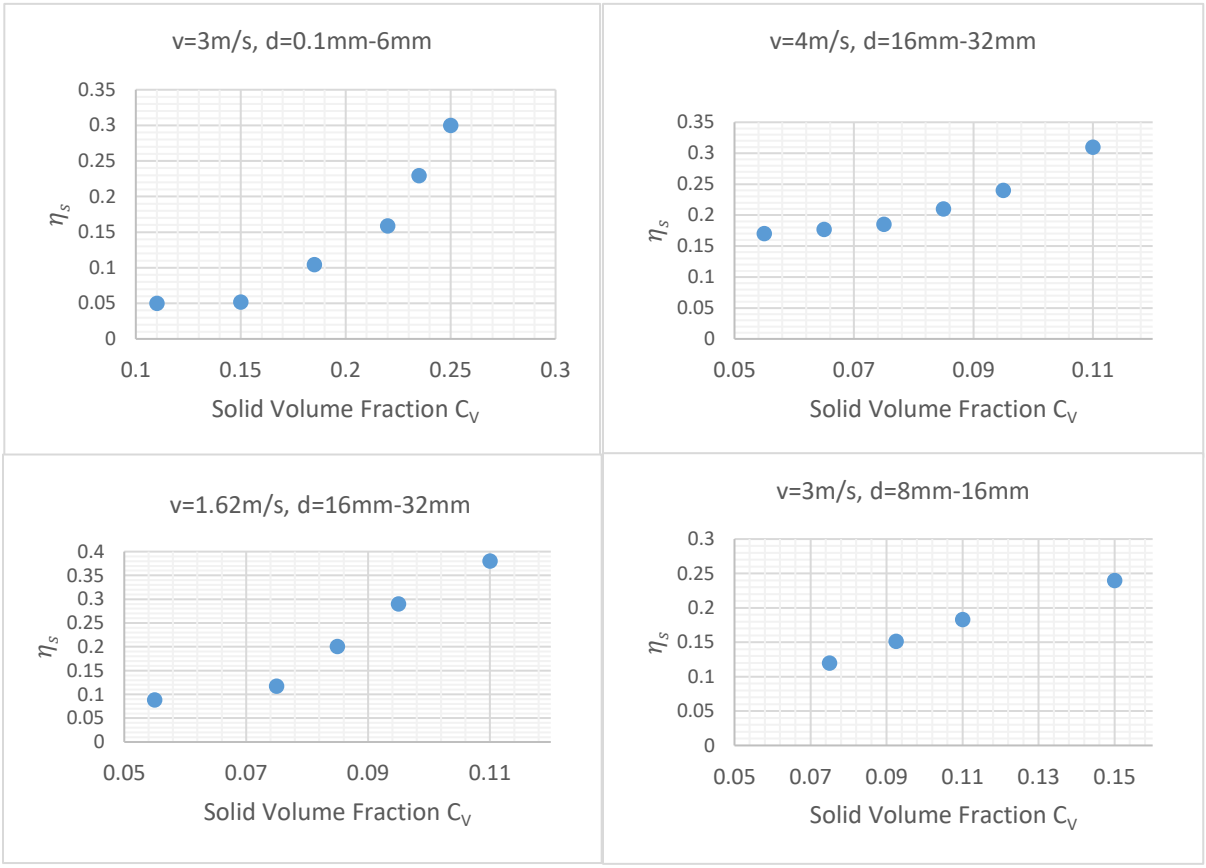

Figure 4-11. The effect of solid particle concentrations on η_s

4.5.3 The Effects of Particle Size on Coefficient of Sliding Friction

To study the effect of solid particle sizes on the solids-wall coefficient of sliding friction, experimental values of the used particle sizes were considered, whilst the operational velocity and solid concentration remained constant. As shown in figure 4.12, the value of η_s is inversely proportional to the particle sizes at low velocities and high velocities. At low velocities, increasing particle sizes help to generate stationary or low movement beds at the bottom of the pipe which lead to a decrease in the friction between solid particles and the pipe wall. At high velocities, decreasing the value of η_s might be due to different dispersion behaviour of fine and coarse particles. In other cases, η_s approaches the maximum by increasing the particle sizes as a result of depositing the solid particles at the bottom of the pipe, and by further increasing the particle size, the slow moving or stationary beds decrease η_s as discussed previously.

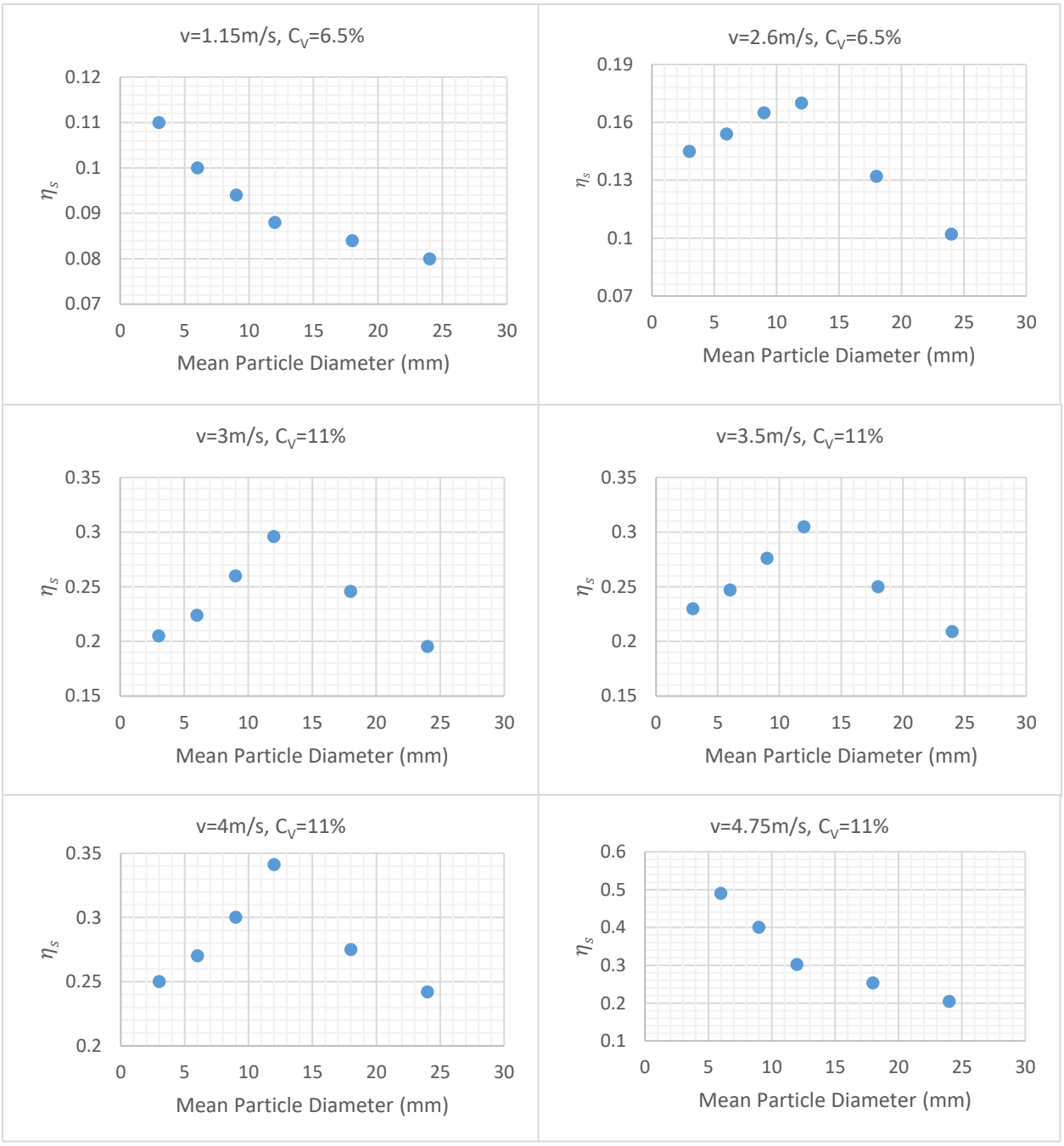

Figure 4-12. The effect of solid particle diameter on η_s

4.6 The Equation of Coefficient of Sliding Friction η_s

As presented in section 4-3, various parameters were used in order to derive an equation for the coefficient of sliding friction between solid particles and the pipe wall. As shown in equations 4-13 and 4-14, the equation is very complicated. Based on the previous analysis of the effects of various parameters on η_s, a new simple equation can be derived.

To derive an equation for the coefficient of sliding friction, many parameters were tested. One of the parameters is the ratio between the velocity in the first layer to the velocity in the second layer v_1/v_2. In order to create this relation, a dimensionless grouping of the other dependent parameters ς was proposed in this research.

$$\varsigma = \log\left({}^{d_{50}}/_{A_k}\right)(1 - C_V) \tag{4.15}$$

As shown in figure 4.13, the maximum values of the coefficient of sliding friction η_s are recorded for different values of ς when the ratio value of $v_1/v_2$is about 1.8 to 2.0. C_V is the delivered solid particles volume fraction, v_1 is the velocity of the upper layer and V_2 is the velocity of the lower layer. The value of ς approaches zero when the values of V1 and V2 approach unity. In addition, η_s settles at 0.1 for any values of v_1/v_2 greater than 3.8. Further research is required to provide experimental evidence of the relation between these parameters in order to give a better understanding of the behaviour of solid-liquid flow in circular smooth pipes.

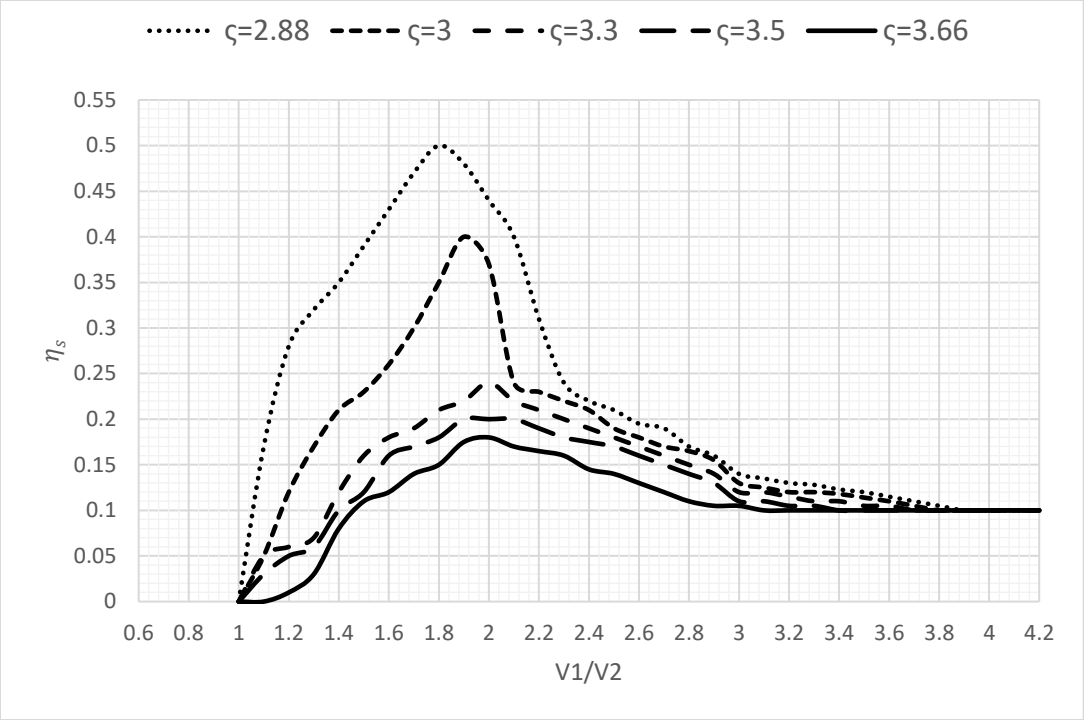

Figure 4-13. The behaviour of the coefficient of sliding friction.

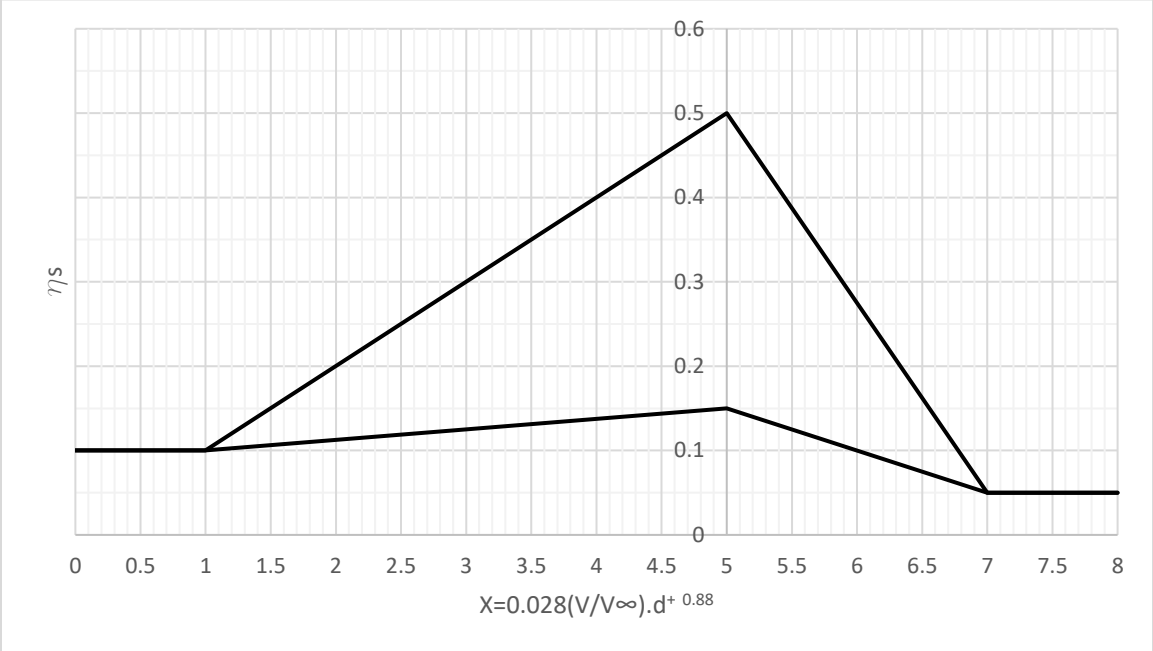

Figure 4-14. The proposed chart for estimating the coefficient of sliding friction: d50=2mm to 24mm, Cv=5% to 25%

According to the analysis presented in the previous section, the effect of all factors can be combined into a single reading graph. The importance of producing this reading graph is to estimate the value of the coefficient of sliding friction η_s for any slurry flow properties. To ensure the relation is dimensionless, (v/v_∞) and the median dimensionless particle diameter d_+ were used instead of operational velocity and median particle diameter respectively. v_∞ is the particle settling velocity and d^+ is defined as:

$$d^+ = d\left(\rho_f(\rho_S - \rho_f)\, g \Big/ {\mu_f}^2\right)^{1/3} \tag{4.16}$$

The maximum values of η_s for different flow properties were explained in the previous section. To define the maximum reachable coefficient of sliding friction for any solid particle sizes and concentration by volume Y^*, the following adjustment is used:

$$Y^* = {C_V}^{0.47} \Big/ {d_+}^{0.013} \text{ or 0.5, whichever is less.} \tag{4.17}$$

The maximum value of the coefficient of friction was found to be 0.5 based on the experimental data. The diagram of coefficient of sliding friction η_s is shown in figure 4.14 and the value of η_s can be read by the steps illustrated in figure 4.15. The dimensionless particle diameter d^+ was computed using equation (4.16). By using equation (4.17), the maximum reachable coefficient of sliding friction Y^* can be computed and the new chart for the current solid particle mean diameter and solid concentration by volume can be drawn.

As shown in figures 4.10 and 4.12, the value of η_s peaks at different values of operational velocity and mean particle diameters, then decreases. However, as

shown in figure 4.11, η_s is directly proportional with the solid particles volume fraction. Accordingly, (v/v_∞) and dimensionless particle diameter d_+ should be considered to compute X^* of figure 4.14 as below:

$$X^* = 0.028\left(v/v_\infty\right).{d_+}^{0.88} \tag{4.18}$$

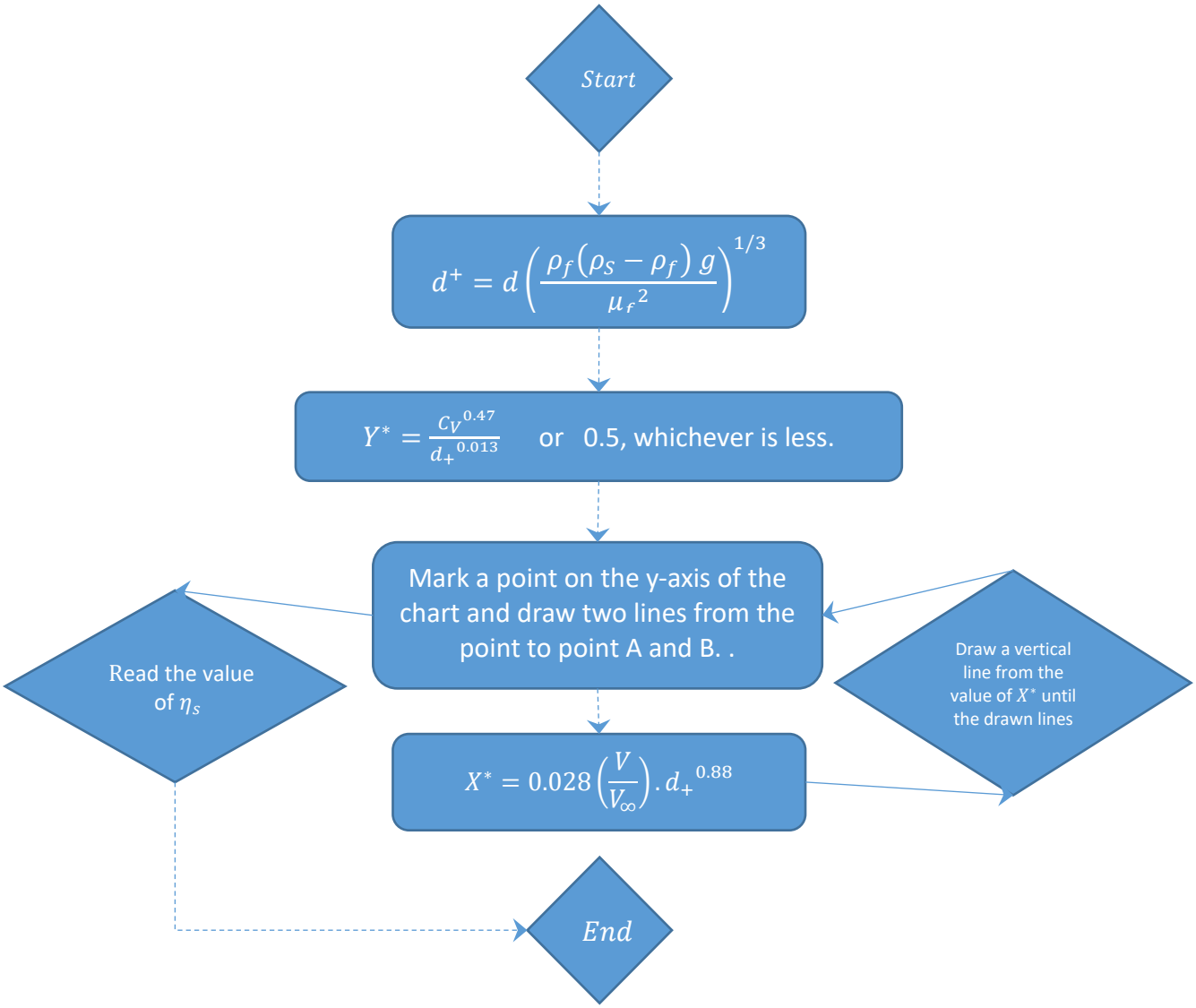

Figure 4-15. Flowchart illustrating the steps of using Coefficient of friction graph.

The proposed graph has been justified for mean particle diameter 2mm to 24mm and solid volume fraction 5% to 25%. Figure 4.16 shows the comparison between the predicted values of η_s using the graph shown in figure 4.14 and the optimum values of η_s as explained is section 4.3. The accuracy of predicting η_s in most cases is less than $\pm$0.05. As shown, the results are not accurate with respect to the experimental data in some instances. There are many factors affecting the results such as the prediction power of the proposed equation and the inaccuracy of the used experimental data. Further researches in this field are necessary to study the limitations of the proposed equation. Generally, the equation proves that the coefficient of sliding friction between solid particles and pipe wall is not constant.

The two-layer model has a number of equations with no graph reading sections. In order to fit the previous works to this model, the graph can easily be replaced by equations.

$$\eta_s = 0.1 \qquad When\ X^* < 1 \tag{4.19a}$$

$$\eta_s = 0.25(Y^* - 0.1)(X^* - 1) + 0.1 \qquad When\ 1 \leq X^* \leq 5 \tag{4.19b}$$

$$\eta_s = 0.5(0.05 - Y^*)(X^* - 7) + 0.05 \qquad When\ 7 \geq X^* \geq 5 \tag{4.19c}$$

$$\eta_s = 0.05 \qquad When\ X^* > 7 \tag{4.19d}$$

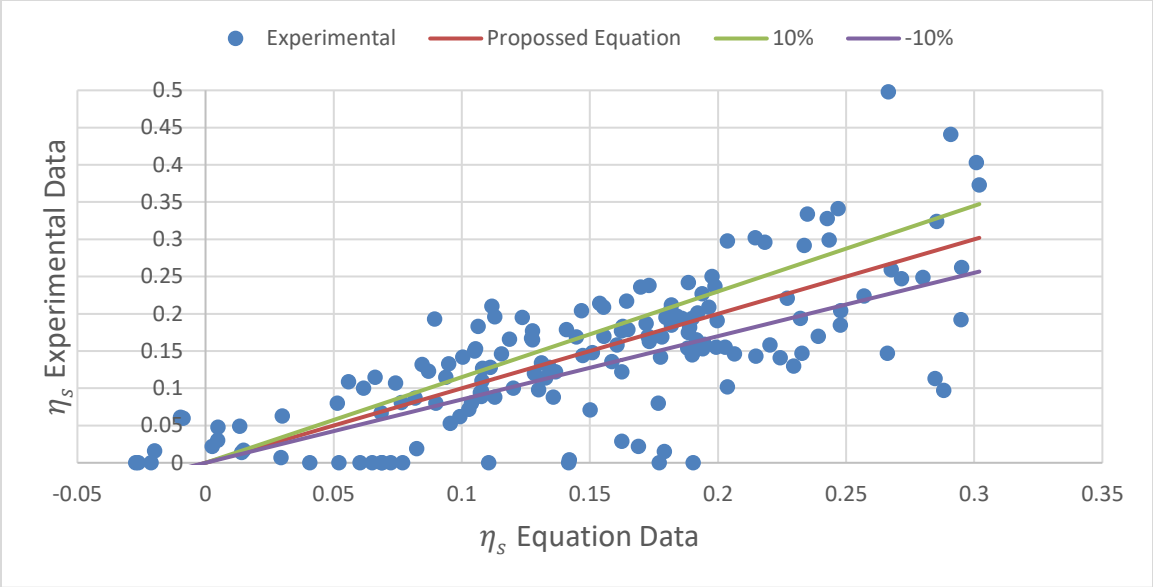

Figure 4-16. The modified model of coefficient of sliding friction

4.7 Applying the Proposed Equation in the Two-Layer Model:

The developed equations of the coefficient of sliding friction η_s were used to predict the pressure drop for the flow of multi-sized particulate slurry through horizontal pipelines based on the two-layer model. In the new model, instead of fixing the value of sliding friction, the proposed equations of the prediction of sliding friction, as presented in equations (4-19) and then the value of η_s are applied in equation (2-23). C_{lim} was defined by applying the proposed equations (4-2) and (4-3) instead of the equation (2-12). In addition, C_{max} was defined by applying the proposed equations (4-11) and (4-12). The momentum for the upper layer, lower layer and entire pipe is expressed in the equations (2.17), (2.18) and (2.19) respectively. The other steps of the determination of pressure drop using the two-layer model were explained in Chapter 2.

The results show better predictions of pressure drop in comparison to using fixed values of η_s, as shown previously in figures 4.3 and 4.4. As shown in figure 4.17,

most experimental data for pressure drop fit are near to the modified model curve by less than +/- 10%. The results are clear proof that the proposed equations are effective in the development of the two-layer model.

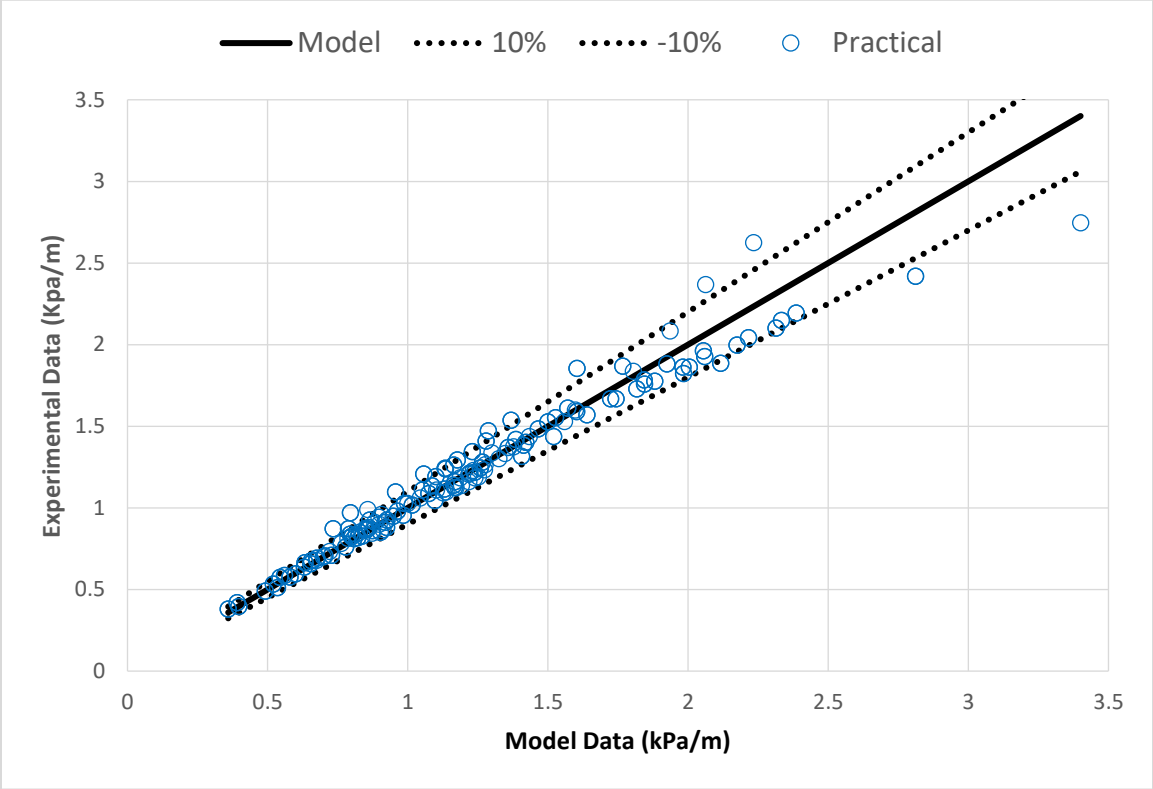

Range of Data Included	
Mean particle diameter	2mm – 24mm
Solid concentration	5% - 25%
Operational velocity	1m/s – 6.5m/s
Density	2650 kg/m3

Figure 4-17. The predicted values of pressure drop using the modified model

4.8 Validation of the Proposed Model Using the Experimental Data

As discussed in the previous chapter, experiments were conducted to transport plastic beads in horizontal pipes using water as a carrier fluid. The used plastic beads have a density of 1329 kg/m3 and diameter of 4.5 mm. The experiments were done with different solid concentrations. Figures 4.18 and 4.19, show a comparison between the experimental data and different models of pressure drop. Figure 4.18 depicts the measured and predicted pressure drop for the flow of plastic beads with 7.5% solid concentration using water as the carrier fluid. As shown, the predicted data of the proposed model has a good fit with the measured data. In addition, the results show good improvements of the proposed model if compared with the Wasp model and the two-layer model.

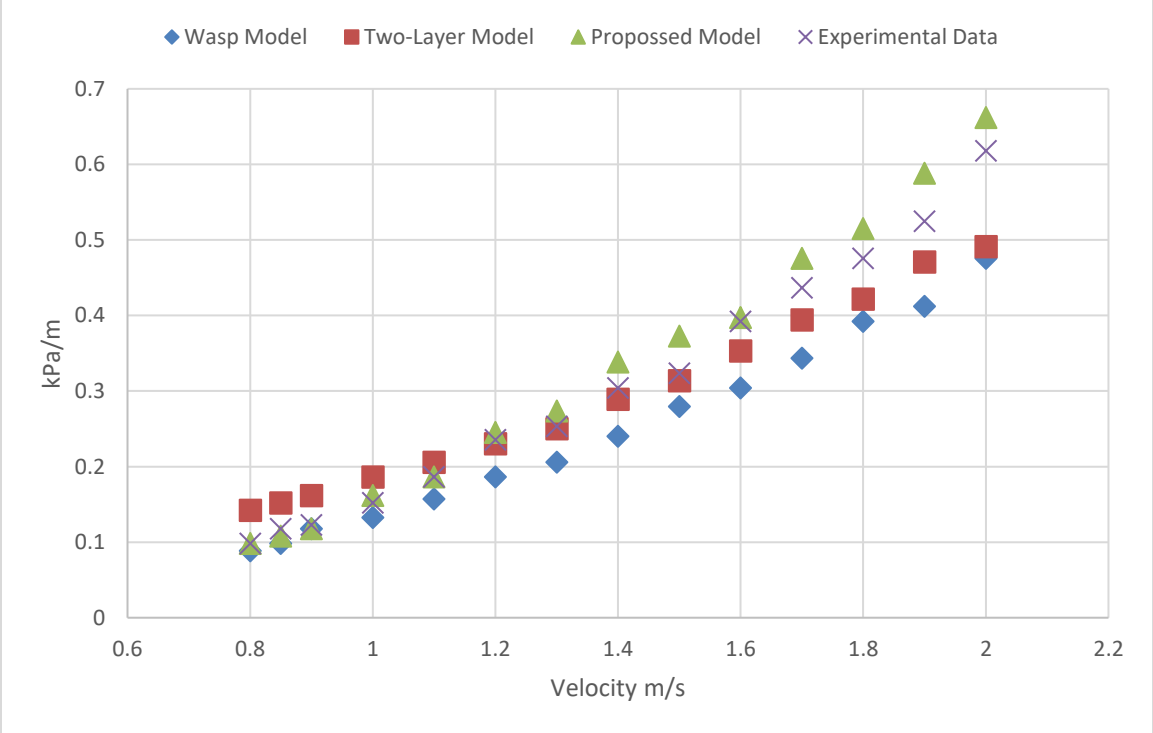

Figure 4-18. The measured and predicted pressure drop for the flow of plastic beads with 7.5% solid concentration.

Figure 4.19 shows the comparison between the measured data of pressure drop and predicted data using different models in low velocities. The two-layer model overestimates the value of head losses in low velocities. In addition, the Wasp model underestimates the pressure drop in most of the tested data.

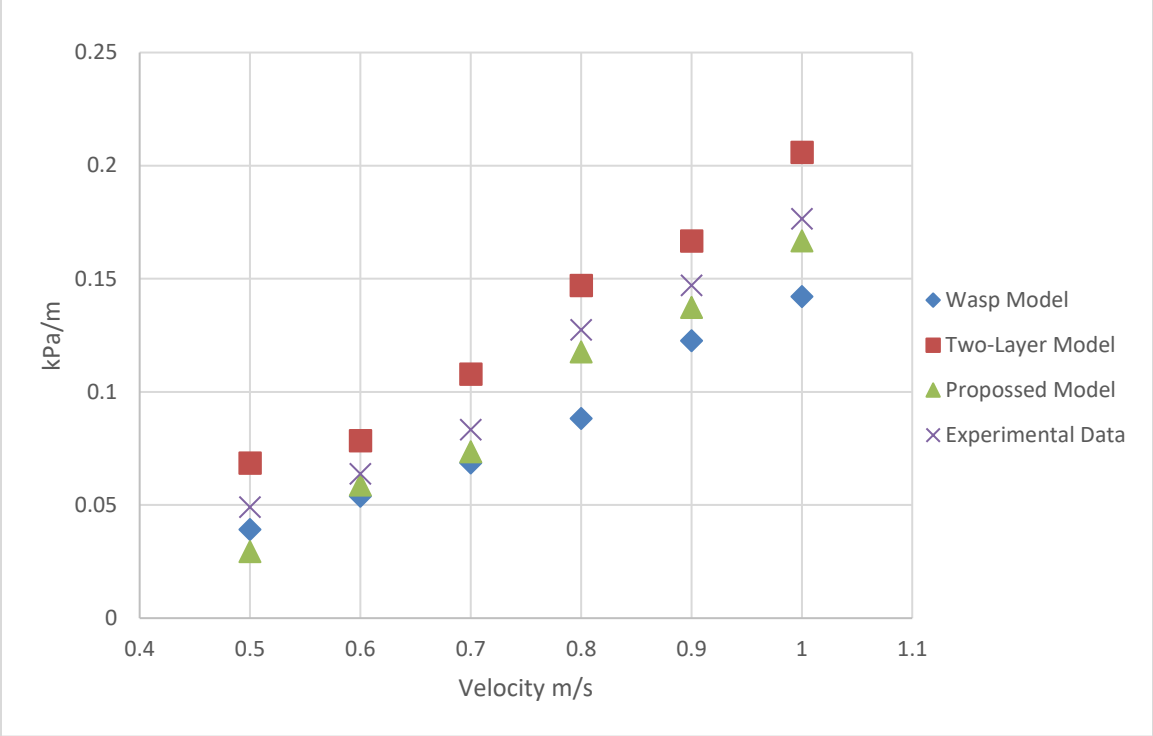

Figure 4-19. The measured and predicted pressure drop for the flow of plastic beads with 10% solid concentration.

4.9 Summary of the Chapter

This chapter focused on the behaviour of the coefficient of sliding friction between solid particles and the pipe wall in a slurry flow pipeline. The study was based on the two-layer model for the prediction of flow properties in horizontal pipelines. An empirical equation was derived for predicting the coefficient of sliding friction in a

coarse slurry pipeline based on the different experimental data. The new equation was applied to the SRC Two-Layer Model. The results show better predictions of pressure drops in comparison to the experimental data.

Figure 4.13 clearly demonstrates that the maximum value the coefficient of friction might reach is 0.5 when the value of v_1/v_2 is around 1.8 to 2. Figure 4.14 and the proposed equations can be used for pre-estimation of the value of the coefficient of sliding friction in the range of d50=2mm to 24mm and C_V=5% to 25%.

The chart can be easily used by students and researchers prior to any experimental investigations, however, further research is required to extend the validity of this chart to wider ranges of d50 and CV.

The proposed model was validated using the experimental data as explained in the previous chapter. The results show that the proposed model has a good fit with the experimental data. The results clearly demonstrate the improvements that are offered by the proposed model with respect to the Wasp model and the two-layer model.

CHAPTER 5 Multi-Layer Model

In the previous chapter, the two-layer model was modified to predict the pressure drop in a horizontal slurry pipeline. The coefficient of friction between solid particles and pipe walls was considered as a variable that changes according to the flow properties. According to the experimental results, the values of velocity and pressure drop are varying continuously across the cross-section of the pipe which is against the concept of two-layer model. In order to have accurate prediction results at any point across the cross-section of pipeline, a multi-layer model has been proposed in the current study. The model was applied to determine the concentration distribution, velocity profile and pressure drop in horizontal pipelines transporting slurries. Furthermore, the equations presented in the previous chapter are used in the model.

5.1 Introduction

In two-layer model, a horizontal hypothetical interface, has been assumed to couple the upper and lower layer. Then each layer is considered to have constant velocity and solid concentration. The logic behind proposing a multi-layer model is to decrease the assumptions and to develop more accurate and realistic model to study the flow properties in horizontal slurry pipelines. This can be achieved by dividing the pipeline into more horizontal layers and considering each layer as a separate region with a different velocity, solid concentration and that contributes to overall local pressure drop.

The first step of the modelling is dividing the cross-section of the pipe into n equal layers by width as shown in figure 5.1. This division will be made in order to study the behaviour of slurry in each layer from top to bottom of the horizontal pipe. As discussed in the literature, the solid concentration varies along the depth; hence designing a prediction model based on the horizontal layers is necessary.

$$A = {}^{\pi}/_{4}\ D^2 = \sum_{i=1}^{n} A_1 + A_2 + A_3 + \cdots + A_n \quad (5.1)$$

The vertical distance of each layer from the bottom of the pipe can be determined as below:

$$(Y_c)_i = \frac{i}{n} D\ , i = 1,2, \ldots\ n \quad (5.2)$$

The chord length of each layer can be calculated as below:

$$X_i = \sqrt{r^2 - (|(r - (Y_c(i)|))^2} \quad (5.3)$$

β_i is layer angle as shown in figure 5.1 and can be calculated as follows:

$$\beta_i = \sin^{-1}\left({}^{X}/_{r}\right) \quad (5.4)$$

AA_i is the cross-section area from the layer to the bottom of the pipe and can be defined as below:

$$AA_i = {D^2}/{4}\,(\beta_i - sin\beta_i\, cos\beta_i) \qquad when\ y_c \le r \tag{5.5}$$

$$AA_i = \frac{D^2}{4}\left(\beta_i - sin(180 - \beta_i)\cos(180 - \beta_i)\right) \qquad when\ y_c \ge r \tag{5.6}$$

Then the area of each layer can be calculated as below:

$$A_i = AA_i - AA_{i-1}, \qquad i = 2,3, \dots n \tag{5.7}$$

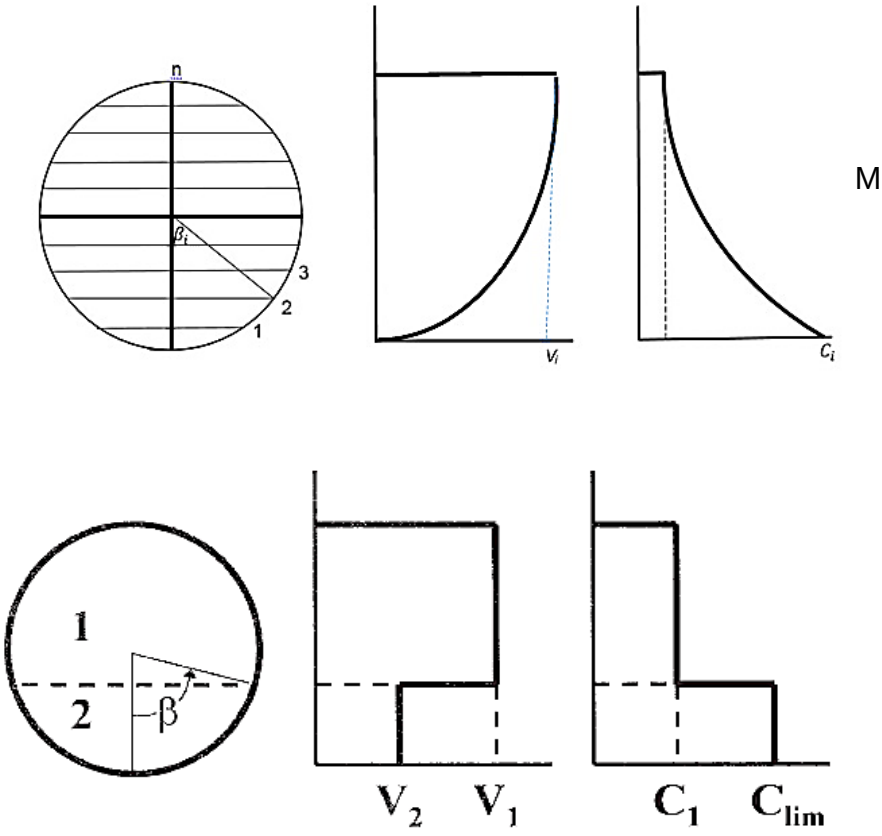

Multi-Layer Model

Multi-Layer Model

Figure 5-1. Idealised velocity and concentration profile used in Multi-Layer Model and Two-Layer models

5.2 Prediction of Concentration Distribution

The concentration distribution of solid particles in slurries varies along the depth of the pipes. In addition, the size ratio of the largest to smallest solid particles in most commercial slurries could be as high as 1000. However, a number of parameters will influence the solid distribution across the pipe cross-section such as flow velocity, particle size, pipe diameter, particle density and solid concentration etc.

In order to optimize the operating conditions for slurry flow and to calculate the energy requirement, the distribution of solid particles across the pipeline must be adequately predicted [1, 97]. There are strong interaction effects of many variables that make the theoretical prediction of concentration distribution almost impossible [4]. Many semi-empirical correlations have been proposed in this regard, as explained in Chapter 2.

The diffusion equations, proposed by Hunt [98], describes vertical diffusion of particles when the diffusivity of solids is uniform and equal to liquid diffusivity.

$$\epsilon_s \left.\partial C_j \right/ \partial_Y + C_j\left(W_j - V_Y\right) = 0, \qquad j = 1,2,\dots,n \tag{5.8}$$

Where,

$$V_Y = \sum_1^n W_i C_i \tag{5.9}$$

For horizontal flow, the following general solution is proposed by Karabelas [60]

$$C_j(Y) = \left.G_j \exp\left(-w_j\, f(Y)\right)\right/ 1 + \sum_1^m G_i \exp\left((-w_i\, f(Y)\right), \qquad j = 1,2,\dots,m \tag{5.10}$$

Where

$$f(Y) = \left.\int_0^Y d_Y \right/ \varepsilon_S(Y) \tag{5.11}$$

G_j is a set of characteristic coefficients of each size fraction but independent of space coordinates, ε_S is the particle diffusivity and w_j is the settling velocity of jth size fraction.

The following equation has been proposed to calculate ε_S [27, 46, 99-101]

$$\varepsilon_S(Y) = \beta\varepsilon_l\,(Y) \tag{5.12}$$

Where,ε_l is liquid diffusivity and can be calculated as suggested by Longwell [102]:

$$\varepsilon_l = 0.369R\,u* \frac{y}{R}\left(1-\frac{y}{R}\right) \qquad for\ 0 \le {}^{y}/_{D} \le 0.337 \tag{5.13a}$$

$$\varepsilon_l = 0.0775R\,u* \qquad for\ 0.337 \le {}^{y}/_{D} \le 0.663 \tag{5.13b}$$

$$\varepsilon_l = 0.369R\,u* \left({}^{y}/_{R}-1\right)\left(2-{}^{y}/_{R}\right) \quad for\ 0.663 \le {}^{y}/_{D} \le 1.0 \tag{5.13c}$$

and β can be calculated as suggested by Kaushal et al [100] as below:

$$\beta = 1 + 0.12504\,e^{4.22054\,{}^{C_{vf}}/_{C_{vss}}} \tag{5.14}$$

$$V_j(Y) = {}^{C_j\,(Y)}\Big/\left(1-\sum_i C_j\,(Y)\right) \tag{5.15}$$

$$\overline{V_j} = \frac{C_{vjf}}{1-C_{vf}} \tag{5.16}$$

The shear velocity $u*$ is obtained as below:

$$u* = \sqrt{{}^{i\,G\,D}/_{4}} \tag{5.17}$$

Where bar denotes the quantities averaged over the pipe cross-section and C_{vjf} is the mean concentration of each particle size. The relative concentration $V_j(Y)$ from equation (5.8) can be expressed as follows:

$$V_j(Y) = G_j \exp\left[-w_j\,f(Y)\right] \tag{5.18}$$

The coefficients G_j are calculated by using equations 5.15, 5.16 and 5.8. In addition, it is assumed that the flow is steady and there is no particle deposition at the bottom of the pipe. Thus, C_{vjf} in the pipe cross-section is constant and already known and the mean relative concentration is constant too.

$$V_j = \frac{1}{A}\int_A V_j(Y)dA = G_j \, {}^{1}\!/_{A} \int_A \exp(-w_j f(Y))dA \tag{5.19}$$

Hence,

$$G_j = {}^{V_j}\!/_{\frac{1}{A}\int_A \exp(-w_j f(Y))dA}, j = 1,2,\dots m \tag{5.20}$$

Where w_j is the actual settling velocity of the j[th] size fraction and can be calculated by using the formula proposed by Richardson and Zaki [103] as below:

$$w_j = v_\infty (1 - C_{vf})^z \tag{5.21}$$

Where:

$$Z = 4.65 + 1.95\left({}^{d_j}\!/_{D}\right) \quad 0.002 < Re_p \leq 0.2 \tag{5.22a}$$

$$Z = \left[4.35 + 17.5\left({}^{d_j}\!/_{D}\right)\right] Re_p{}^{-0.03} \quad 0.2 < Re_p \leq 1.0 \tag{5.22b}$$

$$Z = \left[4.45 + 18\left({}^{d_j}\!/_{D}\right)\right] Re_p{}^{-0.1} \quad 1.0 < Re_p \tag{5.22c}$$

Where Re_p is particle Reynolds number, D is the diameter of the pipe, C_{vf} is volume efflux concentration and d_j is the mean diameter of the J[th] size fraction.

5.2.1 Results of Concentration Distribution Model

The Multi-layer model is proposed in this work to predict the concentration distribution across the pipe cross-section. The model was applied using the MATLAB program. The model was designed as per the following steps:

1. Input a value of pipe diameter D.
2. Input the value of solid throughput (target).
3. Input the size fractions and percentage finer of the solid particles.
4. Calculate Mixture flow rate Q_m using solid throughput and solid concentration.
5. Calculate pressure drop based on the modified two-layer model.
6. Calculate shear velocity using the result of pressure drop from equation (5.17).
7. Calculate liquid diffusivity (equation 5.13).
8. Calculate solid diffusivity (equation 5.12).
9. Calculate actual settling velocity of the j^{th} size fraction.
10. Calculate the relative concentration $V_j(Y)$ (equation 5.18).
11. Apply equation (5-17).

The proposed model was applied for the flow of multisized slurries with 0.22 solid concentration and the following particle diameter (d_p) and percentage finer (S_p):

Pd (mm)	6730	4760	3360	3380	1680	1190	595	210	74
S_p	1	0.942	0.795	0.414	0.085	0.033	0.025	0.017	0.012

The pipe diameter is 0.2631m with an operating velocity of 4.52 m/s. Using 999 kg/m^3 and 2650 kg/m^3 as the densities of water and solids respectively. Figure 5.2 depicts the comparison between the model results and the experimental data using the Karabelas model and the proposed model. In the proposed model, the modified two-layer model was used for the prediction of pressure drop. As shown, the proposed model provides a good match with the experimental data.

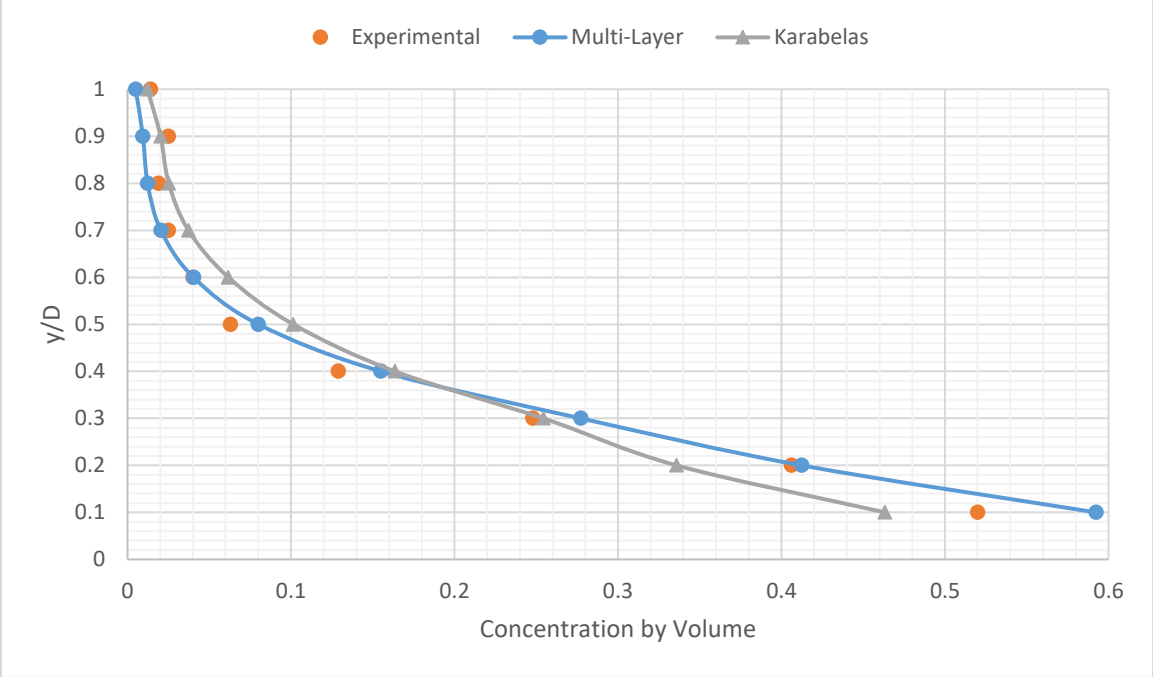

Figure 5-2. comparison between measured and predicted overall concentration profile (Karabelas model and proposed model), V=4.52 m/s.

The model was applied again on the previous example with the median velocity (3.25 m/s) as shown in figure 5.3. The predicted results have good agreement with the measured data.

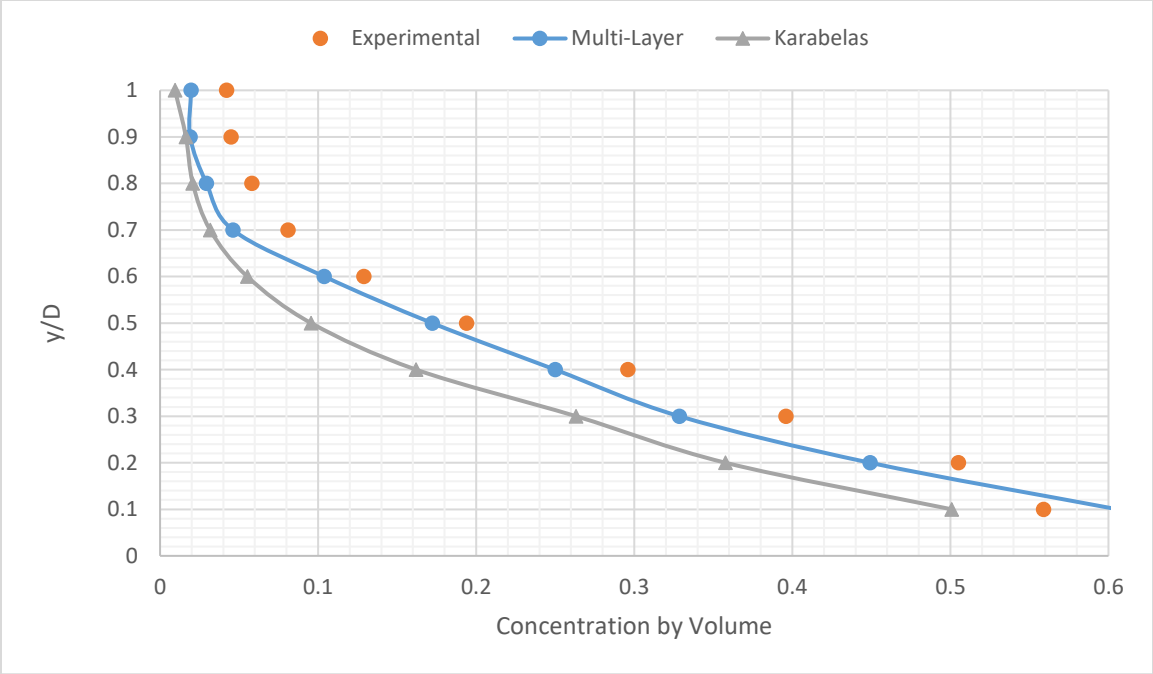

Figure 5-3. comparison between measured and predicted overall concentration profile (Karabelas model and proposed model), V=4.08 m/s.

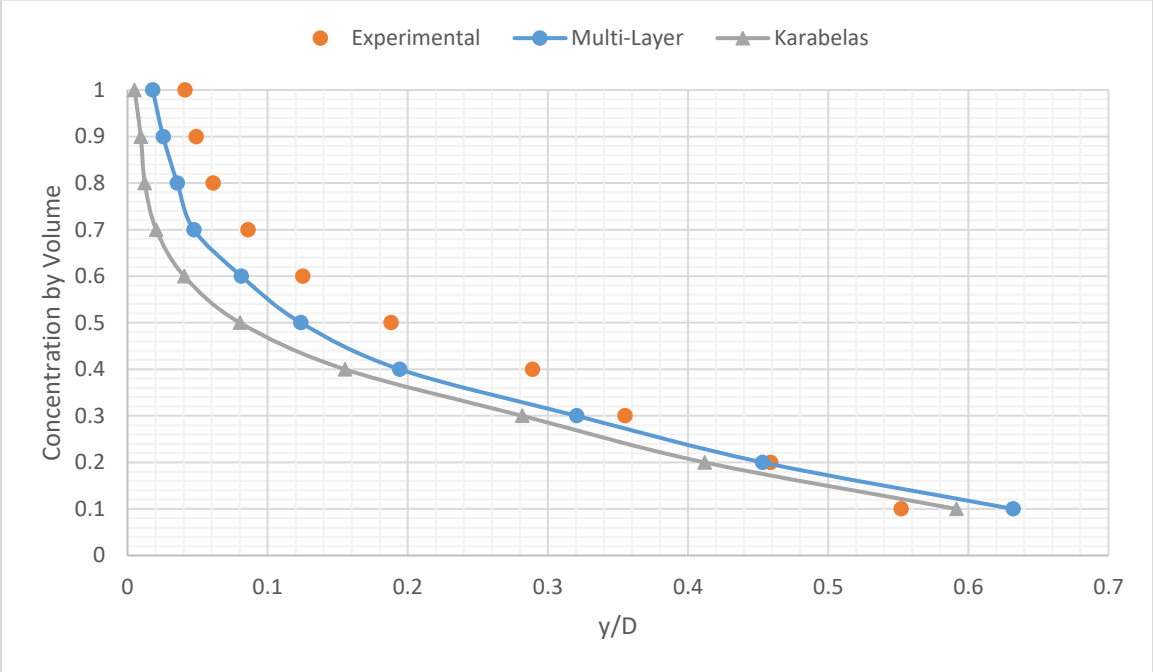

Figure 5-4. comparison between measured and predicted overall concentration profile (Karabelas model and proposed model), V=3.25 m/s

Figure 5.4 depicts the overall comparison between both the Karabelas model and the proposed model with respect to the measured data by Gillies 1993 [6]. As shown, the results of Multi-layer model show a better fit between the measured and predicted data compared to Karabelas model.

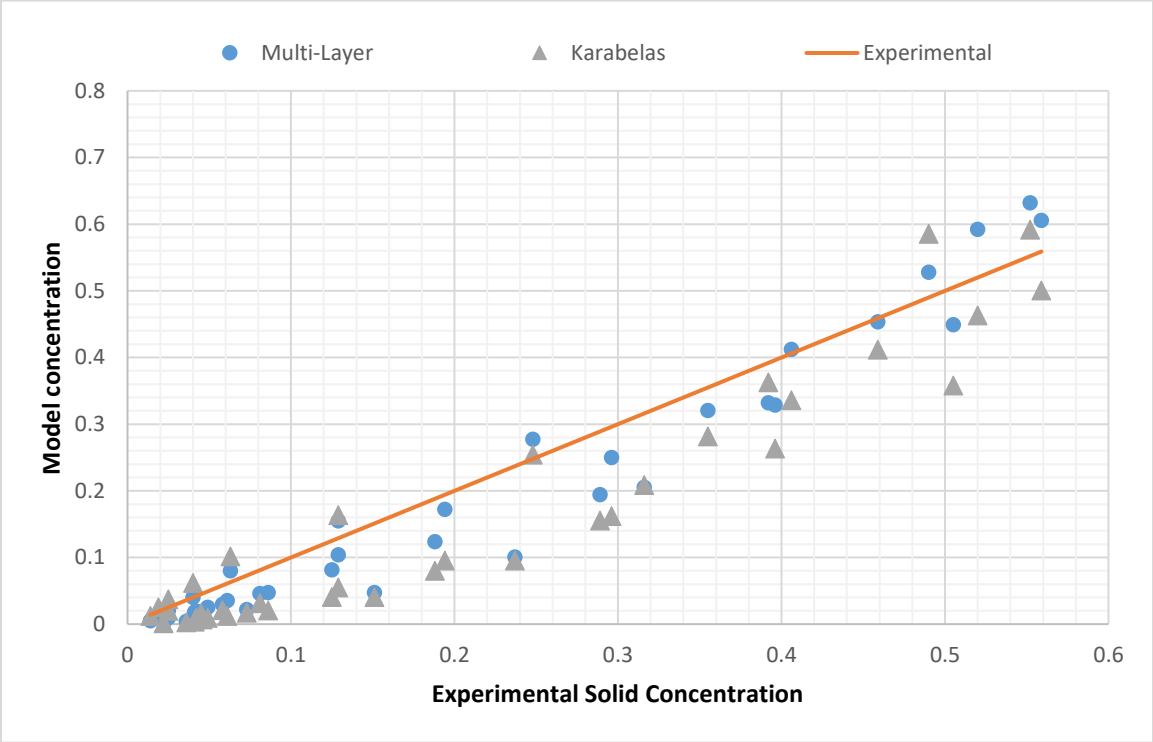

Figure 5-5. comparison between measured and predicted overall concentration profile (Karabelas model and proposed model)

5.3 Prediction of Velocity Profile

The velocity field at a cross-section of the slurry pipeline is an important parameter for its design. A complete knowledge about the velocity field is essential for understanding the complex interrelation between various parameters. The proposed model is based on the computational procedure originally proposed by

Roco and Shook [104] for the prediction of velocity profile across a pipe cross-section. Some modifications are incorporated in order for it to be applied for the prediction of the flow parameters in multi-sized particulate solid-liquid mixtures and to improve the model accuracy.

The Cauchy momentum equation for both liquid and solid phases can be written as:

$$(1-C)\rho_l \, {dV_{Li}}/{dt} = (1-C)\rho_l f_i - (1-C) \, {\partial p}/{\partial x_i} + \sum_{i=1}^{n} {\partial \tau_{Lij}}/{\partial x_j} + (R_{Li})_S \quad (5.23)$$

$$C\rho_s \, {dV_{Si}}/{dt} = C\rho_S f_i - C \, {\partial p}/{\partial x_i} + \sum_{i=1}^{n} {\partial \tau_{Sij}}/{\partial x_j} + (R_{si})_L \quad (5.24)$$

Where τ_{Lij} and τ_{sij} are shear stresses due to liquid phase and solid phase separately. f_i is the specific body force, and both terms $(R_{Li})_s$ and $(R_{si})_l$ are the interaction forces per unit volume of the slurry which are equal in magnitude and opposite in sense. In the particular case of microscopically steady $\left({\partial}/{\partial t} = 0\right)$, uniform $\left({\partial}/{\partial x_3} = 0\right)$ and unidirectional flow in a pipe $(V_1 = V_2 = 0,\ V_3 = V = 0)$, equations (5.23) and (5.24) can be rewritten as below:

$$0 = (1-C)\rho_l f_z - (1-C) \, {\partial p}/{\partial z} + {\partial \tau_{Lzx}}/{\partial x} + {\partial \tau_{Lzy}}/{\partial y} + (R_{Lz})_s \quad (5.25)$$

$$0 = C\rho_s f_z - C \, {\partial p}/{\partial z} + {\partial \tau_{Szx}}/{\partial x} + {\partial \tau_{Szy}}/{\partial y} + (R_{Sz})_s \quad (5.26)$$

The shear stress has two components, one due to a change in viscosity between the adjacent layers and the other due to the mass turbulent exchange between these layers.

$$\tau = \tau_{friction} + \tau_{turbulent} \quad (5.27)$$

The frictional shear stress in the liquid phase can be determined by using Newton's law of viscosity applied to the volume occupied by liquid and turbulent shear stress as derivative of kinetic energy as below:

$$\tau_{Lzx} = \tau_{friction\ L(S)} + {}^{\partial}/_{\partial x}\left[\alpha_{Lzx}(1-C)\rho_l {V_l}^2\right] \quad (5.28)$$

$$\tau_{Szx} = \tau_{friction\ S(L)} + {}^{\partial}/_{\partial x}\left[\alpha_{Szx} C \rho_s {V_s}^2\right] \quad (5.29)$$

Where α_{Lzx} and α_{Szx} are coefficients of turbulence and $\tau_{friction\ L(S)}$ is the shear stress due to the friction between fluid layers in the presence of solid particles.

$$\tau_{friction\ L(S)} = (1-C)\mu_{L(S)}\,{}^{\partial V_L}/_{\partial x} \quad (5.30)$$

$\tau_{friction\ S(L)}$ is considered to be a shear stress as a result of friction between solid particles due to relative motion in the liquid.

By summing both equations (5.25) and (5.26) and considering $(R_{Lz})_s = -(R_{Sz})_L$, the following equation can be created:

$$0 = \rho_m f_z - {}^{\partial p}/_{\partial z} + {}^{\partial(\tau_{Lzx}+\tau_{Szx})}/_{\partial x} + {}^{\partial\left(\tau_{Lzy}+\tau_{Szy}\right)}\Big/_{\partial y} \quad (5.31)$$

Assuming $\alpha_{zx} = \alpha_{zy} = \alpha$, and using equations (5.28), (5.29) and (5.31), the momentum equation in the axial direction becomes:

$$0 = \rho_m f_z - {}^{\partial p}/_{\partial z} + {}^{\partial}/_{\partial x}\left[\mu_m\,{}^{\partial V_m}/_{\partial x} + {}^{\partial\left(\alpha_m \rho_m {V_m}^2\right)}\Big/_{\partial x}\right] + {}^{\partial}/_{\partial y}\left[\mu_m\,{}^{\partial V_m}/_{\partial y} + {}^{\partial\left(\alpha_m \rho_m {V_m}^2\right)}\Big/_{\partial y}\right] \quad (5.32)$$

Where,

$$V_m = {}^{V_L}/_{\beta_L} = {}^{V_S}/_{\beta_S};\ \beta_L > 1,\ \beta_S < 1 \quad (5.33)$$

$$\rho_m = (1-C)\rho_l + C\rho_S \quad (5.34)$$

$$\mu_m = \left(\tau_{friction\ L(S)} + \tau_{friction\ S(L)}\right)\partial m \Big/ \partial V_m \tag{5.35}$$

$m = x$ and is estimated from the expression proposed by Vocaldo and Charles [105],

$$\mu_m = \mu_l \left[exp\left(2.5C - n(c/C_{max})\right) \Big/ \left(1 - (c/C_{max})\right)^n \right] \tag{5.36}$$

n is the experimental coefficient (n=2 for sand) and C_{max} is the maximum packing concentration. In the present study, the two proposed equations of (4.11) and (4.12) are utilised to calculate C_{max} for uni-sized and multi-sized slurries respectively.

For solids of relatively smaller dimensions, the ratio $V_S/V_L = \beta_S/\beta_L \approx 1$. Now the momentum equation can be rearranged as below:

$$d/dz\,(p + \rho_m g h) = \left(\partial^2/\partial x^2 + \partial^2/\partial y^2\right)\left[\left(\pi_m V_m + \rho_m \alpha_m {V_m}^2\right) - (V_m \nabla^2 \mu_m + \nabla \mu_m\, \nabla V_m)\right] \tag{5.37}$$

Where h is measured in downward vertical direction.

The last two terms of equation (5.28) expressing a second order effect of viscosity. By neglecting these two terms in the turbulent flow, the results of cylindrical pipe with any inclination can be expressed as:

$$\nabla^2 \xi = d(p + \rho_m g h)/dz \tag{5.38}$$

Where

$$\xi = \pi_m V_m + \rho_m \alpha_m {V_m}^2 \tag{5.39}$$

Equations (5.38) and (5.39) can be rewritten for a horizontal circular pipeline as below:

$$\xi(r) = \frac{1}{4}\left(-{}^{dp}/_{dz}\right)\left({}^{D^2}/_{4} - r^2\right) \tag{5.40}$$

and

$$V_m(r) = -{}^{\mu_m}/_{2\alpha_{md}} + \sqrt{{}^{{\mu_m}^2}/_{4{\alpha_{md}}^2} + {}^{\xi(r)}/_{\alpha_{md}}} \tag{5.41}$$

Where $\alpha_{md} = \rho_m \alpha_m$ is the dynamic coefficient of turbulence for the solid-liquid mixture. α_{md} can be expressed for slurry as below:

$$\alpha_{md} = \left[(1-C)\rho_l \alpha_{L(S)} {\beta_L}^2 + C\rho_S \alpha_S {\beta_S}^2\right] \tag{5.42}$$

Where β_L and β_S are the ratio of liquid velocity and solid velocity to slurry mixture velocity respectively.

The coefficient of turbulence in the case of water flow and slurry flow can be expressed as:

$$\delta\alpha_{md} = \left[(1-C)\rho_l \phi_{L(S)} {\beta_L}^2 + C\rho_S \phi_S {\beta_S}^2\right]\delta\alpha_0 \tag{5.43}$$

Where $\phi_{L(S)}$ is the ratio between kinematic coefficients for liquid phase in the presence of solid particles, and in the absence of solid particles, and ϕ_S is the ratio between the kinematic coefficient for solid phase and that for clear water. According to Peckenkin [106], $\phi_{L(S)}$ can be related as:

$$\phi_{L(S)} = {}^{\delta\,\alpha_{L(S)}}\Big/_{\delta\,\alpha_0} = 1 - {}^{C}/_{C_{max}} \tag{5.44}$$

Equation (5.44) was modified by Mishra [4] based on his experimental data as below:

$$\phi_{L(S)} = {}^{\delta\,\alpha_{L(S)}}\Big/_{\delta\,\alpha_0} = 1 - \left({}^{C}/_{C_{max}}\right)^b \tag{5.45}$$

Where $\alpha_{L(S)}$ and α_0 are kinematic coefficients of liquid phase in presence of solid phase and in absence of solid phase respectively. b is a coefficient which was

found to be independent of efflux concentration and flow velocity with a value of 0.5.

The expression of ϕ_S as proposed by Mishra [4] is:

$$\phi_S = {\delta\ \alpha_S}/{\delta\ \alpha_0} = exp\left({\left({1}/{Fr}\right)}\Big/{\left(1-\left({C}/{C_{max}}\right)^{a}\right)}\right) \tag{5.46}$$

Where

$$Fr = {U_*^{\,2}}\Big/{g\ d_{av}\ (S_S - 1)} \tag{5.47}$$

a is the experimental coefficient independent of efflux concentration and flow velocity and was found to be 0.7, d_{av} is the weighted mean diameter of the particles and U_* is the shear velocity.

In equation (5.43), $\phi_{L(S)}$ approaches zero when the value of C approaches C_{max} because when the solid concentration in solid-liquid flow reaches static settled concentration there is no diffusion between the layers. Furthermore, when C approaches zero, $\phi_{L(S)}$ becomes unity which is true for representing the flow of clear water. An evaluation has been made for both coefficients of a and b based on the comparison between calculated velocity distribution along different planes and measured flow rate.

The dynamic coefficient of turbulence for flow of clear water is given by the following semi-empirical equation [104]:

$$\alpha_0 = \frac{D}{4}\left(1 - {4\,r^2}/{D^2}\right)\left[8.5 - 5.75\ log\left(k + 3.3\,{\frac{v}{U_*}}\Big/{\left(\frac{D}{2} - r\right)}\right)\right]^{-2} \tag{5.48}$$

To calculate the dynamic coefficient for slurries α_{md}, the distance $\left(\frac{D}{2}-r\right)$ is replaced by Y_{eq}.

$$\frac{Y_{eq}}{dY}=\frac{1}{(1-C)\,\phi_{L(S)}\,\beta_L{}^2+C_S\,\phi_S\,\beta_S{}^2}=\frac{1}{\phi(C)} \tag{5.49}$$

The expression of Y_{eq} from at the n[th] increment of distance from the pipe wall is:

$$Y_{eq}=\sum_{i=1}^{n}{}^{\delta\,Y_i}/_{\phi(C_i)} \tag{5.50}$$

Where C_i is the solid concentration at the midpoint of distance increment δ_{Yi}. Experimentally, Y_{eq} is considered to be smaller than the summation value of equation (5.50) from the point under consideration vertically to the bottom of the pipe, and from the any considered point radially to the pipe wall.

In this proposed model, the value of the coefficient of sliding friction is considered as a variable, which is assumed to depend on particle diameter, solid concentration, operational velocity and settling velocity as explained in the previous chapter.

5.3.1 Results of the Proposed Velocity Profile Model

The proposed model is based on the proposed equations that were explained in the previous chapter, such as the equation of maximum settled concentration for uni sized and multi sized slurries. In addition, both proposed models of concentration distribution and pressure drop that were illustrated in the previous sections have been used. The model is designed as per the following steps:

1. Input a value of pipe diameter D.
2. Input the value of solid throughput (target).

3. Input the size fractions and percentage finer of the solid particles.
4. Calculate mixture flow rate Qm using solid throughput and solid concentration.
5. Calculate pressure drop based on modified two-layer model.
6. Calculate shear velocity using the result of pressure drop (equation 5.10).
7. Calculate liquid diffusivity, solid diffusivity and actual settling velocity of the jth size fraction (equations 5.13, 5.12 and 5.21).
8. Calculate the relative concentration $V_j(Y)$ and apply equation (5-8).
9. Apply equation (5.47) to calculate Fr.
10. Apply equations (4-11) and (4.12) to calculate C_{max}.
11. Apply equation (5.46) to calculate ϕ_S.
12. Apply equation (5.45) to calculate $\phi_{L(S)}$.
13. Apply the dynamic turbulent using equation (5.40), (5.41) and (5.42).
14. The coefficient of turbulence can be found by applying equation (5.35) and (5.36).
15. Apply equations (5.42) and (5.43).

For unisized particulate slurry flow, the predicted results of the proposed model have been compared with the experimental data and CFD results of Nabil et al [107]. As shown in figure 5.6, the predicted results for 0.2mm sand slurries with 10% concentration and 2 m/s velocity are compared with experimental data and

CFD results [107]. Both the results show an inaccurate fit with the experimental data in dilute slurries.

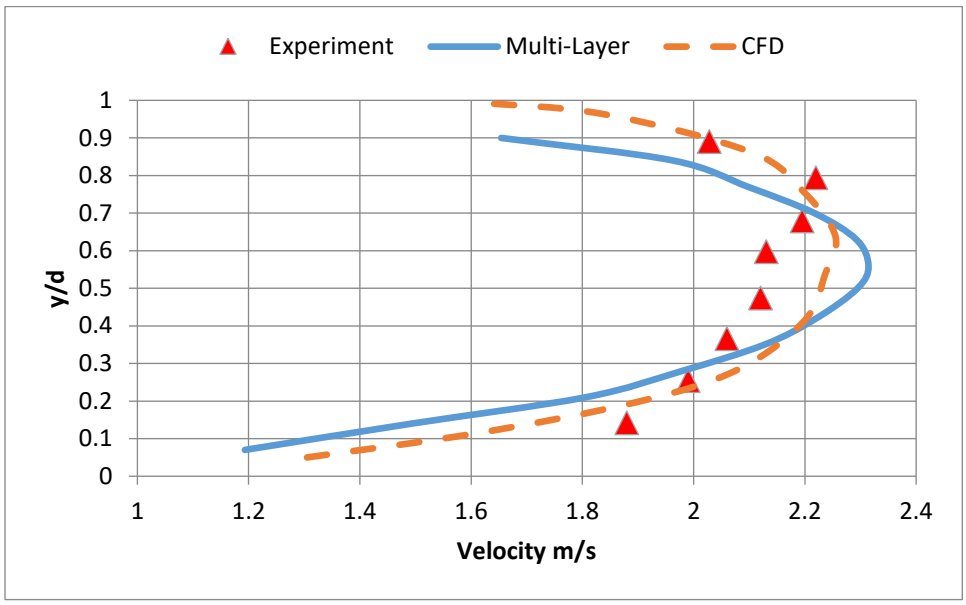

Figure 5-6. Velocity profile for flow of 0.2mm sand particle at 10% concentration and 2 m/s

Figure 5.7 depicts a comparison study between measured and predicted data for fine dense particle slurries with 30% concentration and 1.4mm particle diameter. As shown, the results of multi-layer model show a better fit between the measured and predicted data compared to figure 5.6.

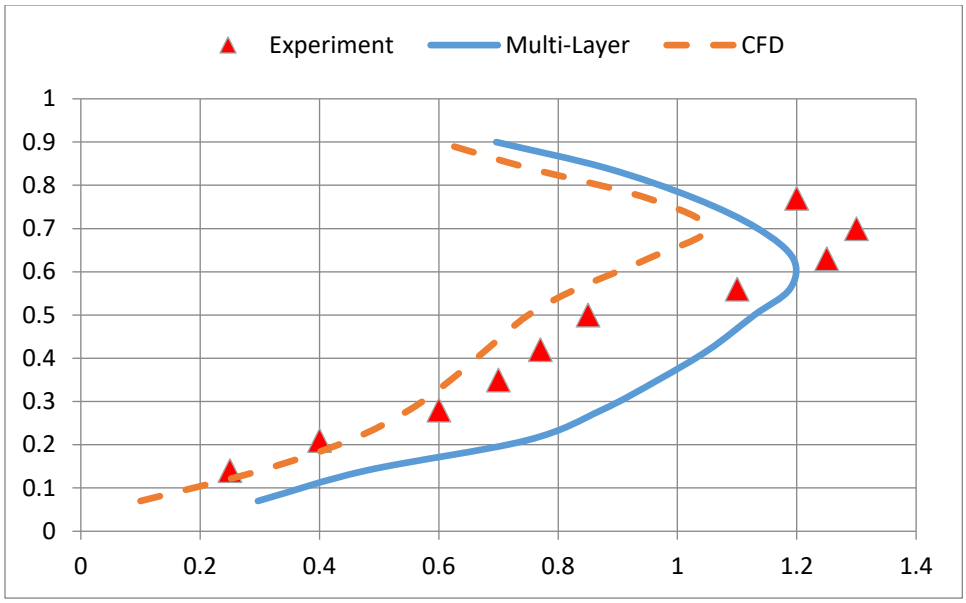

Figure 5-7. Velocity profile for flow of 1.4mm sand particle at 30% concentration and 1m/sec

Figure 5.7 shows a comparison between the measured and predicted velocity profile for 0.7mm particles slurries with 20% concentration and 1 m/s velocity. The results show a better fit between the measured and predicted data compared to Figures 5.6 and 5.7.

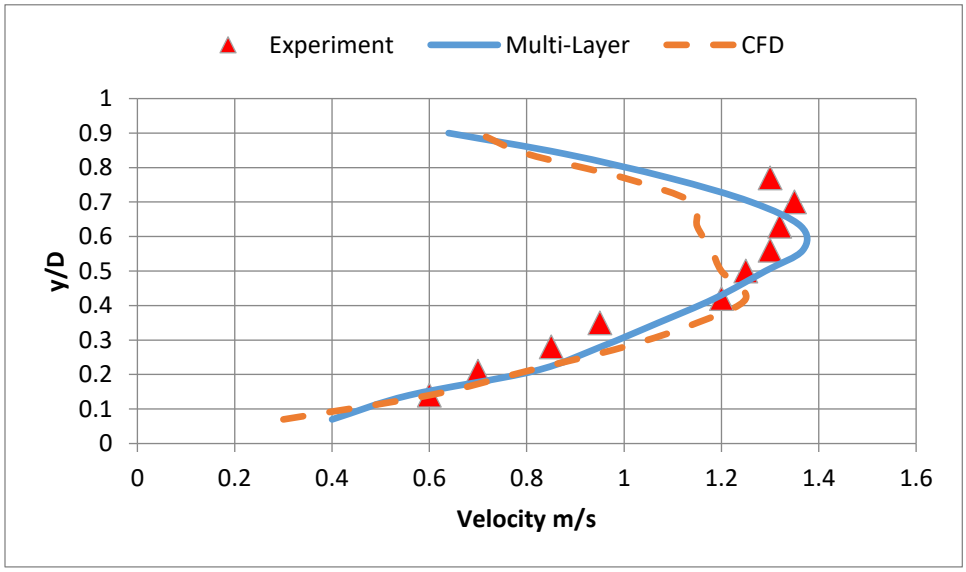

Figure 5-8. Velocity profile for flow of 0.7mm sand particle at 20% concentration and 1m/sec

For dense unisized particles slurries, slurry with 0.7mm sand particles and 20% and 30% concentration by volume have been studied. As shown in Figures 5.9 and 5.8, the mixture flows at 3 m/s and the concentrations are 20% and 30% respectively. The predicted results of the multi-layer model show a reasonable fit with the experimental data.

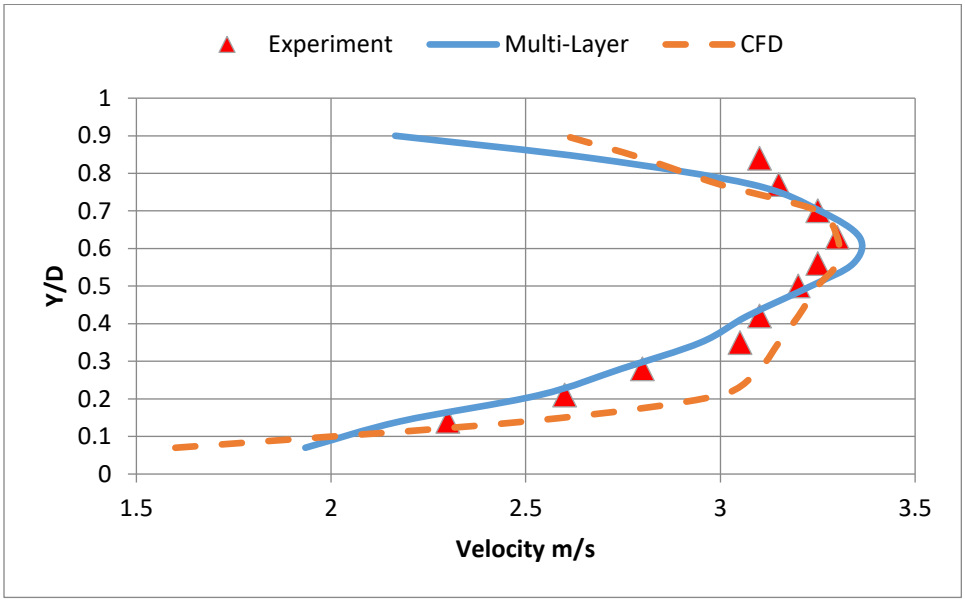

Figure 5-9. Velocity profile for flow of 0.7mm sand particle at 20% concentration and 3m/sec

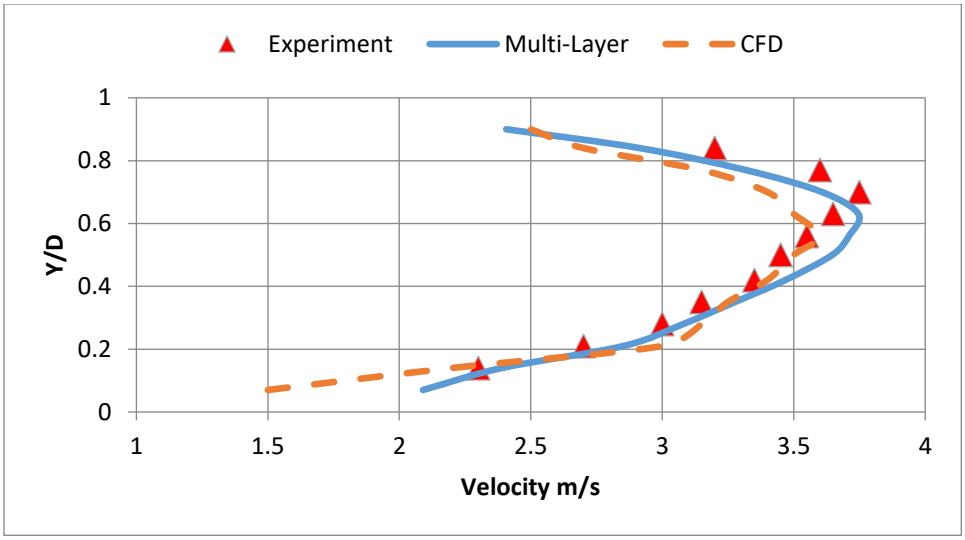

Figure 5-10. Velocity profile for flow of 0.7mm sand particle at 30% concentration and 3m/sec

Figure 5.10 depicts the comparison between the predicted results and experimental results for dense slurries at a high operating velocity. The slurry contains 30% concentration by volume of 0.7mm sand and flows with 5 m/s velocity. The predicted results using the multi-layer model show a reasonable fit with the experimental data.

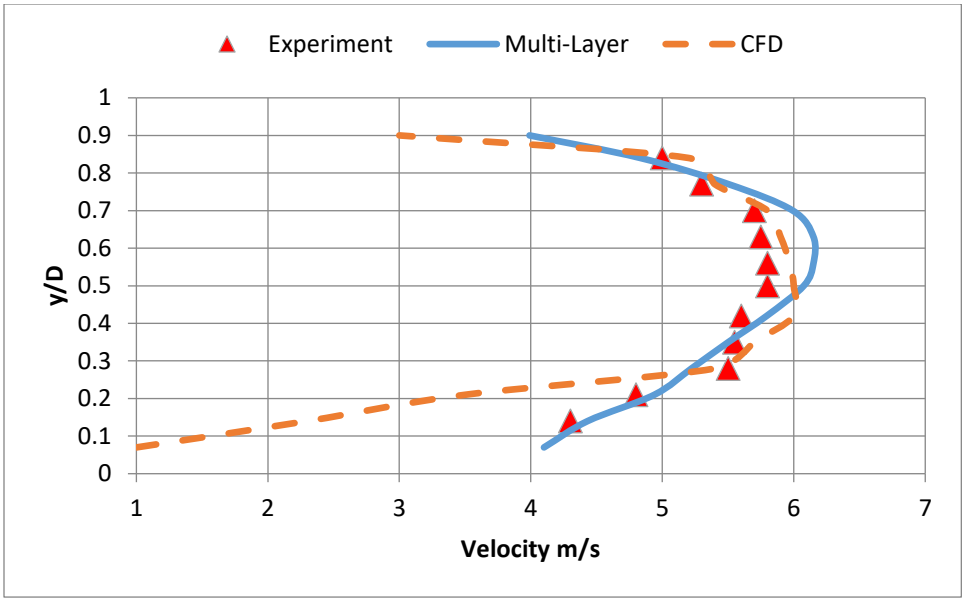

Figure 5-11. Velocity profile for flow of 0.7mm sand particle at 30% concentration and 5 m/s

For multi-sized particulate slurries, the experimental data of Gillies (1993) [9] has been used. Figures 5.11 and 5.12 show the velocity profile of 15% concentration multi-sized particulate slurries with operating velocity of 1.83 m/s and 3.05 m/s respectively through a 0.0532m diameter pipe. The results show a better fit at lower operating velocities.

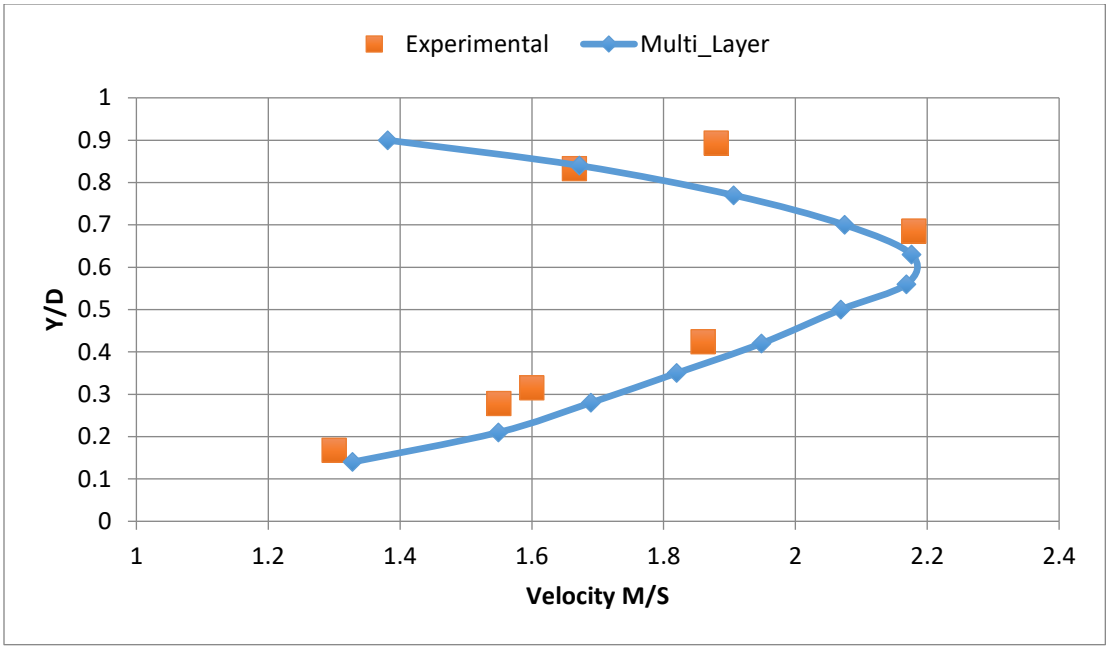

Pd (mm)	0.595	0.420	0.297	0.210	0.149	0.074
Sp	1	0.998	0.951	0.571	0.147	0.005

Figure 5-12 Velocity profile for flow of multi-sized sand particles in 0.0532m diameter pipe at 15% concentration and 1.83 m/sec

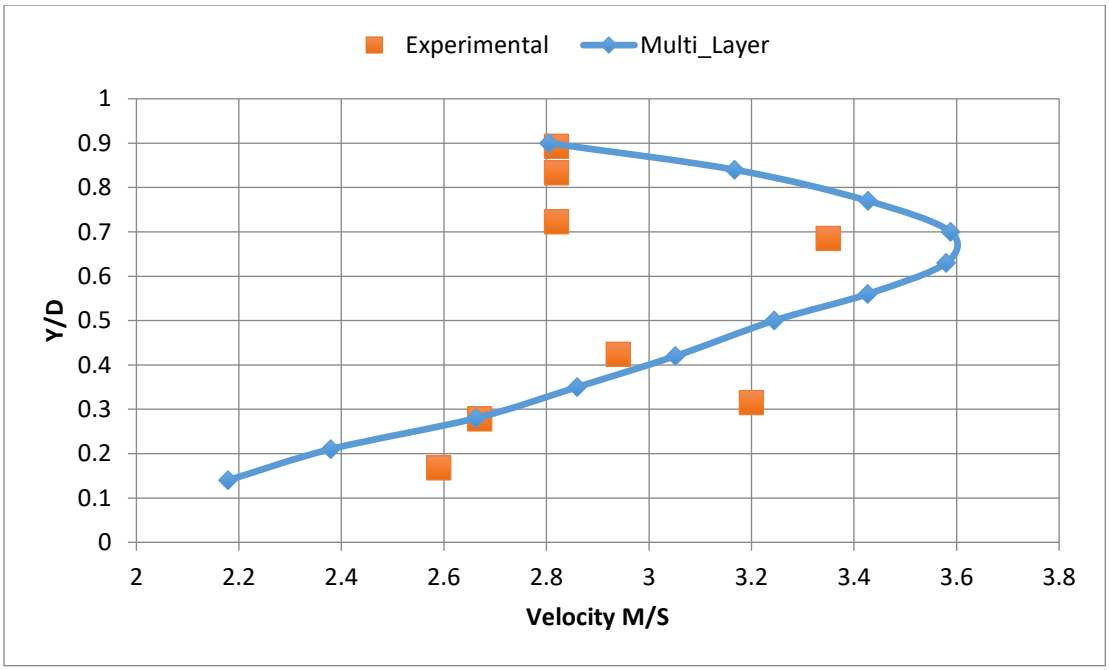

Pd (mm)	0.595	0.420	0.297	0.210	0.149	0.074
Sp	1	0.998	0.951	0.571	0.147	0.005

Figure 5-13. Velocity profile for flow of multi-sized sand particles in 0.0532m diameter pipe at 15% concentration and 3.05 m/sec

For studying other examples, coarser multi-sized particulate slurries were used containing 2.38mm diameter to 0.007mm diameter particles. As shown in figures 5.13 and 5.14, the model has a reasonable fit with the experimental data with operating velocities of 1.8 m/s and 3.05 m/s respectively.

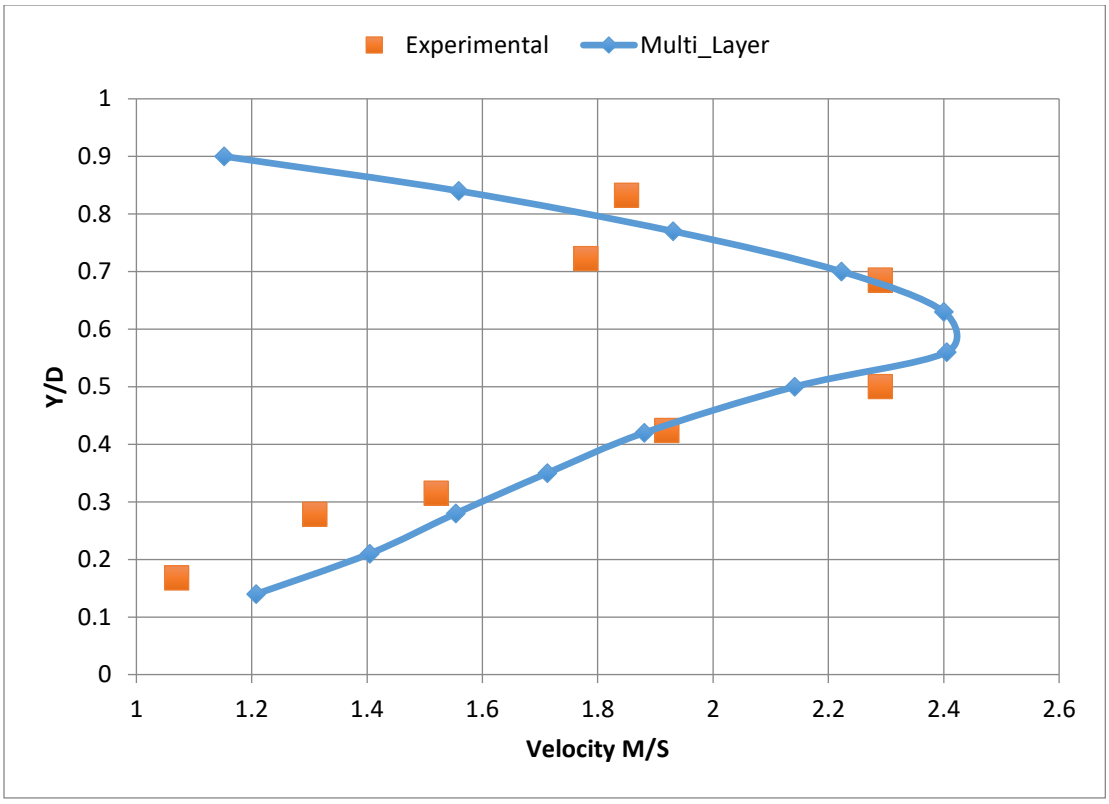

Pd (mm)	2.380	1.190	0.841	0.595	0.420	0.297	0.210	0.074
Sp	1	0.962	0.881	0.674	0.237	0.039	0.008	0.007

Figure 5-14. Velocity profile for flow of multi-sized sand particles in 0.0532m diameter pipe at 15% concentration and 1.8m/sec

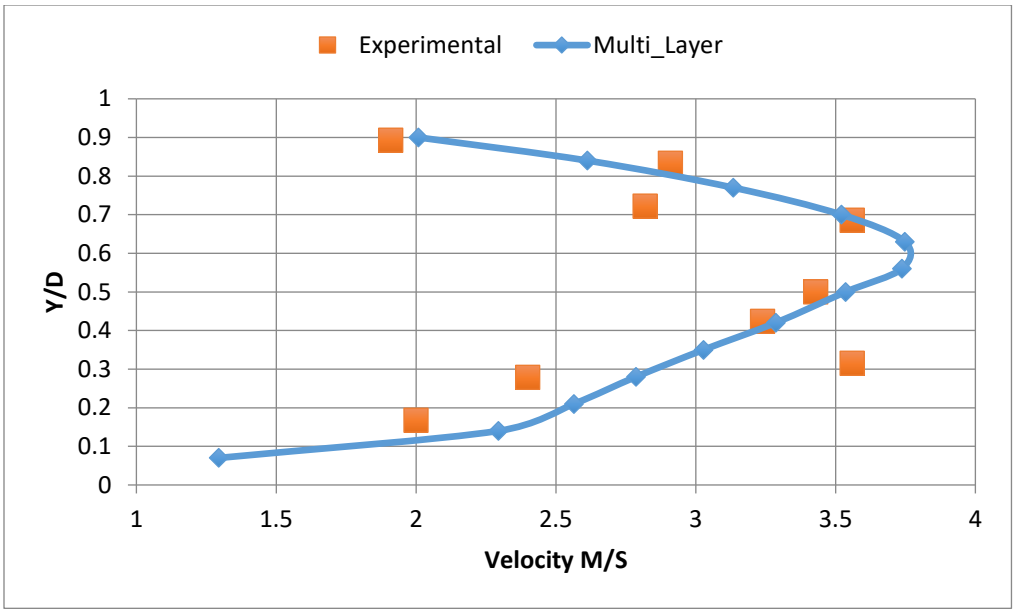

Pd (mm)	2.380	1.190	0.841	0.595	0.420	0.297	0.210	0.074
Sp	1	0.962	0.881	0.674	0.237	0.039	0.008	0.007

Figure 5-15. Velocity profile for flow of multi-sized sand particles in 0.0532m diameter pipe at 15% concentration and 3.05m/sec.

The same mixture was tested again with a bigger pipe diameter (0.2136m). Figures 5.15 and 5.16 show a comparison between the measured and predicted results of the velocity profile at high operation velocities of 4.21m/s and 4.65 m/s respectively. The results show an acceptable match between the measured and predicted data.

As shown in the figures, the model gives more accurate results in low velocities than high velocities. In addition, the particle size also has effective role in the results. In coarse particle slurries, the model result has a good fit with the experimental data.

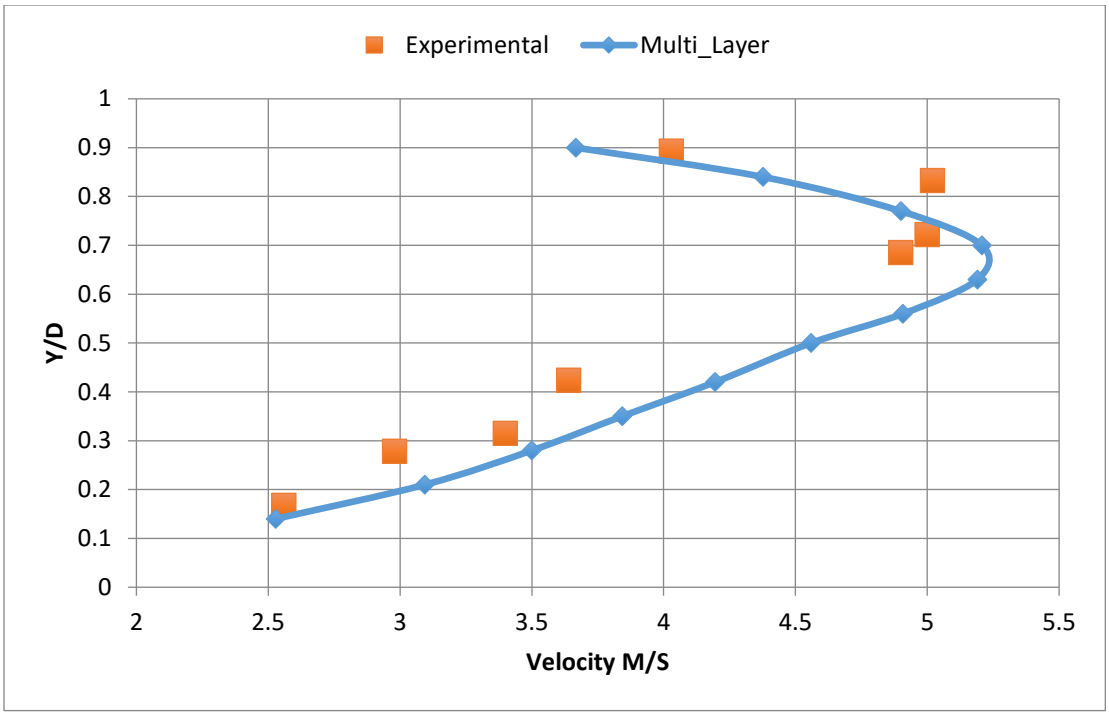

Pd(mm)	2.380	1.190	0.841	0.595	0.420	0.297	0.210	0.074
Sp	1	0.962	0.881	0.674	0.237	0.039	0.008	0.007

Figure 5-16. Velocity profile for flow of multi-sized sand particles in 0.2136 diameter pipe at 15% concentration and 4.21 m/sec

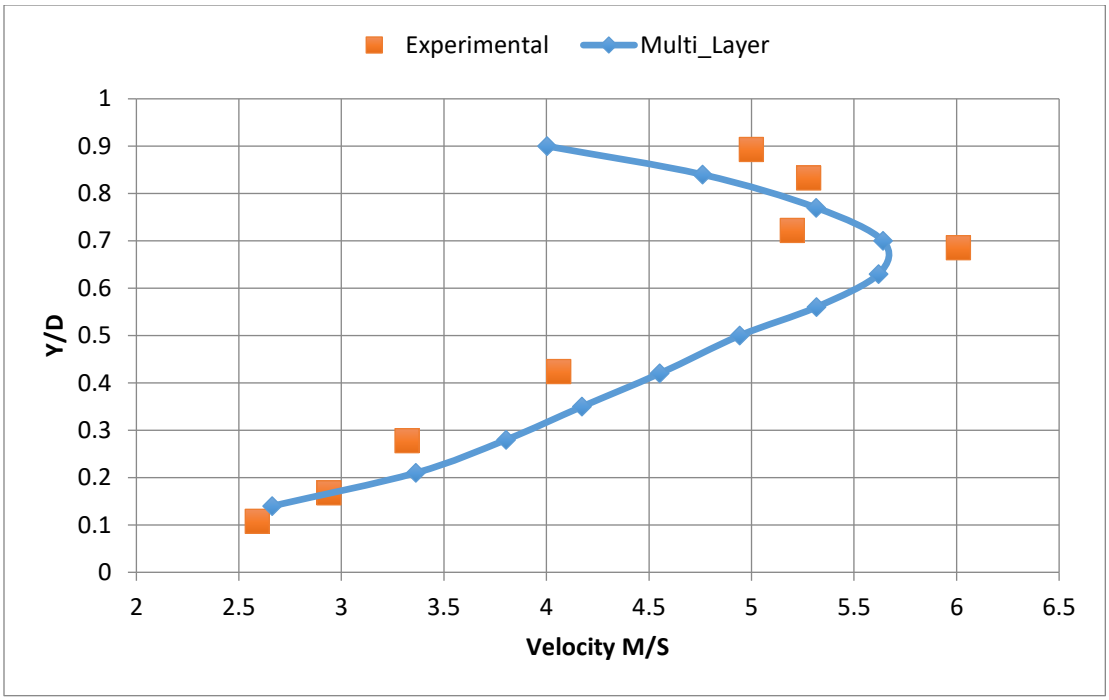

Pd(mm)	2.380	1.190	0.841	0.595	0.420	0.297	0.210	0.074
Sp	1	0.962	0.881	0.674	0.237	0.039	0.008	0.007

Figure 5-17. Velocity profile for flow of multi-sized sand particles in 0.2136 diameter pipe at 15% concentration and 4.65 m/sec

5.4 Prediction of Pressure Drop

The prediction of head loss is essential in the design of a slurry pipeline in order to estimate the energy requirement under various operating conditions. Most of the proposed models to predict the head loss are empirical in nature [27, 30, 46]. These models have been developed based on experimental data for both equi-sized and narrow size range particles. The flow of most commercial slurry pipelines is generally turbulent with a heterogeneous distribution of solid particles across the pipe cross-section. Under these conditions, the prediction of head loss becomes

complex. The prediction of pressure drop in the current study is based on the SRC two layer model as explained in detail in the previous chapter. However, the model has been modified from two-layer to multi-layer. The number of layers should be specified as a basic input of the model. The idea of this modification is to build a model as close as possible to reality and to improve its power of prediction.

To define the ultrafine particles (d_{cf}), equation (1.8) is used. C_f is determined from C_t and the particle size distribution and C_r is determined using equation (4.4). C_c is the actual concentration of coarse particle in each layer which is the sum of j^{th} size fraction in that layer.

The density of the carrier fluid can be defined as below:

$$\rho_f = \left[\rho_l(1 - C_t) + \rho_S\, C_f\right] \Big/ \left[1 - C_t + C_f\right] \tag{5.52}$$

The discharge of the mixture is a constant value which equal to the sum of the actual discharge in each layer as below:

$$AV = \sum_{i=1}^{n} A_i\, V_i \tag{5.52}$$

However,

$$F_f = \sum_{i=1}^{n} C_f\, [(1 - C_i)A_i V_i] \Big/ (1 - C_r) \tag{5.53}$$

The flux of ($-d_{cf}$) particles.

$$Q_c = \sum_{i=1}^{n} C_{c_i} A_i V_i \tag{5.54}$$

The delivered solid flowrate (including - d_{cf} particles)

$$C_V AV = C_{f1} AV + Q_c + F_f \tag{5.55}$$

Mixture density in each layer

$$\rho_i = \rho_f\left(1 - C_i + C_f\right) + \rho_S\, C_f \tag{5.56}$$

Force balance for n-layers

For layer 1:

$$i_1 \rho_i g = (\tau_1 S_1 - \tau_{12} S_{12})/A_1 \quad (5.57a)$$

For layer n:

$$i_n \rho_i g = \left(\tau_n S_n + \tau_{n,(n-1)} S_{n,(n-1)}\right)/A_n \quad (5.57b)$$

For layers 2 to n:

$$i \rho_i g = \left(\tau_i S_i - \tau_{ij} S_{ij} + \tau_{ki} S_{ki}\right)\Big/_{A_n};\ where\ i = 2,3,\dots,(n-1),\ j = i+1,\ k = i-1 \quad (5.57c)$$

The sign of $-\tau_{ij}$ is determined by $V_i > V_{i-1}$

The total pressure drop in the pipe can be defined as an average of the local pressure drops in n layers. The detailed steps for applying the proposed model were presented in figure 5.17.

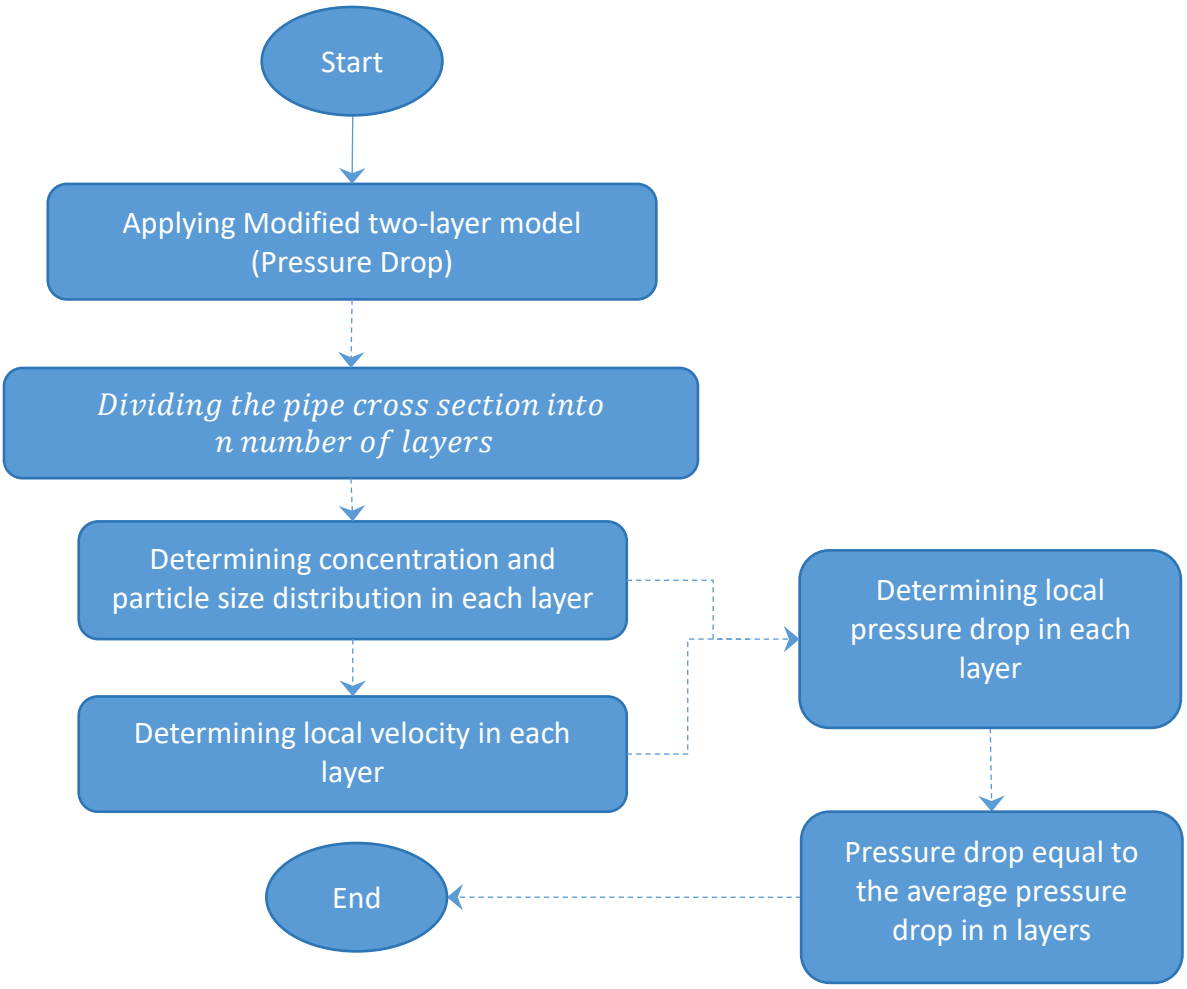

Figure 5-18. Flowchart for applying the Multi-layer model

5.4.1 Validation of the Proposed Model of Pressure Drop

In the previous section, a Multi-layer model for predicting the pressure drop of solid-liquid flow in circular pipelines has been discussed. In order to validate the model, two main methods were used. First the model was validated against experimental data and the prediction power of the proposed model was compared with the modified two layer model and wasp model. For this purpose, a solid-liquid flow loop was developed in order to generate new experimental data as explained

in Chapter 3. In addition, many published experimental data were used from refs. [4, 9, 45, 83, 84].

Figure 5.18 depicts the comparison between the experimental data and predicted data using different models with operating velocity range (1.5m/s to 5.5 m/s). As shown, the proposed model has good prediction power and provides a good match with the experimental data.

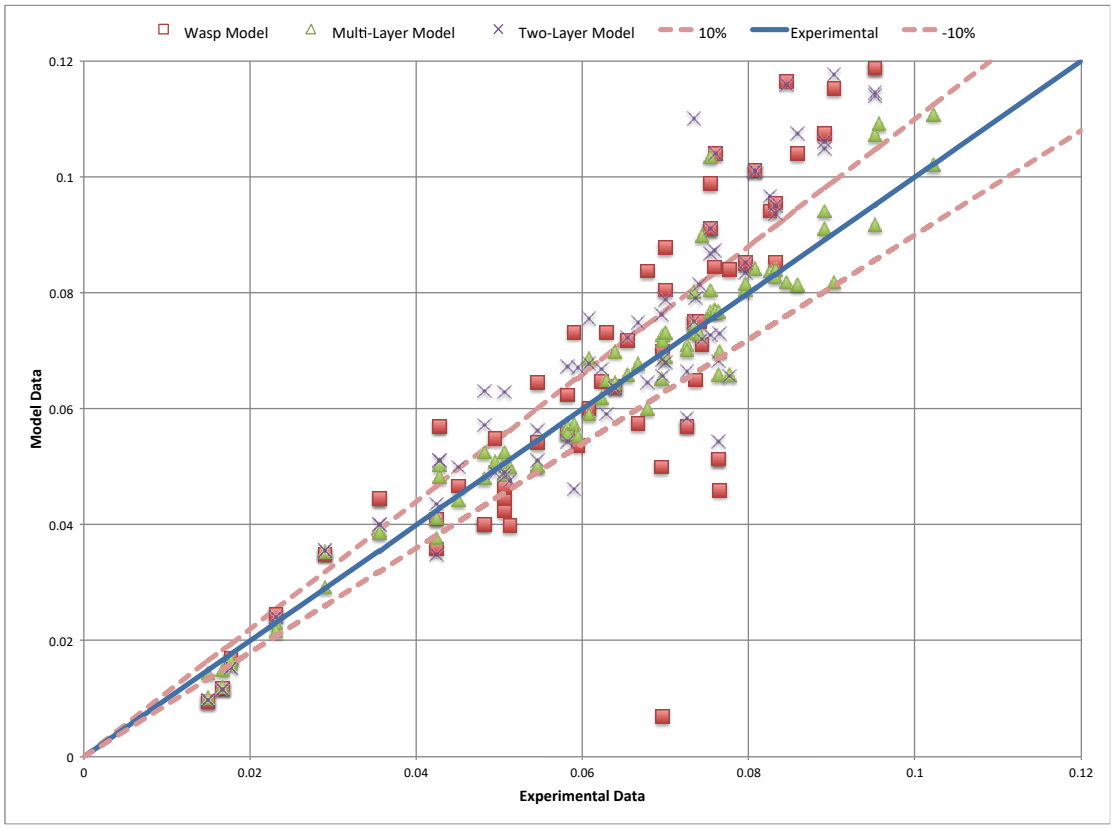

Figure 5-19. comparison between measured and predicted overall pressure drop (using the two-layer model, Wasp model and proposed model)

5.5 Summary of the Chapter

In this chapter, a new model (the Multi-layer model) was introduced for the prediction of pressure drop, concentration distribution and velocity profile for solid-liquid flow in horizontal circular pipelines. The proposed model contains many empirical and semi empirical equations, some of which were proposed in the current study based on extensive data analysis.

The proposed multi-layer model of concentration distribution prediction has been designed based on the Karabelas model and two-layer model. The results were compared with the experimental data (by Gillies 1993) and predicted results (using the Karabelas model). Figure 5.4 depicts the improved prediction power of the proposed model if compared with the Karabelas model.

The second part of the multi-layer model was a model for prediction of the velocity profile. The model was developed based on the computational procedure originally proposed by Roco and Shook [104] for the prediction of the velocity profile across the pipe cross-section. The model was tested on both uni-sized and multi-sized particulate slurries. As shown in the results, further improvements are needed in order to get a model with better prediction power. In addition, more researches with accurate experimental investigations are needed in this field.

The last part of the multi-layer model is the prediction model of pressure drop. This model has been proposed based on the two-layer model. The model was designed based on n number of layers, which can be specified by the user. The mass balance and force balance equations were applied in each layer and the local pressure drop in each layer was defined. The total pressure drop at any point along

the pipeline can be defined as the average of the pressure drop in specified layers. As shown in figure 5.5, the proposed model has a good data fit with the experimental results.

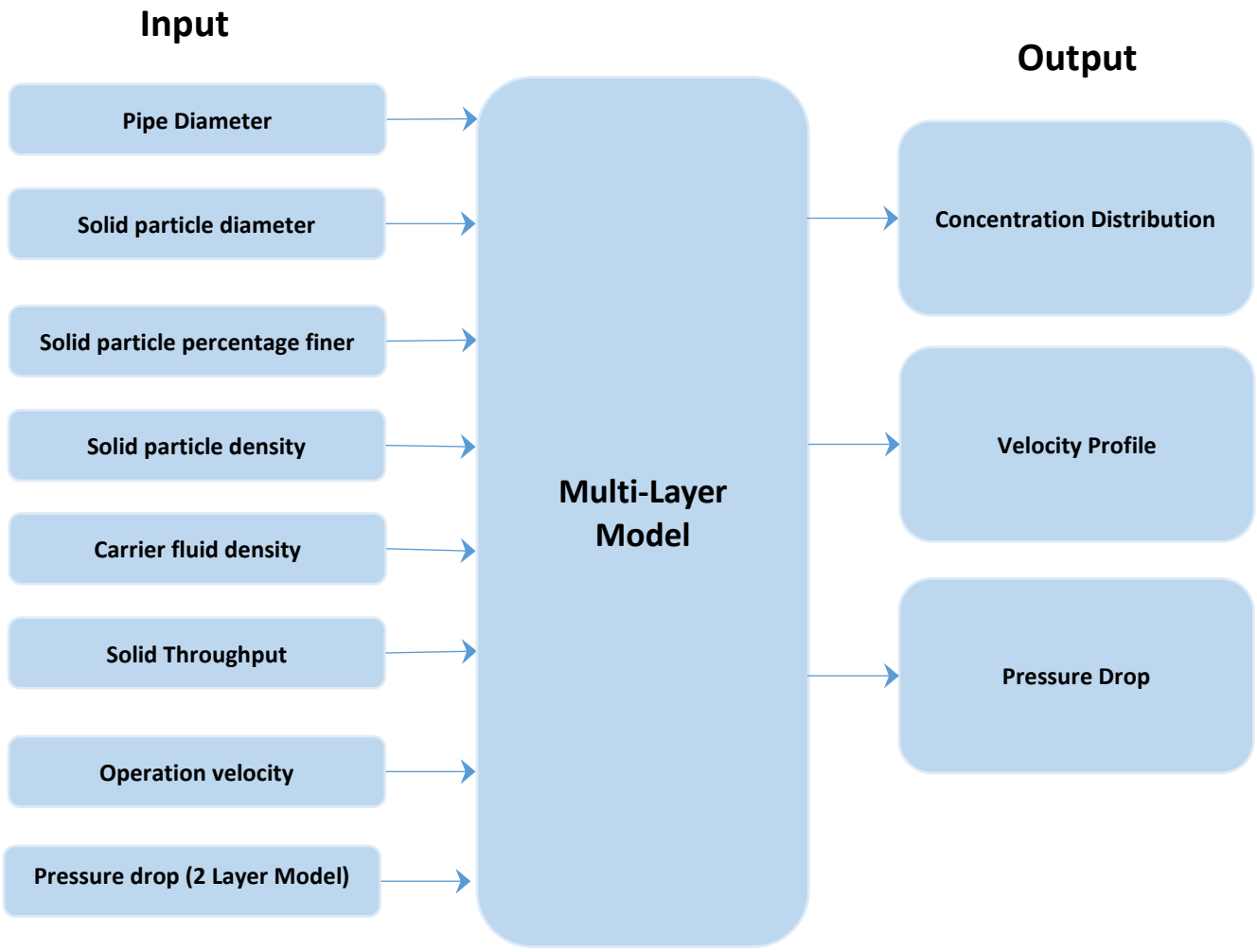

Figure 5-20. Flow chart of applying the Multi-Layer model

CHAPTER 6 Optimisation of horizontal pipelines transporting slurries

The optimisation of solid-liquid two-phase flow pipelines is essential, as commercial viability is concerned in the design of these pipelines. In the Literature review (Chapter 2), some of the existing optimisation models were highlighted. Different methods have been utilised in the presented models such as mechanical design and hydraulic design. In this work, an optimisation methodology has been developed based on both mechanical and hydraulic design.

6.1 Introduction

The least-cost principles method and the proposed prediction models that are explained in the previous chapters were used. All these models are interconnected together to take both the design standards of acceptability and commercial validity into consideration. Robustness and user-friendliness are two main features of the proposed model.

6.2 Developed Least Cost Principle Method

The least cost principle model intends to optimize the design in order to have minimum cost. The cost of a pipeline includes the manufacturing cost and operation cost of the system. This model can also be applied to a slurry pipeline system.

The total cost of a slurry pipeline can be defined as the following:

$$C_T = C_{manufacturing} + C_{Operating} \quad (6.1)$$

In order to have an accurate and meaningful total cost, we have to calculate both the manufacturing and operating costs in specified time period. The operating cost can easily be calculated as per one-year of operation. However, the manufacturing cost can also be considered per year by using system depreciation.

6.3 Manufacturing Cost

The manufacturing cost of most slurry systems can be divided into the pumping station cost and pipeline cost. The design selection of any pumping station is based on many parameters such as the minimum required solid throughput, the mixture properties, pipeline type and length.

$$C_{Manufacturing} = C_{pump} + C_{pipe} \quad (6.2)$$

The net annual cost of pipe per unit pipe length C_{pipe} is given by Chermisinoff [3] as a function of net annual cost of pipe per unit weight of pipe material C2:

$$C_{pipe} = \pi\ D\ t\ \gamma_p\ C_2 \quad (6.3)$$

where:

t : Thickness (m)

$\gamma_p = \rho_p g$ = Specific weight of the pipe ($^{N}/_{m^3}$)

ρ : Density ($^{Kg}/_{m^3}$)

The standard dimension ratio SDR is the ratio of pipe diameter to the wall thickness of the pipe. Hence, the cost of the pipe would be:

$$C_{pipe} = {}^{\pi\ D^2\ \gamma_p\ C_2}/_{SDR} \quad (6.4)$$

6.4 System Depreciation

Depreciation is an accounting method in order to allocate the total cost of any system over its expected operation life. Usually the depreciation method is used for calculating taxes and for other accounting purposes. In this work, depreciation can be used in order to calculate the manufacturing cost per one year of operation. There are different depreciation methods such as declining balance method and straight-line method. In this work, the straight-line method was used due to simplicity of the system and its applicability to the optimization model.

$$Depreciation\ rate = {(System\ Value - Salvage\ value)}/{Useful\ Life}$$

(6.5)

6.5 Cost of Power

The cost power for operating the system for one hour can be expressed as:

$$C_{Power/hr} = C_1 * P \quad (6.6)$$

Where C_1 is the unit cost of power per one KW-Hr and P is the power needed for operating the pump. The power needed for operating the system can be defined as:

$$P = {\gamma_m\ Q\ \Delta P}/{\eta} \quad (6.7)$$

Where:

$\gamma_m = \rho_m g$: Specific weight of the mixture (N/m^3)

Q_m: Mixture flow rate (m^3/sec)

ΔP: Pressure drop (m/m)

η: Efficiency of the Pumping Unit (%)

The mixture density can be defined as:

$$\rho_m = (C_v\ \rho_s) + (1 - C_v\ \rho_l) \quad (6.8)$$

Where:

ρ_s : Solid density (Kg/m^3)

ρ_l : Carrier fluid density (Kg/m^3)

The total cost of power for operating the pipeline for one year can be expressed as:

$$C_{Power} = {C_1 \gamma_m Q_m \Delta P L_P H_{day} D_{year}}/{\eta} \quad (6.9)$$

where:

L_P : Length of the pipe (m)

H_{day} : Operating hours per day (Hr/Day)

D_{year} : Operating days per year ($Day/Year$)

The mixture flow rate can be expressed as a function of the pipe cross-sectional area and operational velocity as below:

$$Q_m = {\pi D^2}/{4} V \quad (6.10)$$

V : Flow Velocity (m/sec)

The pressure drop has been measured in this model based on the multi-layer model as explained in the previous chapter. In addition to the mentioned major losses, there are minor losses such as the loses due to pipe fittings and bends [77] and the losses due to crushing of particles [78]. For a long pipeline, the effect of these minor losses will be negligible [78].

6.6 The Optimisation Model

An optimisation model has been proposed in this work based on developed least cost principles and prediction models that were proposed in the previous chapter. The optimisation model can be run as per the following steps with the input value of the solid throughput.

1- Assume a value of D using for loop from 0.05 to 0.2 using step 0.05.

The value of solid throughput is known (target).

2- The pipeline length is given.

3- Assume the value of solid concentration.

4- Mixture flow rate Q_m can be calculated using solid throughput and solid concentration.

5- For each value of D, the mixture flow velocity can be calculated using mixture flow rate and pipe cross-section area.

6- Calculating the cost of pipes depends on the information regarding the pipe materials and the market price.

7- For each value of D, find the optimum value of velocity to reach the required value of solid throughput.

8- Assume the pumping unit efficiency (0.6 – 0.75) and then keep it fixed.

9- Calculate the pressure drop using multi-layer model.

10- Find out the power requirement for the system.

11- Assume the useful life of the pipeline, such as 20 years.

12- Calculate the power cost of the pipeline for the period of useful life of the pipeline (20 years operation).

13- Calculate the pipeline total cost (Pipeline cost + operation cost) for the useful life period (20 years).

14- Save the data for each value of D and find the case where the value of the total cost is minimal.

6.7 Design Case Studies

6.7.1 Optimisation for Uni-size Slurry Pipeline

Case Study 1:

An optimal design is needed for a high dense polyethylene pipeline transporting 700 mm diameter gravel with 20% concentration. The solid density is 2650 kg/m3 and the carrier fluid is water with 999 kg/m3 density. The required solid throughput is 65 kg/hr. Assume that the cost of unit power is C1=1.4 per KwH, the pipe density is 960 kg/m3 and C2=1.

By applying the proposed model of optimisation, the results shown in Table 6-1 were obtained.

Table 6-1 Variations in total cost and pumping velocity w.r.t pipe diameter for Case study 1

D (m)	$C_{Manufacturing}$ (£)	C_{Power} (£)	C_{Total} (£)	Operating Velocity (m/s)
0.08	86.86	936.90	1023.76	4.88
0.09	109.93	519.49	629.42	3.86
0.10	135.71	307.14	442.86	3.13
0.11	164.21	191.24	355.45	2.58
0.12	195.43	124.26	319.68	2.17
0.13	229.36	83.66	313.02	1.85
0.14	266.00	58.06	324.06	1.59
0.15	305.36	41.36	346.72	1.39
0.16	347.43	30.13	377.56	1.22
0.17	392.21	22.39	414.61	1.08

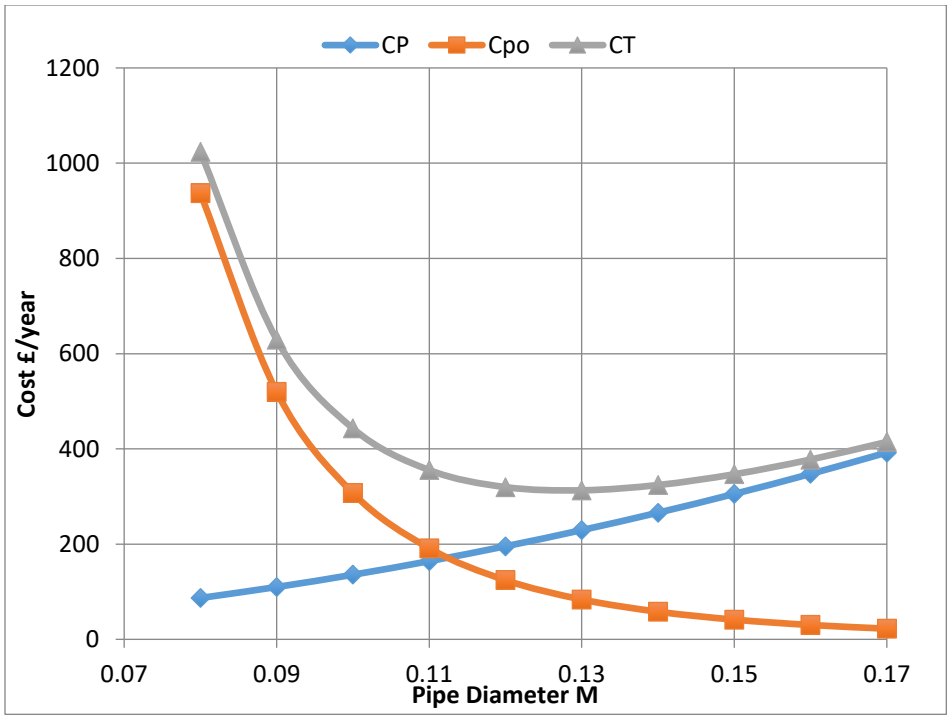

Figure 6.1. Variation of various slurry pipeline costs for case study 1.

6.7.2 Optimisation for Multi-Size Slurry Pipeline

Case Study 2:

An optimal design is needed for a high density polyethylene pipeline transporting multi-sized slurries with 15% concentration. The solid density is 2650 kg/m3 and the carrier fluid is water with 999 kg/m3 density. The required solid throughput is 60 kg/hr. Assume that the cost of unit power is C1=1.4 per KwH, the pipe density is 960 kg/m3 and C2=1. The solid size fractions and percentage finer are as follows:

Pd	2380	1190	841	595	420	297	210	74
Sp	1	0.962	0.881	0.674	0.237	0.039	0.008	0.007

By applying the proposed model of optimisation, the results shown in Table 6-2 were obtained.

Table 6-2 Variations in total cost and pumping velocity w.r.t pipe diameter for case study 2

D (m)	$C_{Manufacturing}$ (£)	C_{Power} (£)	C_{Total} (£)	Operating Velocity (m/s)
D	CP	Cpo	CT	V
0.08	86.86	644.74	731.60	4.51
0.09	109.93	357.32	467.25	3.56
0.10	135.71	211.16	346.88	2.89
0.11	164.21	131.42	295.64	2.39
0.12	195.43	85.36	280.79	2.00
0.13	229.36	57.45	286.81	1.71
0.14	266.00	39.86	305.86	1.47
0.15	305.36	28.38	333.74	1.28
0.16	347.43	20.67	368.10	1.13
0.17	392.21	15.36	407.57	1.00
0.18	439.71	11.61	451.33	0.89

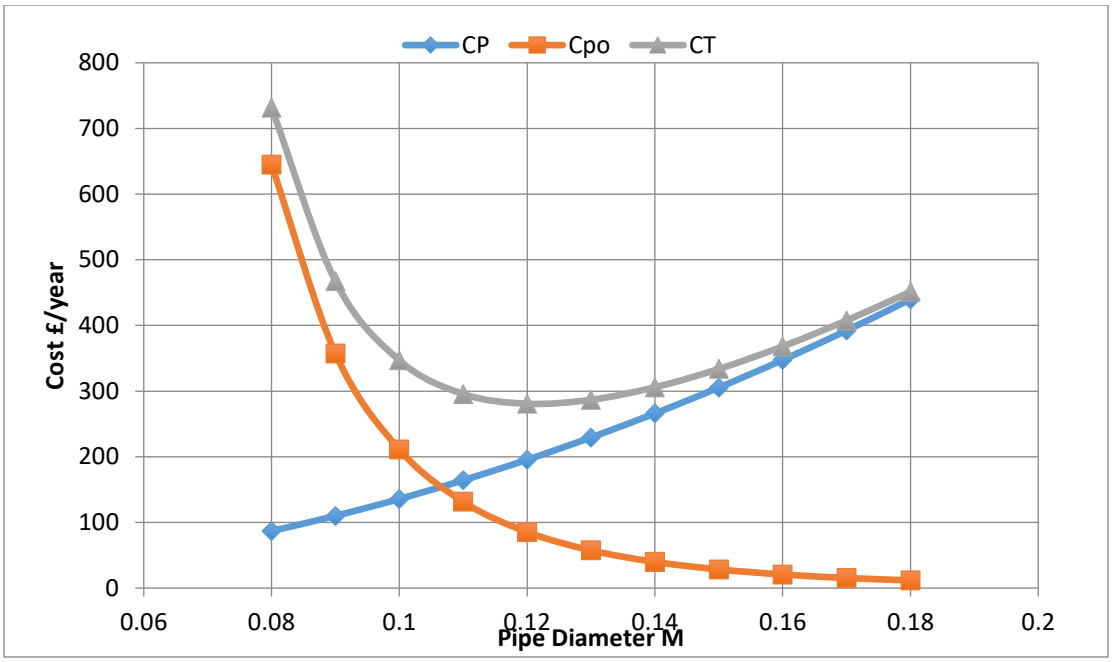

Figure 6.2. Variation of various slurry pipeline costs for case study 2.

Case Study 3:

An optimal design is needed for a high density polyethylene pipeline transporting multi-sized slurries with 15% concentration. The solid density is 2650 kg/m3 and the carrier fluid is water with 999 kg/m3 density. The required solid throughput is 70 kg/hr. Assume that the cost of unit power is C1=1.4 per KwH, the pipe density is 960 kg/m3 and C2=1. The solid size fractions and percentage finer are as the following:

Pd	595	420	297	210	149	74
Sp	1	0.998	0.951	0.571	0.147	0.005

By applying the proposed model of optimisation, the results shown in Table 6-3 were obtained.

Table 6-3 Variations in total cost and pumping velocity w.r.t pipe diameter for case study 3

D (m)	$C_{Manufacturing}$ (£)	C_{Power} (£)	C_{Total} (£)	Operating Velocity (m/s)
D	CP	Cpo	CT	V
0.09	109.93	558.88	668.81	4.16
0.10	135.71	329.85	465.56	3.37
0.11	164.21	205.04	369.25	2.78
0.12	195.43	133.02	328.45	2.34
0.13	229.36	89.44	318.80	1.99
0.14	266.00	61.99	327.99	1.72
0.15	305.36	44.10	349.46	1.50
0.16	347.43	32.10	379.52	1.32
0.17	392.21	23.83	416.04	1.17

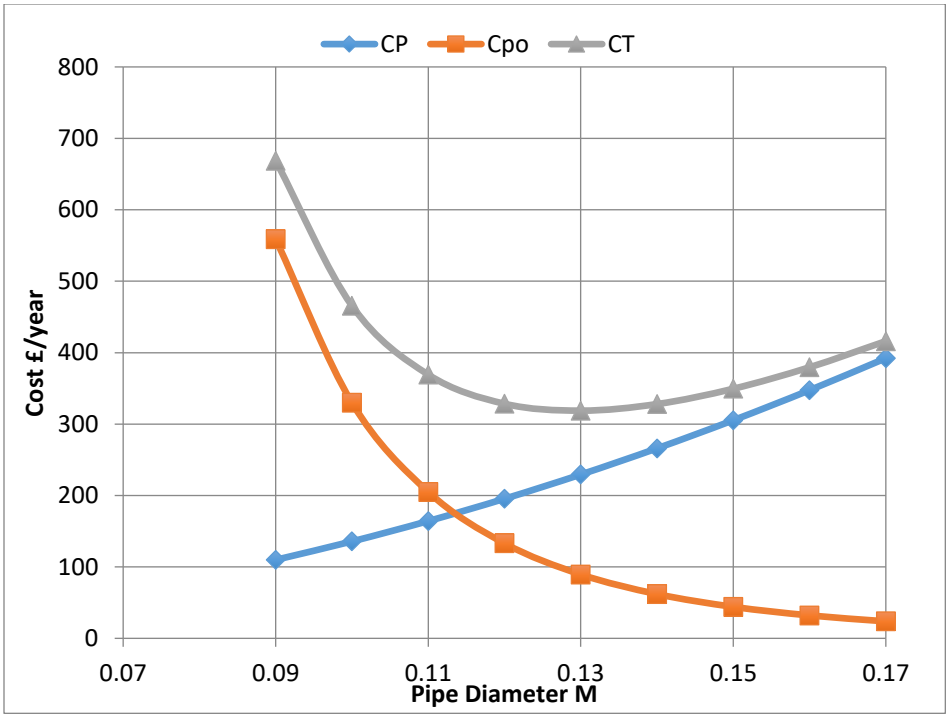

Figure 6.3. Variation of various slurry pipeline costs for case study 3.

Figure 6.4 depicts the variations in the pumping velocity and total head loss in the slurry pipeline for different pipe diameters. It is a fact that the mixture velocity is directly proportional with the pipe diameter. In addition, the figure clearly demonstrates that the total pressure drop is directly proportional to the operating velocity. Hence, this result supports the results of pumping power required for various pipeline diameters.

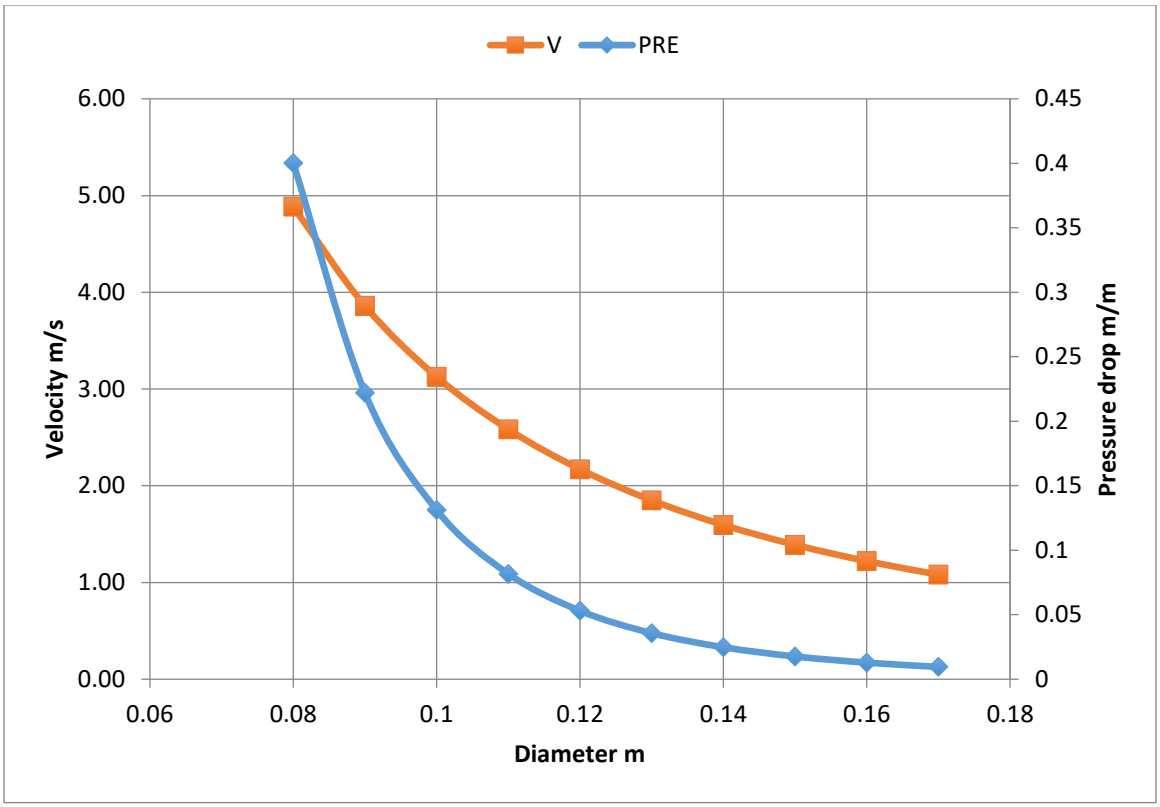

Figure 6.4. Variations of operating velocity and total head loss for various pipeline diameters for case study 3.

6.7 Summary of the Optimisation Model

A detailed cost analysis of pipelines transporting slurries with fixed solid throughput gives the following results:

- The manufacturing cost is directly proportional to the pipe diameter as shown in figures 6.1, 6.2 and 6.3.
- The operating cost is inversely proportional to the pipe diameter as shown in figures 6.1, 6.2 and 6.3.
- The total cost is inversely proportional with diameters less than the diameter at the optimal point, as shown in figures 6.1, 6.2 and 6.3.

- The total cost is directly proportional with diameters greater than the diameter in the optimal point, as shown in figures 6.1, 6.2 and 6.3.
- The total head loss is inversely proportional to the pipe diameter and directly proportional with mixture velocity as depicted in figure 6.4.
- For the same concentration of case studies (2&3), the coarser particle size has a smaller optimal pipe diameter than the finer particles slurries. This is due to a higher pressure drop in the flow of the fine particle slurries.
- The useful life of any pipeline is an important parameter in the optimisation model. This value must be accurately assumed by the designer based on the special mathematical equations according to the quality of the used materials.

CHAPTER 7 Conclusion and Discussion

From the results obtained in the previous chapters regarding the solid-liquid multi-phase flow in horizontal pipes, and the development of a prediction model for predicting slurry flow properties, detailed conclusions are drawn in this chapter. In addition, the major achievements are referenced back to the initial aims of this research and contributions to the existing knowledge base are summarised. Finally, the next steps to complete this ongoing study and the future work are planned and explained.

7.1 Research Problem Synopsis

Transport of solid particles through pipelines is extensively used in chemical engineering and many other applications. However, the majority of research studies carried out on slurry flow in circular pipelines are based on either empirical or semi empirical correlations and assumptions which lack a mathematical basis and detailed investigations about the complex flow behaviour within such pipelines. Since the middle of the last century, several models have been proposed to predict slurry flow behaviour within pipelines. However, the prediction power of the proposed models changes based on different operating conditions. Thus, extensive works were undertaken in this thesis in order to propose a model with better prediction power which is suitable for a wider range of operational conditions.

From the comprehensive review of the literature presented in Chapter 2, a number of limitations were found which are concerned with the above mentioned issues. To improve the prediction model for complex solid-liquid flow in horizontal pipes a set of aims and objectives were identified which represent the scope of this study.

7.2 Research Aims and Major Achievements

The main aims of the current study are outlined in Chapter 1.

Research Aim #1: Experimental based flow diagnostics for solid-liquid flow.

Achievement: The available multiphase flow loop facility in the University of Huddersfield, which was previously used for the flow of solid-liquid mixture in

vertical and inclined pipes, was adopted for horizontal flow experiments. A new 90mm pipeline was installed and used to collect the experimental data. The study involved the observation of slurry flow through the transparent pipe section. Moreover, experiments were performed to collect data that have been used for proposing empirical equations as explained in Chapter 4.

Research Aim #2: Numerical flow diagnostic and design of horizontal pipes transporting slurries.

Achievement: This study provides a detailed numerical based investigation of solid-liquid two-phase flow in horizontal pipelines. The model is able to predict pressure drop along the pipeline, concentration distribution and velocity profile across the pipe cross-section based on some basic input data, which are the pipe diameter and pipe wall roughness, the physical properties and volume fraction of solid particles, the physical properties of the carrier fluid and the operational velocity. Furthermore, any of the input data can be optimised based on the analysis of wide range of data according to the requirement of the design.

Research Aim #3: Development of an analytical model for the optimum design of pipelines transporting slurries.

Achievement: In the current study, a prediction and optimisation model for pipelines transporting slurries was proposed. The model is an improvement of the

Least Cost Principle method. The model is capable of predicting the optimal diameter of a pipeline in order to have the least manufacturing and operation cost. The models of pressure drop, concentration distribution and velocity profile that are proposed in this work have been used in the model.

7.3 Report Conclusions:

A comprehensive study has been conducted in the area of solid-liquid flow in horizontal pipes in order to support the existing literature and to contribute to the knowledge in this regard. The main conclusions of this report can be summarised as follows:

Research Objective #1: To develop a robust prediction model for predicting the pressure drop of multi-sized particulate slurry flow in horizontal pipes.

Conclusion #1: This research suggests some improvements on the two-layer model. These modifications were applied by developing a prediction model for the prediction of pressure drop of solid-liquid flow in horizontal pipes. The modified model contains semi-empirical correlations that were provided by the available literature, and new equations proposed in this study.

The model was developed based on studying the effects of different parameters on pressure drop. The considered design parameters are pipe diameter, solid particle size and solid concentration by volume. Then the effects of each parameter on pressure drop were presented. Then an empirical equation was developed

which considers these effects. The most important outcome of this work is considering the coefficient of sliding friction between solid particles and the pipe wall as a variable parameter. An equation was derived in order to predict the value of sliding friction based on the mentioned design parameters.

The proposed model was validated by comparing the results with the experimental data. In addition to the experimental results that are explained in Chapter 3, different experimental data were used in order to check the prediction power of the model. Furthermore, the model was also compared with the Wasp model and the two-layer model. As shown in the presented graphs, the proposed model has good prediction power with respect to the other prediction models.

Research Objective #2: To determine the effects of the solid-liquid mixture properties, operational velocity and pipe diameter on the pressure drop within the pipelines.

Conclusion #2: The effects of the solid-liquid mixture properties, operational velocity and pipe diameter on the pressure drop were studied based on their effects on the coefficient of sliding friction between the solid particles and pipe wall. In Chapter 4, all these effects have been explained in detail. The chapter clearly demonstrated that these factors have direct effects on the value of the coefficient of sliding friction. Hence, this coefficient cannot be considered as a fixed value as suggested by many previous works.

A computer based numerical program was designed to find the ideal value of the coefficient of sliding friction for given flow properties. Hundreds of experimental data cases were applied. The results were analysed based on the effect of particle size, concentration of solids in the mixture, operational velocity and pipe diameter. The effect of each factor was studied separately and depicted in a graph. In the next step, these data were joined together in order to develop semi-empirical relations for the friction factor and pressure drop in horizontal pipeline transporting slurries.

Research Objective #3: The development of a semi-empirical equation for the coefficient of friction in the solid-liquid flow system.

Conclusion #3: The coefficient of friction between particle-particle and particle-wall is the dominant factor causing pressure drops in coarse slurry flow in cylindrical pipelines. Many parameters were found to be greatly important in determining the magnitude of the overall frictional coefficient, such as, the ratio of operating velocity to the particle settling velocity $\frac{v}{v_c}$ and the ratio of the solid concentration in the lower layer to the solid concentration in the upper layer based on the two-layer model. There are also other parameters found to have less effect on the coefficient of friction, such as the ratio of particle diameter to the wall roughness in smooth wall horizontal pipelines.

An empirical equation was derived for predicting the coefficient of friction in a coarse slurry pipeline based on the experimental data. The new equation was

applied to the SRC Two-Layer Model. The results show better predictions of pressure drops in comparison to the experimental data.

Research Objective #4: To develop a Multi-Layer model for predicting the solid concentration distribution for the flow of multi-sized particulate slurries across a cross-section of horizontal pipes.

Conclusion #4: A Multi-layer model was proposed to predict the concentration distribution of solid particles across the cross-section of horizontal slurry flow pipelines. The proposed model is based on the general solution of diffusion equations [60, 98]. The model can be considered as a modified Karabelas model and is capable of predicting the concentration of each particle size fraction in any layer across a cross-section of such pipes.

The proposed model was validated by comparing the results with the experimental data. For this purpose, different experimental works in the literature were used. Furthermore, the model was also compared with the Karabelas model and the two-layer model. As shown in the comparison graphs, the proposed model has acceptable prediction power with respect to the other prediction models. Further analysis of the model results is needed to show the prediction power of the model.

Research Objective #5: To develop a Multi-Layer model for predicting the velocity profile of multi-sized particulate slurry flow across a cross-section of horizontal pipes.

Conclusion #5: A Multi-layer model has been proposed to predict the velocity profile of multi-sized particulate slurry flow across the cross-section of horizontal slurry flow pipelines. The proposed model is based on the computational procedure originally proposed by Roco and Shook [104] and modified equations of the dynamic coefficient of turbulence for the solid-liquid mixture proposed by Mishra [4]. In this work, in addition to the structure of the multi-layer model, the proposed equations that are illustrated in Chapter 4 have been used.

The proposed model was validated by comparing the results with the experimental data for both uni-sized and multi-sized slurries. In the case of uni-sized slurries, in addition to the experimental data, the predicted data was compared with the predicted CFD results by Nabil et al [107]. As shown in the figures of the results in Chapter 5, the model has reasonable agreements with the experimental data. The accuracy of the proposed model depends on the operation velocity, solid concentration and particle size. In low velocities, the model gives more accurate results than high velocities as shown in figures 5.9 and 5.10. In addition, a better match between the model data and experimental data was noticed in lower concentration slurries as depicted in Figures 5.8 and 5.9. Furthermore, the model gives better prediction results in coarse particles slurries than fine slurries as shown in Figures 5.12 and 5.14. Further analysis of the model results and accurate and reliable experimental works are needed in order to evaluate the prediction power of the proposed model.

Research Objective #6: To determine the effects of the solid-liquid mixture properties, operational velocity and pipe diameter on the velocity profile within the pipelines.

Conclusion #6: From the investigations regarding the effect of the solid-liquid mixture properties, operational velocity and pipe diameter on the velocity profile within the pipelines, carried out in this study, it can be concluded that all the mentioned factors have significant effects on the velocity profile. All the mentioned relations have been clearly explained in Chapter 5. This conclusion is true for both uni-sized and multi-sized particulate slurries. The results were analysed based on the effect of particle size, concentration of solids in the mixture, operational velocity and pipe diameter. The effect of each factor was studied separately and depicted using graphs. As shown in figures 5.8 and 5.9, at 20% solid concentration, the maximum velocity was recorded at Y/D=0.6, however, at 30% solid concentration the maximum velocity was recorded at Y/D=0.68 for the same operational velocity and particle size. In addition, for the same concentration and particle size slurries, by increasing the operational velocity, the maximum velocity will be at a lower Y/D value as shown in figures 5.9 and 5.10. Moreover, particle size also has a significant effect on velocity profile. As shown in figures 5.12 and 5.14, maximum velocity will be at a higher Y/D for fine slurries than coarse slurries. More studies and experimental investigations are needed in order to develop equations to predict accurate velocity profiles based on the mentioned understandings.

Research Objective #7: To develop a Multi-Layer model for predicting the pressure drop of multi-sized particulate slurry flow across a cross-section of horizontal pipes.

Conclusion #7: The prediction of pressure drop in the current study is based on the SRC Two Layer Model as explained in detail in Chapter 3. However, the model was modified from two-layer to multi-layer based on the general structure of the model. The number of layers were specified as a basic input of the model. The idea of this modification is to build a model as close as possible to reality and to improve its power of prediction. The main point of the improvement in this model is applying the force balance equation in each layer according to the local velocity and solid concentration of the layers.

Research Objective #8: Development of a robust optimisation model for a solid-liquid flow system based on the least-cost principle.

Conclusion #8: From the proposed optimisation model that is explained in Chapter 6 regarding the horizontal pipeline transporting slurries, it can be concluded that, for a fixed solid throughput in such a pipeline, the diameter size is directly proportional with the manufacturing costs. On the other hand, it can also be concluded that the diameter size is inversely proportional with the head loss. Therefore, by increasing the diameter, the operational cost will decrease as a result of decreasing the required pumping power. In addition, the pumping velocity is also an effective factor in optimisation methodology. As shown in the results, when the optimal diameter is selected, the operating velocity must be within the

acceptable range, otherwise different diameters should be taken into consideration. The solid throughput is the only input in the proposed optimisation model in the present study and it can be considered as robust and user-friendly.

7.4 Research Contributions

The current study has some contributions and novelties. The major research contributions and the description of the novelties are summarized below:

Contribution #1:

One of the major contributions of the current research is the development of a new equation for the coefficient of sliding friction between solid particles and pipe wall of the horizontal pipeline transporting slurries over a wide range of flow conditions. Most of the available literature either defined this coefficient as a constant value or reported as its value changes according to the flow properties without proposing an equation for measuring its value. In the current study the effects of many flow parameters on the coefficient of sliding friction were studied. The effects of the diameter of solid particles, solid particles distribution, pipe diameter and system operating velocity were also taken into consideration. Furthermore, a novel equation for predicting the coefficient of sliding friction was developed over a wide range of flow conditions. The equation was derived based on extensive numerical investigations and taking hundreds of experimental data of different flow conditions into consideration. The proposed equation can be used for estimating the value of the coefficient of sliding friction in different flow conditions, which is an important parameter in pressure drop prediction modelling.

Contribution #2:

The second major contribution of the current research study is modifying the SRC Two-Layer Model for the prediction of pressure drop in horizontal pipelines transporting slurries. The model data were analysed based on the experimental data and the gaps of the model were identified. Furthermore, the model has been improved based on the proposed equations of the current study which are the proposed equations of coefficient of sliding friction, C_{lim} and C_{max}. The proposed novel pressure drop prediction model can be run using a computer-based program, such as MATLAB, and the value of pressure drop in horizontal pipelines transporting slurries can be accurately predicted. In addition, the model can be used for both uni-sized and multi-sized particulate slurries.

Contribution #3:

Another major contribution of the current research study is the extensive study of available models for the prediction of concentration distribution in horizontal pipelines transporting slurries. The available models have been analysed based on experimental data and the gaps of the models were identified. Furthermore, an improved model for the prediction of concentration distribution of solid particles in horizontal slurry pipeline was proposed. The proposed model can be considered as an improved version of the Karabelas model. The proposed novel pressure drop prediction model can be run using a computer-based program, such as MATLAB, and the concentration distribution of a horizontal slurry pipeline can be reasonably

accurately predicted. In addition, the model can be used for both uni-sized and multi-sized particulate slurries.

Contribution #4:

Another major contribution of the current research is improving the available models for the prediction of velocity profile in horizontal pipelines transporting slurries. The model data were analysed based on experimental data and the gaps of the model have been identified. Furthermore, the proposed model was developed based on the proposed equations in the current study. The proposed velocity profile prediction model can be run using a computer-based program, such as MATLAB, and the results of the velocity profile in horizontal pipelines transporting slurries can be predicted with acceptable prediction power. In addition, the model can be used for both uni-sized and multi-sized particulate slurries.

Contribution #5:

The optimisation methodology is another contribution of the current research study. Horizontal slurry pipelines are widely used in many chemical industries as a method of transportation, and consequently, having an improved optimisation model for the design of slurry pipeline is highly recommended. An improved optimisation model has been proposed in the current research study based on least cost principle method. In addition, an improved pressure drop model has been used for calculating the cost of power. The robustness and user-friendliness are two of the most important features of the proposed model. Furthermore, the model can be used for the design of horizontal pipelines transporting both uni-sized and multi-sized particulate slurries.

7.5 Future Works

In the present research study, the prediction and optimization models for horizontal pipelines transporting slurries have been proposed to bridge the gaps that were identified in the literature. The research study has been concluded in the previous section and the vast potential for future research clear. Below are the main suggested areas for future work to be performed regarding the prediction and optimization methodology for horizontal pipelines transporting slurries.

Recommendation #1:

One of the main problems in slurry flow in pipelines is the wear rate that is the result of sliding friction between solid particles and the pipe wall. In addition to the prediction of pressure drop, concentration distribution and velocity profile, prediction of wear rate is also a very important factor that should be taken into consideration. The proposed multi-layer model could be beneficial for the development of a wear rate prediction model. Furthermore, the proposed equation of the coefficient of sliding friction between solid particles and the pipe wall is also an addition in this field.

Recommendation #2:

Most of the existing slurry systems in the real world contain an amount of gas phase such as air. In order to have accurate results and applicable prediction models, the amount of gas phase inside the pipeline should be taken into consideration. The proposed multi-layer model can be developed to predict the flow properties of three-phase liquid-solid-gas flow inside pipelines.

Recommendation #3:

The optimization methodology that was proposed in the current research study is one of the fields that needs further research and development. The estimated manufacturing cost for one year is based on an assumption of the useful life of the pipeline. In order to get more accurate results, a new equation for the prediction of the useful life of the pipeline based on the mechanical properties of the pipes and the slurry mixture is highly recommended. In addition, the maintenance cost of the system should be also taken into consideration in the optimization methodology.

- **Reference**

[1] U. Kumar, R. Mishra, S. N. Singh, and V. Seshadri, "Effect of particle gradation on flow characteristics of ash disposal pipelines," Powder Technology, vol. 132, no. 1, pp. 39-51, 2003.

[2] J. S. Marshall and S. Li, Adhesive Particle Flow. Cambridge University Press, 2014.

[3] K. C. Wilson, G. R. Addie, A. Sellgren, and R. Clift, Slurry transport using centrifugal pumps. Springer Science & Business Media, 2006.

[4] R. Mishra, "A study on the flow of multisized particulate solid-liquid mixtures in horizontal pipelines," 1996.

[5] S. M. Peker and S. S. Helvaci, Solid-liquid two phase flow. Elsevier, 2011.

[6] R. Mishra, S. Singh, and V. Seshadri, "Velocity measurement in solid–liquid flows using an impact probe," Flow Measurement and Instrumentation, vol. 8, no. 3, pp. 157-165, 1998.

[7] D. Kaushal, T. Thinglas, Y. Tomita, S. Kuchii, and H. Tsukamoto, "CFD modeling for pipeline flow of fine particles at high concentration," International Journal of Multiphase Flow, vol. 43, pp. 85-100, 2012.

[8] R. Durand and E. Condolios, "Experimental investigation of the transport of solids in pipes," Deuxieme Journée de lhydraulique, Societé Hydrotechnique de France, 1952.

[9] R. G. Gillies, "Pipeline flow of coarse particle slurries," 1993.

[10] M. Vaezi and A. Kumar, "Development of correlations for the flow of agricultural residues as slurries in pipes for Bio-refining," Biosystems Engineering, vol. 127, pp. 144-158, 2014.

[11] H. Hashimoto, K. Noda, T. Masuyama, and T. Kawashima, "Influence of pipe inclination on deposit velocity," in Proceedings of the 7th International Conference on the Hydraulic Transport of Solids in Pipes, 1980, pp. 231-244.

[12] R. B. Spelay, "Solids transport in laminar, open channel flow of non-Newtonian slurries," The University of Saskatchewan, 2007.

[13] K. B. Hill, "Pipeline flow of coarse particles in fluids with yield stresses," 1996.

[14] R. B. Bird, W. E. Stewart, and E. N. Lightfoot, Transport phenomena. John Wiley & Sons, 2007.

[15] B. E. Abulnaga, Slurry systems handbook. McGraw-Hill New York, 2002.

[16] D. Newitt, J. Richardson, M. Abbott, and R. Turtle, "Hydraulic conveying of solids in horizontal pipes," Trans. Inst. Chem. Eng, vol. 33, pp. 93-113, 1955.

[17] G. R. Addie, "Slurry pipeline design for operation with centrifugal pumps," in PROCEEDINGS OF THE INTERNATIONAL PUMP USERS SYMPOSIUM, 1996, pp. 193-212: TEXAS A&M UNIVERSITY SYSTEM.

[18] R. G. Gillies, C. A. Shook, and J. Xu, "Modelling heterogeneous slurry flows at high velocities," The Canadian Journal of Chemical Engineering, vol. 82, no. 5, pp. 1060-1065, 2004.

[19] D. G. Thomas, "Transport characteristics of suspension: VIII. A note on the viscosity of Newtonian suspensions of uniform spherical particles," Journal of Colloid Science, vol. 20, no. 3, pp. 267-277, 1965.
[20] S. W. Churchill, "Friction-factor equation spans all fluid-flow regimes," Chemical Engineering, vol. 84, no. 24, pp. 91-92, 1977.
[21] A. Metzner and J. Reed, "Flow of non-newtonian fluids—correlation of the laminar, transition, and turbulent-flow regions," AIChE Journal, vol. 1, no. 4, pp. 434-440, 1955.
[22] F. Pinho and J. Whitelaw, "Flow of non-Newtonian fluids in a pipe," Journal of Non-Newtonian Fluid Mechanics, vol. 34, no. 2, pp. 129-144, 1990.
[23] D. Dodge and A. Metzner, "Turbulent flow of non-Newtonian systems," AIChE Journal, vol. 5, no. 2, pp. 189-204, 1959.
[24] K. C. Wilson and A. D. Thomas, "A new analysis of the turbulent flow of non-newtonian fluids," The Canadian Journal of Chemical Engineering, vol. 63, no. 4, pp. 539-546, 1985.
[25] C. A. Shook and M. C. Roco, Slurry flow: Principles and practice. Elsevier, 1991.
[26] M. Charles, "TRANSPORT OF SOILDS BY PIPELINE," in Presented at the 1st International British Hydromechanics Research Association Hydraulic Transport of Solids in Pipes Conference, Warwichshire Univ., Coventry, Eng., Sept. 1-4, 1970., 1970, no. A3 Proceeding.
[27] G. W. Govier and K. Aziz, The flow of complex mixtures in pipes. Richardson, TX: Society of Petroleum Engineers; 2nd ed., 1972.
[28] C. Shook, R. Gillies, D. Haas, W. Husband, and M. Small, "Flow of coarse and fine sand slurries in pipelines," Journal of Pipelines, vol. 3, no. 1, pp. 13-21, 1982.
[29] K. Wilson, "A unified physically-based analysis of solid-liquid pipeline flow," in Proc. Hydrotransport, 1976, vol. 4, pp. A1-1. BHRA Cranfield, UK.
[30] R. Gillies, C. Shook, and K. Wilson, "An improved two layer model for horizontal slurry pipeline flow," The Canadian Journal of Chemical Engineering, vol. 69, no. 1, pp. 173-178, 1991.
[31] C. A. Shook, R. G. Gillies, and R. S. S. Sanders, Pipeline Hydrotransport: With Applications in the Oil Sand Industry. SRC Pipe Flow Technology Centre, 2002.
[32] G. Houzeaux et al., "High-Performance Computing: Do's and Dont's," 2018.
[33] E. Mitsoulis, "Flows of viscoplastic materials: models and computations," Rheology reviews, vol. 2007, pp. 135-178, 2007.
[34] C. G. Litzenberger, "Rheological study of kaolin clay slurries," 2003.
[35] K. Wilson and A. Thomas, "Analytic Model of Laminar-Turbulent Transition for Bingham Plastics," The Canadian Journal of Chemical Engineering, vol. 84, no. 5, pp. 520-526, 2006.
[36] R. Silva, F. A. Garcia, P. M. Faia, and M. G. J. T. J. o. C. M. F. Rasteiro, "Evaluating the performance of the Mixture Model coupled with High and Low Reynolds Turbulence closures in the numerical description of concentrated solid-liquid flows of settling particles". The Journal of Computational Multiphase Flows, vol. 7, no. 4, pp. 241-257, 2015.

[37] T. H. H. Alzuhd, "Pressure losses associated with slurry flow in horizontal pipelines," 2003.
[38] R. Mishra, S. Singh, and V. Seshadri, "Hydraulic Conveying-Improved Model for the Prediction of Pressure Drop and Velocity Field in Multi-Sized Particulate Slurry Flow Through Horizontal Pipes," Powder Handling and Processing, vol. 10, no. 3, pp. 279-288, 1998.
[39] R. Gillies, W. Husband, and M. Small, A Study of Flow Conditions Arising in Horizontal Coarse Slurry Short Distance Pipelining Practice Phase 1: Sand-slurry Tests in a 250 Mm Pipeline: Interim Report. Saskatchewan Research Council, 1985.
[40] R. G. Gillies and C. A. Shook, "Modelling high concentration settling slurry flows," The Canadian journal of chemical Engineering, vol. 78, no. 4, pp. 709-716, 2000.
[41] R. Gillies and C. Shook, "Concentration distributions of sand slurries in horizontal pipe flow," Particulate science and technology, vol. 12, no. 1, pp. 45-69, 1994.
[42] D. P. Gillies, "Particle contributions to kinematic friction in slurry pipeline flow," University of Alberta, 2013.
[43] R. Spelay, S. A. Hashemi, R. G. Gillies, R. Hegde, R. S. Sanders, and D. G. Gillies, "Governing Friction Loss Mechanisms and the Importance of Off-Line Characterization Tests in the Pipeline Transport of Dense Coarse-Particle Slurries," in ASME 2013 Fluids Engineering Division Summer Meeting, 2013, pp. V01CT20A013-V01CT20A013: American Society of Mechanical Engineers.
[44] D. Kaushal and Y. Tomita, "An improved method for predicting pressure drop along slurry pipeline," Particulate science and technology, vol. 20, no. 4, pp. 305-324, 2002.
[45] D. Kaushal and Y. Tomita, "Solids concentration profiles and pressure drop in pipeline flow of multisized particulate slurries," International Journal of multiphase flow, vol. 28, no. 10, pp. 1697-1717, 2002.
[46] E. J. Wasp, Kenny, J.P., Gandhi, R.L.,, "Solid Liquid Flow Slurry Pipeline Transportation," Trans. Tech. Publications, Clausthal, Germany, vol. first ed., 1977.
[47] R. J. Phillips, R. C. Armstrong, R. A. Brown, A. L. Graham, and J. R. Abbott, "A constitutive equation for concentrated suspensions that accounts for shear-induced particle migration," Physics of Fluids A: Fluid Dynamics (1989-1993), vol. 4, no. 1, pp. 30-40, 1992.
[48] K. C. Wilson, R. S. Sanders, R. G. Gillies, and C. A. Shook, "Verification of the near-wall model for slurry flow," Powder Technology, vol. 197, no. 3, pp. 247-253, 2010.
[49] P. Vlasak, B. Kysela, and Z. Chara, "Flow structure of coarse-grained slurry in a horizontal pipe," Journal of Hydrology and Hydromechanics, vol. 60, no. 2, pp. 115-124, 2012.
[50] A. A Kumar and B. J. Y. I. J. o. R. Singh, "CFD modeling for silica sand slurry in horizontal pipeline system," vol. 3, 2015b.

[51] H. P. Singh, S. Pandey, and D. Kaushal, "A NEW CORRELATION FOR PARTICLE DIFFUSIVITY IN SLURRY FLOW THROUGH PIPELINE," in 18th International Conference on Transport, 2017, p. 327.
[52] V. Seshadri, S. Singh, and M. Ahmed, "Prediction of concentration and size distribution of solids in a slurry pipeline," 1997.
[53] M. P. O'Brien, "Review of the theory of turbulent flow and its relation to sediment-transportation," Eos, Transactions American Geophysical Union, vol. 14, no. 1, pp. 487-491, 1933.
[54] H. Rouse, "Modern conceptions of the mechanics or fluid turbulence," Transactions of the American Society of Civil Engineers, vol. 102, no. 1, pp. 463-505, 1937.
[55] H. M. Ismail, "Turbulent transfer mechanism and suspended sediment in closed channels," Transactions of the American Society of Civil Engineers, vol. 117, no. 1, pp. 409-434, 1952.
[56] E. Wasp, T. J. Regan, J. Withers, P. Cook, and J. J. P. L. N. Clancey, "Cross Country Coal Pipe Line Hydraulics," Pipe Line News, vol. 25, no. 7, 1963.
[57] E. Wasp and T. Aude, "Deposition velocities, transition velocities, and spatial distribution of solids in slurry pipelines," in Presented at the 1st International British Hydromechanics Research Association Hydraulic Transport of Solids in Pipes Conference, War Wickshire Univ, Conventry, England, Sept. 1-4, 1970., 1970, no. H4 Proceeding.
[58] C. Shook and S. Daniel, "Flow of suspensions of solids in pipelines: Part I. Flow with a stable stationary deposit," The Canadian Journal of Chemical Engineering, vol. 43, no. 2, pp. 56-61, 1965.
[59] C. Shook, S. Daniel, J. Scott, and J. Holgate, "Flow of suspensions in pipelines (Part 2: Two mechanisms of particle suspension)," The Canadian Journal of Chemical Engineering, vol. 46, no. 4, pp. 238-244, 1968.
[60] A. Karabelas, "Vertical distribution of dilute suspensions in turbulent pipe flow," AIChE Journal, vol. 23, no. 4, pp. 426-434, 1977.
[61] J. Hunt, "The turbulent transport of suspended sediment in open channels," in Proceedings of the Royal Society of London A: Mathematical, Physical and Engineering Sciences, 1954, vol. 224, no. 1158, pp. 322-335: The Royal Society.
[62] V. Seshadri, R. Malhotra, and K. Sundar, "Concentration and size distribution of solids in a slurry pipeline," in Proc. 11th Natl. Conf. on FMFP, BHEL Hyderabad, India, 1982.
[63] V. Seshadri, S. Singh, D. J. P. s. Kaushal, "A model for the prediction of concentration and particle size distribution for the flow of multisized particulate suspensions through closed ducts and open channels," Particulate science and and technology, vol. 24, no. 2, pp. 239-258, 2006.
[64] K. P. S. A Kumar, S Gupta and D R Kaushal, "CFD modeling for solid-liquid flow in pipeline," YMCAUST international journal of research vol. volume 3, pp. 105-109 2015a.
[65] M. K. Gopaliya, D. J. J. o. H. Kaushal, and Hydromechanics, "Modeling of sand-water slurry flow through horizontal pipe using CFD," Journal of Hydrology and Hydromechanics, vol. 64, no. 3, pp. 261-272, 2016.

[66] K. P. Singh, A. Kumar, D. R. J. R. Kaushal, and R. J. o. Physics, "Computation Modelling for Fine Particle Flow in Horizontal Slurry Pipelines," Journal of Physics, vol. 8, no. 1, pp. 1-6, 2018.
[67] P. Doron, D. Granica, and D. J. I. J. o. M. F. Barnea, "Slurry flow in horizontal pipes—experimental and modeling," International Journal of Multiphase Flow, vol. 13, no. 4, pp. 535-547, 1987.
[68] Å. Sundqvist, A. Sellgren, and G. J. P. t. Addie, "Slurry pipeline friction losses for coarse and high density industrial products," Powder technology, vol. 89, no. 1, pp. 19-28, 1996.
[69] R. Gillies, K. Hill, M. Mckibben, and C. Shook, "Solids transport by laminar Newtonian flows," Powder Technology, vol. 104, no. 3, pp. 269-277, 1999.
[70] K. C. Ghanta and N. J. T. C. J. o. C. E. Purohit, "Pressure drop prediction in hydraulic transport of bi-dispersed particles of coal and copper ore in pipeline," The Canadian Journal of Chemical Engineering, vol. 77, no. 1, pp. 127-131, 1999.
[71] K. Wilson, R. Clift, and A. J. P. t. Sellgren, "Operating points for pipelines carrying concentrated heterogeneous slurries," Powder technology, vol. 123, no. 1, pp. 19-24, 2002.
[72] D. Kaushal, K. Sato, T. Toyota, K. Funatsu, and Y. Tomita, "Effect of particle size distribution on pressure drop and concentration profile in pipeline flow of highly concentrated slurry," International Journal of Multiphase Flow, vol. 31, no. 7, pp. 809-823, 2005.
[73] M. A. Garman, "Local particle velocity measurements in slurry flow in pipes and centrifugal pumps using ultrasound technique," Case Western Reserve University, 2015.
[74] T. Nabil, I. El-Sawaf, and K. El-Nahhas, "Computational fluid dynamics simulation of the solid-liquid slurry flow in a pipeline," in Proc. 17th International Water Technologies Conference IWTC17, 2013, pp. 5-7.
[75] G. V. Messa, M. Malin, and S. Malavasi, "Numerical prediction of fully-suspended slurry flow in horizontal pipes," Powder Technology, vol. 256, pp. 61-70, 2014.
[76] T. A. Akintola and O. J. L. J. o. S. Solomon, "Optimum pipe size selection for turbulent flow," Leonardo Journal of Sciences, vol. 8, no. 14, pp. 112-123, 2009.
[77] T. Asim, R. Mishra, S. Pradhan, and K. Ubbi, "A study on optimal sizing of pipeline transporting equi-sized particulate solid-liquid mixture," in Journal of Physics: Conference Series, 2012, vol. 364, no. 1, p. 012072: IOP Publishing.
[78] L. E. Kollár, R. Mishra, and T. J. P. C. Asim, "Particle size effects on optimal sizing and lifetime of pipelines transporting multi-sized solid-liquid mixtures," Procedia CIRP, vol. 11, pp. 317-322, 2013.
[79] C. F. J. I. J. o. M. P. Ihle, "A cost perspective for long distance ore pipeline water and energy utilization. Part I: Optimal base values," International Journal of Mineral Processing, vol. 122, pp. 1-12, 2013.

[80] B. Yildiz, A. B. Altan-Sakarya, A. M. J. C. E. Ger, and E. Systems, "Optimum design of slurry pipelines by genetic algorithm," Civil Engineering and Environmental Systems, vol. 31, no. 4, pp. 311-330, 2014.
[81] A. J. I. J. o. M. P. Thomas, "Scale-up methods for pipeline transport of slurries," International Journal of Mineral Processing, vol. 3, no. 1, pp. 51-69, 1976.
[82] R. H. Dieck, Measurement uncertainty: methods and applications. ISA, 2007.
[83] G. Ming, L. Ruixiang, N. Fusheng, and X. Liqun, "Hydraulic transport of coarse gravel–a laboratory investigation into flow resistance," in Global dredging congress, 2007, pp. 703-710.
[84] N. Fusheng, Z. Lijuan, X. Liqun, and W. Valsblom, "A model calculation for flow resistance in the hydraulic transport of sand," in Florida, USA: Proceedings of the 18th World Dredging Congress, 2007.
[85] S. Miedema, "Slurry Transport: Fundamentals, a historical overview and the Delft Head Loss & Limit Deposit Velocity Framework," 2016.
[86] V. Matoušek, "Predictive model for frictional pressure drop in settling-slurry pipe with stationary deposit," Powder Technology, vol. 192, no. 3, pp. 367-374, 2009.
[87] P. Vlasák, Z. Chára, J. Krupička, and J. Konfršt, "Experimental investigation of coarse particles-water mixture flow in horizontal and inclined pipes," Journal of Hydrology and Hydromechanics, vol. 62, no. 3, 2014.
[88] K. C. Wilson, "Slip point of beds in solid-liquid pipeline flow," Journal of the Hydraulics Division, vol. 96, no. 1, pp. 1-12, 1970.
[89] K. Wilson, M. Streat, and R. Bantin, "Slip model correlation of dense two phase flow," in Proc. 2nd Int. Conf. on Hydraulic Transport of Solids in Pipes, BHRA, Cranfield, UK, Paper B, 1972, vol. 1.
[90] K. Wilson, "A unified physically-based analysis of solid-liquid pipeline flow," in Proc. Hydrotransport, 1976, vol. 4, pp. 1-16.
[91] R. G. Gillies, J. Schaan, R. J. Sumner, M. J. McKibben, and C. A. Shook, "Deposition velocities for Newtonian slurries in turbulent flow," The Canadian Journal of Chemical Engineering, vol. 78, no. 4, pp. 704-708, 2000.
[92] C. E. Brennen, Fundamentals of multiphase flow. Cambridge University Press, 2005.
[93] K. Wilson, A. Sellgren, and G. Addie, "Near-wall fluid lift of particles in slurry pipelines," Zeszyty Naukowe Akademii Rolniczej we Wroclawiu. Konferencje (Poland), 2000.
[94] F. N. Krampa, "Two-fluid modelling of heterogeneous coarse particle slurry flows," 2009.
[95] M. Eesa, "CFD studies of complex fluid flows in pipes," University of Birmingham, 2009.
[96] T. Mali, V. Khudabadi, A. Rana, A. Vijay, and M. Adarsh, "Slurry flow pressure drop in pipes with modified wasp method," in SME Annual Meeting/Exhibit. Salt Lake City, 2014.

[97] A. Biswas, B. Gandhi, S. Singh, and V. Seshadri, "Characteristics of coal ash and their role in hydraulic design of ash disposal pipelines," Indian Journal of Engineering and Materials Sciences, vol. 7, no. 1, pp. 1-7, 2000.
[98] J. Hunt, "On the turbulent transport of a heterogeneous sediment," The Quarterly Journal of Mechanics and Applied Mathematics, vol. 22, no. 2, pp. 235-246, 1969.
[99] D. R. Kaushal, "Prediction of particle distribution in the flow of multisized particulate slurries through closed ducts and open channels," INDIAN INSTITUTE OF TECHNOLOGY, DELHI INDIA, 1995.
[100] D. Kaushal, V. Seshadri, and S. Singh, "Prediction of concentration and particle size distribution in the flow of multi-sized particulate slurry through rectangular duct," Applied Mathematical Modelling, vol. 26, no. 10, pp. 941-952, 2002.
[101] I. C. Walton, "Eddy diffusivity of solid particles in a turbulent liquid flow in a horizontal pipe," AIChE Journal, vol. 41, no. 7, pp. 1815-1820, 1995.
[102] P. A. Longwell, "Mechanics of Fluid flow," ed. New York: McGraw-Hill, 1977.
[103] J. Richardson and W. Zaki, "The sedimentation of a suspension of uniform spheres under conditions of viscous flow," Chemical Engineering Science, vol. 3, no. 2, pp. 65-73, 1954.
[104] M. Roco and C. Shook, "Computational method for coal slurry pipelines with heterogeneous size distribution," Powder Technology, vol. 39, no. 2, pp. 159-176, 1984.
[105] J. Vocaldo and M. Charles, "Prediction of pressure gradient for the horizontal turbulent flow of slurries," in 2nd International Conference on the Hydraulic Transport of Solids in Pipes, Coventry, UK, Paper, 1972, no. C1, pp. 1-12.
[106] M. Pechenkin, "EXPERIMENTAL STUDIES OF FLOWS WITH HIGH SOLID PARTICLE CONCENTRATIONS," 1969.
[107] T. Nabil, I. El-Sawaf, and K. J. I. W. T. J. El-Nahhas, "Sand-water slurry flow modelling in a horizontal pipeline by computational fluid dynamics technique," Int. Water Technol. Journal, vol. 4, pp. 1-17, 2014.

- **Appendices**

- **Appendix 1: The Regression Data of Equation (4.13)**

η_S (Practical)	V2/Vc	C2/(1-C2)	D50-Ak/Ak	η_S (MODEL)
0	1.016425856	0.276324186	0.87455	0.002032095
0.06	1.010934579	0.358142062	0.87455	0.006878223
0	2.01545	0.399776036	8.5	0.00848133
0	1.92745	0.40390285	8.5	0.009369649
0	2.62605	0.373437715	8.5	0.011114353
0	1.015821501	0.287664177	0.87455	0.013111402
0.048	1.011929825	0.348435814	0.87455	0.014389906
0	2.17895	0.393728223	8.5	0.015393379
0.014	1.01349162	0.341381623	0.87455	0.018737907
0.017	1.01356546	0.340842049	0.87455	0.019037535
0	1.015309168	0.296512382	0.87455	0.019502547
0.016	2.17975	0.388696014	8.5	0.020227882
0.007	1.013860104	0.329256945	0.87455	0.024120832
0	1.014909091	0.307360439	0.87455	0.024340352
0	1.014439024	0.319261214	0.87455	0.025822274
0.061	2.27975	0.383508578	8.5	0.029340163
0.03	1.73175	0.410437236	8.5	0.030113942
0.049	2.4158	0.378359752	8.5	0.036853852
0.063	1.020417537	0.206418145	1.63245	0.045466141
0.08	1.016659292	0.216397032	1.63245	0.047816544
0.022	1.031062992	0.196315349	1.63245	0.050220862
0.1	0.175866667	0.509433962	74	0.05310373
0	1.013478261	0.226542377	1.63245	0.055958292
0.107	1.005775656	0.229558588	1.63245	0.06017907
0.067	0.103	0.542020046	74	0.065169604
0.019	1	0.235635735	1.63245	0.068052634
0.123	0.994065657	0.239310943	1.63245	0.073533067
0.081	0.131833333	0.537279016	74	0.074227873
0.08	0.242066667	0.502178158	74	0.076042833
0.087	0.153733333	0.533272002	74	0.080153998
0	1.428133333	0.448016218	74	0.084266759

0.053	0.974176904	0.246261216	1.63245	0.085392149
0.133	0.987798408	0.247816321	1.63245	0.085859412
0.109	1.47005	0.416631251	8.5	0.089746762
0.115	0.1957	0.526717557	74	0.092335538
0.142	0.979083333	0.255650427	1.63245	0.097832954
0.072	0.959921671	0.256123603	1.63245	0.100674107
0.08	0.217966667	0.52578578	74	0.102596329
0.167	0.346466667	0.487652484	74	0.106822996
0.134	0.226266667	0.477104874	16.5	0.10695823
0.128	0.2387	0.523925632	74	0.110462779
0.146	0.2629	0.518833536	74	0.114594249
0.15	0.964375	0.267427123	1.63245	0.115209445
0.062	0.156966667	0.515151515	36.5	0.115416289
0.089	0.938444444	0.265983036	1.63245	0.115948309
0.166	0.282233333	0.514233798	74	0.116748158
0.11	0.187233333	0.506704837	36.5	0.117234312
0.17	0.272233333	0.465630954	16.5	0.120420251
0.153	0.960795107	0.272102786	1.63245	0.121310153
0.094	0.944637681	0.270809506	1.63245	0.121389336
0.12	0.2451	0.490979574	36.5	0.123289121
0.093	0.938651026	0.272750414	1.63245	0.124237783
0.214	1.511566667	0.426737052	36.5	0.125516015
0.004	1.2764	0.452011035	74	0.128880474
0.096	0.931957831	0.276976121	1.63245	0.129574675
0.183	0.943142857	0.27844541	1.63245	0.130165471
0.1	0.178866667	0.510802236	16.5	0.130516146
0.088	0.168466667	0.520912548	36.5	0.131146855
0.122	0.290733333	0.468213185	16.5	0.131832946
0.128	0.2248	0.497005988	16.5	0.132420073
0.148	0.422433333	0.482579689	74	0.134449772
0.114	0.246633333	0.499475184	36.5	0.136793385
0.071	0.418466667	0.486104919	74	0.137221877
0.193	1.2933	0.422272792	8.5	0.137483446
0.088	0.2227	0.501726986	16.5	0.138709909
0.179	0.356466667	0.507386192	74	0.141639641
0.127	0.89224359	0.286835671	1.63245	0.141741109
0.115	0.39385	0.490090896	8.5	0.142128058

0.146	0.912386935	0.437814522	12	0.143320247
0.155	0.889216216	0.443834825	12	0.144526977
0.143	0.916382488	0.429388222	12	0.144828859
0.204	1.2298	0.460280374	74	0.145244764
0.155	0.872877907	0.449695564	12	0.146081471
0.098	0.209	0.517220452	36.5	0.146386105
0.022	1.4338	0.429592566	36.5	0.146500055
0.217	0.300533333	0.479508803	16.5	0.147816066
0.153	0.876182965	0.457088737	12	0.148663406
0.154	0.341133333	0.455815985	16.5	0.14887132
0.236	1.4212	0.431434297	36.5	0.149599243
0.122	0.230033333	0.513775356	36.5	0.151641277
0.156	0.849094077	0.464343242	12	0.1534518
0.169	0.265666667	0.504438092	36.5	0.154595213
0.136	0.282566667	0.491869312	16.5	0.154717408
0.165	0.834130435	0.46713615	12	0.155507987
0.179	0.300633333	0.486325803	16.5	0.156218463
0.15	0.840261194	0.469075951	12	0.157114256
0.158	0.322766667	0.486988848	36.5	0.157172351
0.029	1.166233333	0.454968718	74	0.158729375
0.142	0.899295775	0.47080453	11.5	0.159626059
0.145	0.835647059	0.472320377	12	0.159976914
0.209	1.178266667	0.463914507	74	0.160711977
0.17	0.356633333	0.476886723	36.5	0.161285375
0.144	0.260633333	0.510117789	36.5	0.161413366
0.163	0.514466667	0.47579693	74	0.161844581
0.132	0.46465	0.482799526	8.5	0.161926063
0.169	0.873715847	0.479946722	11.5	0.170044635
0.177	0.4343	0.503985562	74	0.170383159
0.183	0.316666667	0.499250375	36.5	0.172003015
0.195	0.847857143	0.484119917	11.5	0.17552281
0.21	1.12445	0.432459533	8.5	0.176823333
0.194	0.368366667	0.476668636	16.5	0.177378546
0.237	0.389233333	0.467566774	16.5	0.178387998
0.187	0.495733333	0.494991778	74	0.17990139
0.205	0.820460526	0.488538255	11.5	0.181085163
0.13	1.425	0.39431121	16.5	0.183719696

0.182	0.607866667	0.470372004	74	0.183909712
0.238	1.071333333	0.466490688	74	0.185972275
0.196	0.60175	0.464343242	8.5	0.187833761
0.197	0.807883212	0.494544911	11.5	0.189292733
0.212	0.378766667	0.491869312	36.5	0.190348542
0.194	0.79048	0.498127341	11.5	0.193978183
0.102	1.262266667	0.43328078	36.5	0.19462173
0.185	0.5546	0.491869312	74	0.194634976
0.298	1.2526	0.435338022	36.5	0.196865465
0.195	1.01	0.438434983	8.5	0.196990067
0.175	0.789482759	0.502403846	11.5	0.200680046
0.159	0.925533333	0.459640928	74	0.201224942
0.147	0.468333333	0.446759259	16.5	0.201253057
0.191	0.746	0.464986815	74	0.203220919
0.25	0.437766667	0.484119917	36.5	0.205372135
0.221	0.474566667	0.457301078	16.5	0.207004207
0.165	0.74415	0.454757056	8.5	0.207487542
0.177	0.89675	0.447596989	8.5	0.208812056
0.242	0.9412	0.471886959	74	0.208980172
0.201	0.651	0.485663349	74	0.21017453
0.302	1.174	0.440507058	36.5	0.216726296
0.227	0.863633333	0.476668636	74	0.218081502
0.209	0.747733333	0.482359917	74	0.220270334
0.158	0.530433333	0.468644441	36.5	0.223117407
0.141	1.132066667	0.438434983	36.5	0.226639049
0.194	0.580733333	0.459640928	36.5	0.231864429
0.296	0.530066667	0.477978126	36.5	0.231994079
0.259	1.223933333	0.398992725	16.5	0.23633883
0.147	0.6043	0.436575205	16.5	0.244118512
0.334	1.0345	0.444251878	36.5	0.245688635
0.292	0.620766667	0.467351431	36.5	0.247112828
0.224	0.615866667	0.448435689	16.5	0.247366129
0.17	1.0153	0.442377037	36.5	0.24858359
0.204	0.714933333	0.45285486	36.5	0.255876391
0.328	0.9295	0.450326323	36.5	0.259740164
0.185	0.8866	0.448225923	36.5	0.261878516
0.247	0.7076	0.439470275	16.5	0.263810621

0.341	0.8239	0.454333915	36.5	0.2644684
0.299	0.757066667	0.462202076	36.5	0.265022127
0.113	0.746266667	0.427755568	16.5	0.270828974
0.249	0.803233333	0.431844215	16.5	0.273439434
0.324	0.841466667	0.425719989	16.5	0.276256497
0.097	0.8738	0.421868335	16.5	0.277542108
0.516	0.936133333	0.415428167	16.5	0.277558224
0.441	0.8517	0.420656343	16.5	0.278597461
0.262	0.9271	0.412828483	16.5	0.280019013
0.192	0.8674	0.416631251	16.5	0.280633398
0.373	0.9204	0.408054069	16.5	0.283991734

SUMMARY

OUTPUT

Regression Statistics	
Multiple R	0.811000033
R Square	0.657721053
Adjusted R Square	0.620245256
Standard Error	0.05598406
Observations	153

ANOVA

	df	SS	MS	F	Significance F		
Regression	15	0.825108207	0.055007214	17.55055543	5.66476E-25		
Residual	137	0.429387453	0.003134215				
Total	152	1.25449566					
	Coefficients	Standard Error	t Stat	P-value	Lower 95%	Upper 95%	Low
Intercept	8.245406796	7.745086877	1.064598361	0.288930468	-7.069969736	23.56078333	-7.0
X Variable 1	0.431438506	0.52501902	0.82175786	0.412642537	-0.606750491	1.469627503	-0.6
X Variable 2	-138.0951061	116.7980047	-1.182341312	0.239118293	-369.0551261	92.86491396	-36
X Variable 3	0.240656883	0.042983748	5.598787742	1.1362E-07	0.155659477	0.325654288	0.1
X Variable 4	0.562985221	1.075255145	0.523582913	0.601414588	-1.563257864	2.689228305	-1.5
X Variable 5	827.965109	681.8199176	1.214345735	0.226704764	-520.2868772	2176.217095	-52
X Variable 6	-0.038930014	0.007645992	-5.091558278	1.15113E-06	-0.054049437	-0.023810591	-0.0
X Variable 7	-1.228163519	0.974493598	-1.260309479	0.209700162	-3.155157575	0.698830538	-3.1
X Variable 8	-2361.554984	1928.494442	-1.224558875	0.222842948	-6175.020087	1451.910118	-61
X Variable 9	0.002400989	0.000491139	4.888612492	2.79924E-06	0.001429795	0.003372183	0.0
X Variable 10	0.618793236	0.395599634	1.564190619	0.120079807	-0.163477827	1.401064299	-0.1
X Variable 11	3219.702645	2647.517928	1.216121187	0.226029983	-2015.581942	8454.987232	-20
X Variable 12	-5.61453E-05	1.16987E-05	-4.799278138	4.10927E-06	-7.92787E-05	-3.30119E-05	-7.9
X Variable 13	-0.097265407	0.058667731	-1.657903013	0.099625087	-0.213276809	0.018745994	-0.2
X Variable 14	-1686.332564	1416.15272	-1.190784398	0.235797353	-4486.677153	1114.012026	-44
X Variable 15	4.08499E-07	8.58677E-08	4.757301984	4.91388E-06	2.38701E-07	5.78296E-07	2.3

- **Appendix 2: Matlab Codes**

Multi Layer Model

```
clc
clear all
CLIMY=zeros(1,11); CLIM=zeros(1,11);
%for KK=1:11;
% V=(KK/2)+0.5;
N=16;
data = xlsread('input.xls');
CWMAX = data(1,1);
AMUL = data(2,1);
ROS = data(3,1);
ROL = data(4,1);
EITA = data(5,1);
PD = data(6,:);
SP = data(8,:);
V = data(9,1);
ER=data(13,1);
D = data(14,1);
M = data(15,1);
AMS = data(16,1);
VMX1 = data(22,1);
VMN1 = data(23,1);
VN1 = data(24,1);
CW = data(25,1);
CV = data(26,1);
PREG = data(18,1);
R=D/2;
YC=zeros (1,N); X=zeros (1,N-1); B=zeros (1,N); AA=zeros (1,N); A=zeros
(1,N);
PD1=zeros(1,M-1);      SP3=zeros(1,M-1);      CFC=0.0;      CVH=zeros(1,M-
1);CBED=zeros(1,M-1); GITA=zeros(1,N);
CT=CV;
CMAX=(CWMAX/ROS)/((CWMAX/ROS)+((1-CWMAX)/ROL));
G=9.81;
SS=ROS/ROL;
DCF=((1.8*((AMUL/ROL).^2)/(G*(SS-1.0))).^0.333)*1000000.0;

for IJJ=1:N;
    CTT(IJJ)=CT;
end
for I=1:M;
    if PD(I)<DCF && I>1
        L=I-1;
        CFC=SP(L)-((PD(L)-DCF)/(PD(L)-PD(I))*(SP(L)-SP(I)));
        break
    end
    if I==N
      L=I-1;
        CFC=SP(L)-((PD(L)-DCF)/(PD(L)-PD(I))*(SP(L)-SP(I)));
    end
end
      CFL=1.0-(CFC);
```

```
      CF=CFC*CT/100;
      CR=CT-CF;
      AMUF=AMUL*(1.0+2.5*CF+10.5*(CF.^2.0));
      ROF=(ROL*(1.0-CT)+ROS*CF)/(1.0-CT+CF);
      CRC=1+6.88*CV;
for i=1:N;
    YC(i)=(i/N)*D;
    if i<N
    X(i)=((R^2)-((abs(R-YC(i)))^2))^0.5;
    end
    if i<=(N/2);
        B(i)=asin(X(i)/R);
    end
    if YC(i)<=R
       AA(i)=((D^2)/4)*(B(i)-sin(B(i))*cos(B(i)));
    end
end
A(1)=AA(1);
for i=2:N
    if i<=N/2;
    A(i)=AA(i)-AA(i-1);
    else
    A(i)=A(N-i+1);
    end
end
for II=1:M-1;
    PD1(II)=PD(II)+PD(II+1)/2.0;
    SP3(II)=SP(II)-SP(II+1);
    PD1(II)=PD1(II)/1000000.0;
    CJBAR(II)=SP3(II)*CT/100.0;
    VNF1(II)=G*(PD1(II).^2.0)*(ROS-ROF)/(18.0*AMUF);
    R18=VNF1(II)*PD1(II)*ROF/AMUF;
    if R18<0.02
        Z=(4.65+1.95*(PD1(II)/D))
    else if R18>0.02 && R18<1.0;
    Z=(4.35+17.5*(PD1(II)/D))*((R18).^(-0.03));
        else
            if R18>1 && R18<1000.0;
                XX=((G*(ROS-ROF)/ROF).^0.72)*(PD1(II).^1.18);
                XX1=((AMUF/ROF).^0.45);
               VNF1(II)=0.2*XX/XX1;
                R18=VNF1(II)*PD1(II)*ROF/AMUF;
               Z=(4.45+(18*(PD1(II)/D)))*((R18).^(-0.1));
            else
             VNF1(II)=sqrt((4.0*G*PD1(II)*(ROS-ROF)/(3.0*0.44*ROF)));
             Z=(4.45+(18*(PD1(II)/D)))*((R18).^(-0.1));
            end
        end
    end
end
G=9.81;
SS=ROS/ROL;
DCF1=((1.8*((AMUL/ROL).^2)/(G*(SS-1.0))).^0.333);
DCF=DCF1*1000000.0;
for I=1:M;
    if PD(I)<DCF && I>1
```

```
        L=I-1;
        CFC=SP(L)-((PD(L)-DCF)/(PD(L)-PD(I))*(SP(L)-SP(I)));
        break
    end
end
CFL=1.0-(CFC);
for I=1:M;
            SP1(I)=SP(I)-CFC;
            SP2(I)=SP1(I)*100.0/CFL;
            if SP2(I)<0.0;
                SP2(I)=0.0;
            end
end
  for II=1:M-1;
             PD1(II)=(PD(II)+PD(II+1)/2.0);
             SP4(II)=SP2(II)-SP2(II+1);
             PD1(II)=PD1(II)/1000000.0;
  end
  sum=0.0;
  DF=0.0;
  DC=0.0;

    %%%% CALCULATING DC THE AVERAGE DIAMETER OF +50% OF PARTICLES
  for i=1:M-1;
      sum=sum+SP4(i);
      if sum<50;
          SPC(i)=SP4(i);
          PDC(i)=PD1(i);
          DC=DC+(PDC(i)*SPC(i)/50);
          CC=sum;
      else if sum==50;
          SPC(i)=SP4(i);
          PDC(i)=PD1(i);
          DC=DC+(PDC(i)*SPC(i)/50);
              break
          else
          SPC(i)=50-CC;
          PDC(i)=PD1(i-1)+(((PD1(i)*sum)-(PD1(i-1)*(sum-
SP4(i))))/(SP4(i)-SP4(i-1)));
          DC=DC+(PDC(i)*SPC(i)/50);
     break
          end
      end
  end

    %%%% CALCULATING DF THE AVERAGE DIAMETER OF -50% OF PARTICLES
    NT=0.0;
    sum=0.0;
  for i=M-1:-1:1;
      NT=NT+1;
      sum=sum+SP4(i);
      if sum<50;
          SPF(NT)=SP4(i);
          PDF(NT)=PD1(i);
          DF=DF+(PDF(NT)*SPF(NT)/50);
          CC=sum;
```

```
      else if sum==50;
          SPF(NT)=SP4(i);
          PDF(NT)=PD1(i);
          DF=DF+(PDF(NT)*SPF(NT)/50);
              break
          else
          SPF(NT)=50-CC;
          if i<2;
              break
          end
          PDF(NT)=PD1(i-1)+(((PD1(i)*sum)-(PD1(i-1)*(sum-
SP4(i))))/(SP4(i)-SP4(i-1)));
          DF=DF+(PDF(NT)*SPF(NT)/50);
     break
          end
       end
  end
         D501=0.0;
 for I=1:M-1;
         D50=PD1(I)*SP4(I)/100;
         D50=D501+D50;
         D501=D50;
 end
for I=2:N;
            if SP2(I)<50;
                J=I-1;
                break
            end
end
           DPC=PD(J)-((SP2(J)-50)*(PD(J)-PD(I))/(SP2(J)-SP2(I)));
           DMD=DPC/1000000.0;
%%%%%%%%%%   PRESSURE DROP %%%%%%%
CT=CV;
AK=0.00002;
P=0.026*((AK/D).^0.225)+0.133*AK/D;  %%% unitless
Q=22.0*((AK/D).^0.44);  %%% unitless
R=1.62*((AK/D).^0.136);   %%% unitless
REE=(ROL*V*D)/AMUL;   %%% unitless
AFA=P+Q*(1./(REE.^R));  %%% unitless
WPL=2.0*AFA*(V.^2.0)/(9.81*D);  %%% unitless
CF=CFC*CT;
AMUF=AMUL*(1.0+2.5*CF+10.5*(CF.^2.0));
ROF=(ROL*(1.0-CT)+ROS*CF)/(1.0-CT+CF);
CRC=1+6.88*CV; %%%%%%%%%%% 945
VINF=(9.81*(D50.^2.0)*(ROS-ROF))/(18.0*AMUF)/CRC;
R8=(VINF*D50*ROF)/AMUF;     %%% Settling Reynolds Number
for K=1:100000;
if R8<1
    break
end
XP=4.0*9.81*(D50.^1.625)*(ROS-ROF)/90.0;
    X11=(ROF.^0.375)*(AMUF.^0.625);
    X22=XP/X11;
    VINF=(X22.^0.727)/CRC;

    R8=VINF*D50*ROF/AMUF;
```

```
    if R8>1000;
        VINF=sqrt((4.0*9.81*D50*(ROS-ROF))/(3.0*0.10*ROF))/CRC;
    end
    R8=VINF*D50*ROF/AMUF;
end

%%%%%%%%%%%%%%%%%%%%%%%%%%%%%%%%    MLAYER    CONCENTRATION    DISTRIBUTION
%%%%%%%%%%%%%%%%%%%%%%%%%%%%%%%%
AMUFM=AMUL*(1.0+(2.5*CT)+10.5*(CT.^2.0));
ROM=ROS*CT+(1.-CT)*ROL;
REM=ROM*V*D/AMUFM;
 if REM<2000.0;
    F1=16.0/(PRI);
 end
P=0.026*((AK/D).^0.225)+0.133*AK/D;  %%%%%%%%%%340
Q=22.0*((AK/D).^0.44);
R=1.62*((AK/D).^0.136);
F1M=P+Q*(1./(REM.^R));
PRE=(2.0*F1M*(V.^2.0)*(ROM/ROL)/(9.81*D));
USTAR=sqrt(PRE*G*D/4.);
for i=1:N;
    if (YC(i)/D) <= 0.337 && (YC(i)/D)>=0.0;
        GCOF=0.369*USTAR*(YC(i)/R);
    else if (YC(i)/D) >= 0.337 && (YC(i)/D)<=0.663
          GCOF=0.0775*R*USTAR;
        else
            GCOF=0.369*R*USTAR*((YC(i)/R)-1)*(2-(YC(i)/R));
        end
    end

    % GITA(i)=GCOF*(1.0+0.12504*exp(4.22054*(CTT(i)/CMAX)));
    % if GITA(i)==0;
    % GITA(i)=0.01;
    % end
end
for IIL=1:M-1;
    CJBAR(IIL)=SP3(IIL)*CT/1.0;
    VNF1(IIL)=G*(PD1(IIL).^2.0)*(ROS-ROF)/(18.0*AMUF);
    R18=VNF1(IIL)*PD1(IIL)*ROF/AMUF;
     Z=(4.65+1.95*(PD1(IIL)/D));
    for RR=1:1000000;
        if R18>0.002 && R18<0.2 ;
           break
        end
        Z=(4.35+17.5*(PD1(IIL)/D))*((R18).^(-0.03));
        if R18>0.2 && R18<1;
            break
        end
        XX=((G*(ROS-ROF)/ROF).^0.72)*(PD1(IIL).^1.18);
        XX1=((AMUF/ROF).^0.45);
        VNF1(IIL)=0.2*XX/XX1;
        R18=VNF1(IIL)*PD1(IIL)*ROF/AMUF;
        Z=(4.45+18*(PD1(IIL)/D))*((R18).^(-0.1));
        if R18>1 && R18<1000.0;
            break
        end
```

```
            VNF1(IIL)=sqrt((4.0*G*PD1(IIL)*(ROS-ROF)/(3.0*0.44*ROF)));
            Z=(4.45+18*(PD1(IIL)/D))*((R18).^(-0.1));
        if R18>1000 && R18<200000.0;
            break
        end
         VNF1(IIL)=sqrt((4.0*G*PD1(IIL)*(ROS-ROF)/(3.0*0.1*ROF)));
           Z=(4.45+18*(PD1(IIL)/D))*((R18).^(-0.1));
    end
    for IN=1:N;
        VINF1(IIL,IN)=VNF1(IIL)*(1.0-CTT(IN).^Z);
    end
end

  for IIL=1:M-1;
    for IN=1:N;
        VINF1(IIL,IN)=VNF1(IIL)*(1.0-CTT(IN).^Z);
    end
  end

    for IJI=1:N;
   YR(IJI)=IJI*(2/(N-1))-(1+(2/(N-1)));
    YD(IJI)=(YR(IJI)+1.0)/2.0;
    if YD(IJI)<=0.337 && YD(IJI)>=0.0
        YYD=YD(IJI)*D;
         GCOF=0.369*(2*YD(IJI))*(1.-(2*YD(IJI)));
    else if YD(IJI)>=0.337 && YD(IJI)<=0.663
       if YD(IJI)<0.5;
           YYD=YD(IJI)*D;
       else
           YYD=D*(1.-YD(IJI));
       end
          GCOF=0.0775;
        else
            YYD=D*(1.-YD(IJI));
           GCOF=0.369*((2*YD(IJI))-1)*(2-(2*YD(IJI)));
        end
    end
       % if GCOF<0.0775
       % GCOF=0.0775;
       % end

        GITA(IJI)=GCOF*(1.0+0.12504*exp(4.22054*(CTT(IJI)/CMAX)));
      if GITA(IJI)==0;
         GITA(IJI)=0.01;
     end
    end
 for III=1:M-1;
    for IM=1:N;
        AKJ(III,IM)=VINF1(III,IM)/(USTAR*GITA(IM));
       for ITH=1:180;
           PI=22/7;
           TH=(ITH)*PI/180;
           FT(ITH)=exp(-AKJ(III,IM)*cos(TH)*sin(TH)*sin(TH));
       end  %}
       DSUM=0.0;
       for IE=2:2:178;
```

```
            DSUM=DSUM+FT(IE);
        end
        DSUM1=0.0;
        for IO=3:2:179;
            DSUM1=DSUM1+FT(IO);
        end
        EKJ(III,IM)=(2/180)*(FT(1)+FT(180)+(2*DSUM1)+(4*DSUM))/3;
        VJB(III)=CJBAR(III)/(1-CT);
     end
  end
     for IJK=1:M-1;
     for IJI=1:N;
         YR(IJI)=IJI*(2/(N-1))-(1+(2/(N-1)));
         YD(IJI)=(YR(IJI)+1)/2;
         P(IJK,IJI)=exp((-AKJ(IJK,IJI)*YR(IJI)));
         if P(IJK,IJI)>1e94;
             P(IJK,IJI)=1e94;
         end
         COF(IJK,IJI)=(VJB(IJK)/EKJ(IJK,IJI))*P(IJK,IJI);
     end
end
     for KII=1:N;
     ECOFJ=0.0;
     for KI=1:M-1;
         ECOF(KII)=COF(KI,KII)+ECOFJ;
         ECOFJ=ECOF(KII);
     end
     end
     CLIM=CMAX-0.074*((V/VINF).^0.44)*((1-CR).^0.189)*(CMAX-CR);
for KFI=1:M-1;
     for KFII=1:N;
         C(KFI,KFII)=COF(KFI,KFII)/(1.0+ECOF(KFII));
%%%%%%%%%%%%%%%%%%%%%%%%%%%%%%%%%%%%%%%%%%%%%%%%%%%%%%%
         CAB1(KFI,KFII)=C(KFI,KFII)/CJBAR(KFI);
     end
end
CNET=zeros(1,N-6);
     for i=1:N-6;
         sum=0.0;
         for j=1:M-1;
             sum=sum+C(j,i+3);
         end
             CNET(i)=sum;
     end
%CLIMY=0.0;
for I=1:N;
     L=C(:,I);
     SUM=0.0;
     for J=1:M-1;
         SUM=SUM+L(J);
     end
     CL(I)=SUM;
     if abs(CL(I)-CLIM)<=0.025;
         CLIMY=I/N;
     end
end
```

```
%%%%%%%%%%%%%%%%%%%%% START EDITING VELOCITY PROFILE %%%%%%%%%%%%%%
%%%%%%%%%%%%%%%% DIVIDING EACH CHORD IN TO 6 PARTS %%%%%%%%%%%%%%%%%%%%
for I=1:N-1;
    XX=X(I)/6;
    XPP(I,1)=0.0;
    for J=2:7;
        XPP(I,J)=XPP(I,J-1)+XX;
    end
end
%%%%%%%%%%%%%%%%%%%%%%%%%%%%%%%%%%%%%%%%%%%%%%%%%%%%%%%%%%%%%%%%%%%%%%%
%%%%%%%%%% DETERMINATION OF RADIAL DISTANCES AND IDENTIFYING DIFFERENT
POINTS ALONG IT%%%%%%%%%%%%%%%%%%%%%%
%%%%%%%%%%%%%%%%%%%%%%%%%%%%%%%%%%%%%%%%%%%%%%%%%%%%%%%%%%%%%%%%%%%%%%%%
for I=1:N-1;
    for J=1:7;
        if YD(I)<0.5
            YD1(I)=(D/2)-(YD(I)*D);    %%%% YVR=YD, YVR1=YD1
        else
            YD1(I)=YD(I)*D-(D/2);
        end
        RZ(I,J)=sqrt((YD1(I)^2)+(XPP(I,J)^2));     %%% DISTANCE TO THE
CENTRE
        RPP(I,J)=(D/2)-RZ(I,J);                  %%% DISTANCE TO THE WALL
    end
end

%%%%%%%%%%%%%%%%%%%% IDENTIFYING POINTS ALONG RADIAL UP TO THE WALL
%%%%%%%%%%%%%%%%%%%%%%%%%%%%%%%%%%%%%%
for I=1:N-1;
    for J=1:7;
        RPN=RPP(I,J)/6;
        RP1(I,J,1)=0.0;
        for K=2:7;
            RP1(I,J,K)=RP1(I,J,K-1)+RPN;
        end
    end
end
%%%%%%%%%%%%%%%%%%%%%%%%%%%%%%%%%%%%%%%%%%%%%%%%%%%%%%%%%%%%%%%%%%%%%%%%
%%%%%%%%%%%%%%%%%%%%%%%%%%%%%%%%%%%%%%
%%%%%%%%%%%%%%%%%%%  CALCULATION OF EQUIVALENT VERTICAL DISTANCES
%%%%%%%%%%%%%%%%%%%%%%%%%%%%%%%%%%%%%%

for I=1:N-1;
        TH1(I,1)=0.0;
        for J=1:7;
            TT=XPP(I,J)/abs((YD(I)*D-(D/2)));
            TH1(I,J)=atan(TT);
           %COS(I,J)=cos(TH1(I,J));
        end
end
 for I=1:N-1;
     for J=1:7;
         for K=1:7;
             if (YD(I)<0.5);
                   FF(I,J,K)=(((D/2)-RP1(I,J,K))*cos(TH1(I,J)));
```

```
                YCC(I,J,K)=((D/2)-FF(I,J,K))/D;

            else
               FF(I,J,K)=(((D/2)-RP1(I,J,K))*cos(TH1(I,J)));
                YCC(I,J,K)=((D/2)+FF(I,J,K))/D;

            end
            if (YCC(I,J,K)<1e-10);
                YCC(I,J,K)=0.0;
            end
        end
    end
 end
X1=zeros(1,4);
X2=zeros(1,4);
[ YD,X2 ] = cinter2( CNET,YD,X2,N);   %%%%%%%%%%%%%%%%%%%%%% CALLING cinter
FUNCTION (cinter.m)
PI=22./7.;
for I=1:N;
    DC1=0.0;
    for II=1:M-1;
        DC(I)=C(II,I)*PD1(II)+DC1;
        DC1=DC(I);
    end
    DC(I)=DC(I)/CTT(I);
    %disp ('DC(I)'); disp (DC(I));
end
[ YD,X2 ] = cinter2( CNET,YD,X2,N);  %%%%%%%%%%%%%%%%%%%%%% CALLING cinter
FUNCTION (cinter.m)
for I=1:N-1;
    for J=1:7;
        for K=1:7;
            PAA=0.0;
            PCC=0.0;
            YLY=YCC(I,J,K);
            for NN=1:4;
                CTTCC(I,J,K)=X1(NN)*(YCC(I,J,K)^(NN-1))+PAA;
                DCC(I,J,K)=X2(NN)*(YCC(I,J,K)^(NN-1))+PCC;
                PAA=CTTCC(I,J,K);
                PCC=DCC(I,J,K);
           end
        end
    end
end

PAPP=1.0;
AC=0.7;
% for WW=1:100000;
POP=zeros(N-3,7,7);
KK=zeros(N-3,7,7);
for I=2:N-1;
    for J=1:7;
        for K=1:7;
            FR1(I,J,K)=USTAR^2.0/(G*DCC(I,J,K)*(SS-1)); % Froude Number
            FILS1(I,J,K)=(1-(CTTCC(I,J,K)/CMAX));  %  Coefficient  for
influence of solid particles on turbulence intensity
```

```
            if FILS1(I,J,K)<0;
                FILS1(I,J,K)=0;
            end
            if FR1(I,J,K)<0.01;
                FR1(I,J,K)=0.01;
            end
            KK(I,J,K)=1/FR1(I,J,K);
            POP(I,J,K)=exp(KK(I,J,K));
            FIS1(I,J,K)=(POP(I,J,K))/((1-(CTTCC(I,J,K)/CMAX)^AC));
            FCC(I,J,K)=(1-
CTTCC(I,J,K))*FILS1(I,J,K)+CTTCC(I,J,K)*SS*FIS1(I,J,K);
        end
    end
end
%%%%%%%%%%% CALCULATION OF Y EQUAVALENT FOR EACH POINT %%%%%%%%
for I=2:N-1;
    for J=1:7;
        YQ1(I,J,1)=0.0;
        RPN=RPP(I,J)/6.0;
        for K=2:7;
            YQ1(I,J,K)=YQ1(I,J,K-1)+(RPN/((FCC(I,J,K)+FCC(I,J,K-
1))/2));
        end
        YYQ(I,J)=YQ1(I,J,7);
    end
end
for I=2:N-1;
    for J=1:7;
        GDR(I,J)=0.25*PRE*ROL*G*(((D^2)/4)-(RZ(I,J)^2));
    end
end

AMUM=AMUL*(1+2.5*CV+10.5*(CV^2));
for I=2:N-1;
    for J=1:6;
        DM1(I,J)=((1-DCC(I,J,7))*ROL)+(DCC(I,J,7)*ROS);
        ALFM1(I,J)=0.25*D*(1-(4*((RZ(I,J)/D)^2)))*((8.5-
5.75*log(abs(((AK+3.3*(AMUM/(DM1(I,J)+0.001))/USTAR))/(YYQ(I,J)+0.01)))
)^(-2))*DM1(I,J); % Dynamic coefficient of Turbulence (5.54) june
        VVM1(I,J)=-AMUM/(2*ALFM1(I,J));          %% (5.47) june
        VVM2(I,J)=(VVM1(I,J)*VVM1(I,J))+(GDR(I,J)/ALFM1(I,J));         %%
(5.47) june
        VVM(I,J)=((VVM1(I,J)+sqrt(VVM2(I,J))));    %% (5.47) june
    end
end

for I=1:N-2;
    for J=1:6;
        VVMM(I,J)=VVM(I+1,J);
    end
end
    VT=VVMM(:,1);
VTM=mean(VT);
while VTM>V;
    for I=1:N-2;
    VT(I)=VT(I)-0.1;
```

```
    end
    VTM=mean(VT);
end

%%%%%%%%%%%%%%%%% END OF VELOCITY PROFILE
VTT=zeros(1,N-1);
VTT(1)=VT(1);
VTT(N)=VT(N-2);
for I=2:N-1
VTT(I)=VT(I-1);
end
```

Optimisation Model

```
clear all;
clc;
pi=22/7; cp=0.2; Lp=1000; CC=0.001; MU=0.7; C22=950; C11=1.4;
PD=zeros(1,40);   SP=zeros(1,20);   SP2=zeros(1,20);   PD1=zeros(1,120);
SP3=zeros(1,40);
AKJ =zeros(50,50); EKJ =0; VP=0.0;
zeros(50,50); CJBAR=zeros(1,50); VJB=zeros(1,50);
YR=zeros(1,50); COF =zeros(50,50); ECOF =zeros(1,50); C=zeros(100,100);
CTT=zeros(1,50); SP4=zeros(1,50);
CTT1=zeros(1,50);     CAB1     =zeros(50,50);     FILS     =zeros(10,50);
FIS=zeros(1,50); DR=zeros(1,50); YV=zeros(1,50);
ALFO=zeros(1,50);     DALFO     =zeros(1,50);     DALFM     =zeros(1,50);
ALFM=zeros(1,50); GDR=zeros(1,50);
VM=zeros(10,50);   VM1=zeros(1,50);   VM2   =zeros(1,50);   YD=zeros(1,50);
DALM=zeros(1,50); FT=zeros(1,500);
CTTW=zeros(1,100); GITA =zeros(1,50); DR1 =zeros(1,50); YQ=zeros(1,50);
FC=zeros(10,50); YD1=zeros(1,50);
YY=zeros(1,101);  AXX  =zeros(1,101);  AA  =zeros(1,20);  OSUM=zeros(1,10);
ESUM=zeros(1,10);
DM=zeros(1,50);   DC   =zeros(1,50);   FR   =zeros(1,50);   VD1=zeros(1,20);
DPW=zeros(1,20); X1=zeros(1,50);
BA1=zeros(1,50);  BAQ  =zeros(1,50);  BQ  =zeros(1,50);  CTTT=zeros(10,50);
EW=zeros(1,50);
CFC=0.0; D50=2.075; SS=0.0; DD50=0.0; DMD=0.0;
SP1=zeros(1,20); SP3=zeros(1,40); SP4=zeros(1,50);
AK=0.0002; F1=0.0; CV1=0.0; AMUFM=0.0; C1=0.0; C2=0.0; VV=zeros(1,20);
DD=[2 3 4 5 6 8 10 12 14 16 18 20 22 24 28];
for i=1:15;
    DD(i)=DD(i)*0.0254;
end
for iq=1:15;
D=DD(iq);
data = xlsread('input.xls');
CWMAX = data(1,1);
AMUL = data(2,1);
ROS = data(3,1);
ROL = data(4,1);
EITA = data(5,1);
PD = data(6,:);
```

```
SP = data(8,:);
%V = data(9,1);
ER=data(13,1);
%D = data(14,1);
N = data(15,1);
AMS = data(16,1);
VMX1 = data(22,1);
VMN1 = data(23,1);
VN1 = data(24,1);
CW = data(25,1);
CV = data(26,1);
PREG = data(18,1);
QS = data(20,1);
A=(pi/4)*(D^2);
QW=(1/CV)*(QS/ROS);
Qm=QW*(1+(CV/(1-CV)));
VV(iq)=Qm/A;
V=VV(iq);
while V>1.0 && V<6.0;

%CMAX=CWMAX;
%PP = data(30,1);
%disp('STATIC SETT. CONC.:'); disp (CWMAX)
disp('VISCOSITY:'); disp (AMUL);
CMAX=(CWMAX/ROS)/((CWMAX/ROS)+((1-CWMAX)/ROL));
PRE=0.0; V2=0.0;
PI=22/7;
G=9.81;
flag=0.0;
if CW==0.0;
    if CV==0;
        return
    end
end
CT=CV;
[ CFC, D50, SS, DD50, DMD, DCF, SP2 ] = part( N, PD, SP, AMUL, ROS, ROL,
PD1, SP2, SP3, SP4 );
disp ('DCF='); disp(DCF); disp ('CT='); disp(CT);
AAK=1;
%AAK = input ('IF DEPOSITION VELOCITY REQUIRED TYPE 0 ELSE POS REAL');
for MM=1:100000; %%%%%%%%%%%% goto 12;
if AAK>0.; %%%% goto 12
     break
  end
AK=0.00020;
%%%%%%%%%%%%%%%%%%%%dp.m%%%%%%%%%%%%%%%
%VP=4.;
%for EETT=1:10000;
VP=4.;
for I=1:1000000;
    if I>11
        disp ('BY TYPING 1 YOU CAN COME OUT OF THE MODULE');
        disp ('WHRITE OTHER NO. TO CONTINUE');
        disp ('THIS PROVISION IS MADE IN CASE OF NON CONVER.');
        OUT = input;
        if OUT==1.0;
```

```
            return
        end
    end
    [PRE,V2,AMUF,ROF,USTAR,VINF, C1, C2,V1,B,EITA, CV1,CT] = pres(C1, C2,
AK,SP2,PD,CMAX,VMN1,VMX1,VN1,ER,CFC,CT,V,AMUL,D,N,EITA,ROS,ROL,D50,DMD,
CV)  %%%%552 (17)
if V2>0.0;
      VP=VP-.05;

  end
  if V2<0.8
         disp ('DEPOSITION NOT ENCOUNTERED');
      end
    break
end
  %if PRE<=PREG
  if V2<0.0;
  disp ('V2='); disp (V2);
  disp ('DEPOSITION VELOCITY'); disp (VP);
  return
  end


%EITA1=input('if estimate of deposition velocity is already available
change EITA to match the two values give new value of Eita else type
0.0');
 % if EITA1==0.0;
  %        break
  %end
   %EITA=EITA1;
%end
break
  %end
end
for UU=1:10000; %%%%%%%%%%%%%%%%%%%%%%%%%%%%%%%%%%%%%%%%   goto 16
for ZZ=1:10000; %%%%%%%%%%%%%%%%%%%%%%%%%%%%%%%%%%%%%%%%%%%%%%%%
    %for PREGGG=1:10000000
[PRE,V2,AMUF,ROF,USTAR,VINF,  C1,  C2,V1,B,EITA,  CV1,CT]  =  pres(C1,  C2,
AK,SP2,PD,CMAX,VMN1,VMX1,VN1,ER,CFC,CT,V,AMUL,D,N,EITA,ROS,ROL,D50,DMD,
CV)  %%%%552 (17)
%disp ('PRESSSURE DROP PRE'); disp (PRE);
%disp ('VELOCITY V'); disp (V);
%disp ('CONCENTRATION CT'); disp (CT);
%disp ('CV1'); disp (CV1);
% if PRE<=PREG
      %  break
%end

%EITA=EITA-0.001;
    %end

if CV1==100.0;
% PREX = input ('GIVE VALUE OF MEASURED GRADIENT IF AVAILABLE ELSE WRITE
0.0 EXPERIMENTAL VALUE');
 PREX=0.0;
```

```
 flag=222.0;
      break   %%%%%%%%%%% goto 22  (goto 34)
end
CV1D=abs(CV-CV1);
if CV1D>0.01;
    disp   ('MASS   BALANCE   NOT   SATISFIED   CARRYING   OUT   ITER');
%%%%%%%%%%%%%%%%%%%%%% (19)
    flag=2121;
else
    PREX=0.0;
   %PREX = input ('GIVE VALUE OF MEASURED GRADIENT IF AVAILABLE ELSE WRITE
0.0 EXPERIMENTAL VALUE');
   CVDST=1;
   %CVDST = input ('TYPE 0. IF CONC. & VELOCITY DISTRIBUTION IS REQUIRED
ELSE POS. REAL');
   if CVDST==0.0;
    flag=333.0;
      break  %%%%%%%%%%% goto 23
   end
end
VCC=((2*9.81*D*(SS-1))^0.5)*1.7951*(CV^(0.1087))*((1-
CV)^(0.2401))*(((ROL*D*((9.81*D*(SS-
1))^(0.5)))/AMUL)^(0.00179))*((D50/D)^(0.06623));
 CVD=CV-CV1;
CV2=abs(CVD);
disp ('CV2='); disp (CV2);
if CV2<0.010
   break   %%%%%%%%%%% goto 22
end
CT=CT+0.01;
disp ('MASS BALANCE NOT SATISFIED CARRYING OUT ITER');
end
if flag==222;
    break
end
USTAR=sqrt(PRE*G*D/4.); %%%%%%%%%%%%%%%%%%%%%%%% (23)
break
end
t=CC*D;
Cp(iq)=pi*D*t*cp*C22*Lp;
P=Qm*PRE/MU;
Co(iq)=C11*P;
Ct(iq)=Cp(iq)+Co(iq);
break
end
end
```

Wasp Model

```
clc
clear all
N=5;
data = xlsread('inputz.xls');
```

```
CWMAX = data(1,1);
AMUL = data(2,1);
ROS = data(3,1);
ROL = data(4,1);
EITA = data(5,1);
PD = data(6,1);
SP = data(8,:);
V = data(9,1);
ER=data(13,1);
D = data(14,1);
M = data(15,1);
AMS = data(16,1);
VMX1 = data(22,1);
VMN1 = data(23,1);
VN1 = data(24,1);
CW = data(25,1);
CV = data(26,1);
PREG = data(18,1);
R=D/2;
YC=zeros (1,N); X=zeros (1,N-1); B=zeros (1,N); AA=zeros (1,N); A=zeros
(1,N);
%PD1=zeros(1,M-1);     SP3=zeros(1,M-1);     CFC=0.0;     CVH=zeros(1,M-
1);CBED=zeros(1,M-1);
CT=CV;
G=9.81;
SS=ROS/ROL;
DCF=((1.8*((AMUL/ROL).^2)/(G*(SS-1.0))).^0.333)*1000000.0;
for IJJ=1:N;
    CTT(IJJ)=CT;
end

    if PD<DCF
        CFC=0.0;
    else
        CFC=1.0;
    end
      CFL=1.0-(CFC);
      CF=CFC*CT/100;
      CR=CT-CF;
      AMUF=AMUL*(1.0+2.5*CF+10.5*(CF.^2.0));
      ROF=(ROL*(1.0-CT)+ROS*CF)/(1.0-CT+CF);
      CRC=1+6.88*CV;
for i=1:N;
    YC(i)=(i/N)*D;
    if i<N
    X(i)=((R^2)-((abs(R-YC(i)))^2))^0.5;
    end
    if i<=(N/2);
        B(i)=asin(X(i)/R);
    end
    if YC(i)<=R
       AA(i)=((D^2)/4)*(B(i)-sin(B(i))*cos(B(i)));
    end
end
A(1)=AA(1);
for i=2:N
```

```
    if i<=N/2;
    A(i)=AA(i)-AA(i-1);
    else
    A(i)=A(N-i+1);
    end
end

    PD1=PD/1000000.0;
    CJBAR=CT/100.0;
    VNF1=G*(PD1.^2.0)*(ROS-ROF)/(18.0*AMUF);
    disp ('PD1'); disp (PD1);
    disp ('ROF'); disp (ROF);
    disp ('AMUF'); disp (AMUF);
    R18=VNF1*PD1*ROF/AMUF;
    if R18<0.02
        Z=(4.65+1.95*(PD1/D))
    else if R18>0.02 && R18<1.0;
    Z=(4.35+17.5*(PD1/D))*((R18).^(-0.03));
        else
            if R18>1 && R18<1000.0;
                XX=((G*(ROS-ROF)/ROF).^0.72)*(PD1.^1.18);
                XX1=((AMUF/ROF).^0.45);
               VNF1=0.2*XX/XX1;
                R18=VNF1*PD1*ROF/AMUF;
               Z=(4.45+(18*(PD1/D)))*((R18).^(-0.1));
            else
             VNF1=sqrt((4.0*G*PD1*(ROS-ROF)/(3.0*0.44*ROF)));
             Z=(4.45+(18*(PD1/D)))*((R18).^(-0.1));
            end
        end
    end

G=9.81;
SS=ROS/ROL;
DCF1=((1.8*((AMUL/ROL).^2)/(G*(SS-1.0))).^0.333);
DCF=DCF1*1000000.0;


  sum=0.0;
  DF=0.0;
  DC=0.0;

    %%%% CALCULATING DC THE AVERAGE DIAMETER OF +50% OF PARTICLE

    %%%% CALCULATING DF THE AVERAGE DIAMETER OF -50% OF PARTICLES
           DMD=PD/1000000.0;
%%%%%%%%%%   PRESSURE DROP %%%%%%%
CT=CV;
AK=0.00002;
P=0.026*((AK/D).^0.225)+0.133*AK/D;  %%% unitless
Q=22.0*((AK/D).^0.44);  %%% unitless
R=1.62*((AK/D).^0.136);   %%% unitless
REE=(ROL*V*D)/AMUL;   %%% unitless
AFA=P+Q*(1./(REE.^R));  %%% unitless
WPL=2.0*AFA*(V.^2.0)/(9.81*D);  %%% unitless
```

```
CF=CFC*CT;
AMUF=AMUL*(1.0+2.5*CF+10.5*(CF.^2.0));
ROF=(ROL*(1.0-CT)+ROS*CF)/(1.0-CT+CF);
CRC=1+6.88*CV; %%%%%%%%%%% 945
VINF=(9.81*(PD.^2.0)*(ROS-ROF))/(18.0*AMUF)/CRC;
R8=(VINF*PD*ROF)/AMUF;      %%% Settling Reynolds Number
for K=1:100000;
if R8<1
    break
end
XP=4.0*9.81*(PD.^1.625)*(ROS-ROF)/90.0;
    X11=(ROF.^0.375)*(AMUF.^0.625);
    X22=XP/X11;
    VINF=(X22.^0.727)/CRC;

    R8=VINF*PD*ROF/AMUF;
    if R8>1000;
        VINF=sqrt((4.0*9.81*PD*(ROS-ROF))/(3.0*0.10*ROF))/CRC;
    end
    R8=VINF*PD*ROF/AMUF;
end

%%%%%%%%%%%%%%%%%%%%%%%%%%%%%%%%    MLAYER    CONCENTRATION    DISTRIBUTION
%%%%%%%%%%%%%%%%%%%%%%%%%%%%%%%%
AMUFM=AMUL*(1.0+(2.5*CT)+10.5*(CT.^2.0));
ROM=ROS*CT+(1.-CT)*ROL;
REM=ROM*V*D/AMUFM;
 if REM<2000.0;
F1=16.0/(PRI);
     end
P=0.026*((AK/D).^0.225)+0.133*AK/D;  %%%%%%%%%%340
Q=22.0*((AK/D).^0.44);
R=1.62*((AK/D).^0.136);
F1M=P+Q*(1./(REM.^R));
PRE=(2.0*F1M*(V.^2.0)*(ROM/ROL)/(9.81*D));
USTAR=sqrt(PRE*G*D/4.);

for i=1:N;
    if (YC(i)/D) <= 0.337 && (YC(i)/D)>=0.0;
        GCOF=0.369*USTAR*(YC(i)/R);
    else if (YC(i)/D) >= 0.337 && (YC(i)/D)<=0.663
          GCOF=0.0775*R*USTAR;
        else
            GCOF=0.369*R*USTAR*((YC(i)/R)-1)*(2-(YC(i)/R));
        end
    end
    %GITA(i)=GCOF*(1.0+0.12504*exp(4.22054*(CTT(i)/CMAX)));
    %if GITA(i)==0;
     %  GITA(i)=0.01;
    % end
end


    CJBAR=CT/100.0;
    VNF1=G*(PD1.^2.0)*(ROS-ROF)/(18.0*AMUF);
```

```
  R18=VNF1*PD1*ROF/AMUF;
  Z=(4.35+17.5*(PD1/D))*((R18).^(-0.03));
  CD=24*((R18).^(-1));
  for RR=1:1000000;
      if R18<1;
          break
      end
      XX=((G*(ROS-ROF)/ROF).^0.72)*(PD1.^1.18);
      XX1=((AMUF/ROF).^0.45);
      VNF1=0.2*XX/XX1;
      R18=VNF1*PD1*ROF/AMUF;
      Z=4.45*((R18).^(-0.1));
      CD=(24/R18)*(1+(0.15*(R18).^0.687));
      if R18>1 && R18<1000.0;
          break
      end
          VNF1=sqrt((4.0*G*PD1*(ROS-ROF)/(3.0*0.44*ROF)));
          Z=2.39;
          CD=0.44;
     if R18>1000 && R18<200000.0;
          break
     end
      VNF1=sqrt((4.0*G*PD1*(ROS-ROF)/(3.0*0.1*ROF)));
       Z=2.39;
  end


  for IN=1:N;
      VINF1(IN)=VNF1*(1.0-CTT(IN).^Z);
  end

  IBED=0.0;
SP3=1.0;
    CVH=10.^(-1.8*(VINF1/(0.41*USTAR)));
    CBED=(SP3-CVH)/100;
    IB=82*PRE*CBED*((9.81*D*(SS-1))/(V^2)*(Z^0.5)^1.5);
    IBED=IBED+IB;

PRI=PRE+IBED;
for KK=1:1000;
    USTAR=sqrt(PRE*G*D/4.);
IBED=0.0;

    CVH=10.^(-1.8*(VINF1/(0.41*USTAR)));
    CBED=(SP3-CVH)/100;
    IB=82*PRE*CBED*((9.81*D*(SS-1))/(V^2)*(Z^0.5)^1.5);
    IBED=IBED+IB;

KK=PRE+IBED;
ZK=KK/PRI;
PRI=KK;
if ZK<=1.05 && ZK>=0.95
    break
end
end
```

Karabelas Model

```
clc
clear all
N=16;
data = xlsread('input.xls');
CWMAX = data(1,1);
AMUL = data(2,1);
ROS = data(3,1);
ROL = data(4,1);
EITA = data(5,1);
PD = data(6,:);
SP = data(8,:);
V = data(9,1);
ER=data(13,1);
D = data(14,1);
M = data(15,1);
AMS = data(16,1);
VMX1 = data(22,1);
VMN1 = data(23,1);
VN1 = data(24,1);
CW = data(25,1);
CV = data(26,1);
PREG = data(18,1);
R=D/2;
YC=zeros (1,N); X=zeros (1,N-1); B=zeros (1,N); AA=zeros (1,N); A=zeros
(1,N);
PD1=zeros(1,M-1);      SP3=zeros(1,M-1);      CFC=0.0;      CVH=zeros(1,M-
1);CBED=zeros(1,M-1);
CT=CV;
CMAX=(CWMAX/ROS)/((CWMAX/ROS)+((1-CWMAX)/ROL));
G=9.81;
SS=ROS/ROL;
DCF=((1.8*((AMUL/ROL).^2)/(G*(SS-1.0))).^0.333)*1000000.0;
for IJJ=1:N;
    CTT(IJJ)=CT;
end
for I=1:M;
    if PD(I)<DCF && I>1
        L=I-1;
        CFC=SP(L)-((PD(L)-DCF)/(PD(L)-PD(I))*(SP(L)-SP(I)));
        break
    end
    if I==N
      L=I-1;
        CFC=SP(L)-((PD(L)-DCF)/(PD(L)-PD(I))*(SP(L)-SP(I)));
    end
end
      CFL=1.0-(CFC);
      CF=CFC*CT/100;
```

```
      CR=CT-CF;
      AMUF=AMUL*(1.0+2.5*CF+10.5*(CF.^2.0));
      ROF=(ROL*(1.0-CT)+ROS*CF)/(1.0-CT+CF);
      CRC=1+6.88*CV;
for i=1:N;
    YC(i)=(i/N)*D;
    if i<N
    X(i)=((R^2)-((abs(R-YC(i)))^2))^0.5;
    end
    if i<=(N/2);
        B(i)=asin(X(i)/R);
    end
    if YC(i)<=R
       AA(i)=((D^2)/4)*(B(i)-sin(B(i))*cos(B(i)));
    end
end
A(1)=AA(1);
for i=2:N
    if i<=N/2;
    A(i)=AA(i)-AA(i-1);
    else
    A(i)=A(N-i+1);
    end
end
for II=1:M-1;
    PD1(II)=PD(II)+PD(II+1)/2.0;
    SP3(II)=SP(II)-SP(II+1);
    PD1(II)=PD1(II)/1000000.0;
    CJBAR(II)=SP3(II)*CT/100.0;
    VNF1(II)=G*(PD1(II).^2.0)*(ROS-ROF)/(18.0*AMUF);
    R18=VNF1(II)*PD1(II)*ROF/AMUF;
    if R18<0.02
        Z=(4.65+1.95*(PD1(II)/D))
    else if R18>0.02 && R18<1.0;
    Z=(4.35+17.5*(PD1(II)/D))*((R18).^(-0.03));
        else
            if R18>1 && R18<1000.0;
                XX=((G*(ROS-ROF)/ROF).^0.72)*(PD1(II).^1.18);
                XX1=((AMUF/ROF).^0.45);
               VNF1(II)=0.2*XX/XX1;
                R18=VNF1(II)*PD1(II)*ROF/AMUF;
               Z=(4.45+(18*(PD1(II)/D)))*((R18).^(-0.1));
            else
             VNF1(II)=sqrt((4.0*G*PD1(II)*(ROS-ROF)/(3.0*0.44*ROF)));
             Z=(4.45+(18*(PD1(II)/D)))*((R18).^(-0.1));
            end
        end
    end
end
G=9.81;
SS=ROS/ROL;
DCF1=((1.8*((AMUL/ROL).^2)/(G*(SS-1.0))).^0.333);
DCF=DCF1*1000000.0;
for I=1:M;
    if PD(I)<DCF && I>1
        L=I-1;
```

```
        CFC=SP(L)-((PD(L)-DCF)/(PD(L)-PD(I))*(SP(L)-SP(I)));
        break
    end
end
CFL=1.0-(CFC);
for I=1:M;
            SP1(I)=SP(I)-CFC;
            SP2(I)=SP1(I)*100.0/CFL;
            if SP2(I)<0.0;
                SP2(I)=0.0;
            end
end
  for II=1:M-1;
             PD1(II)=(PD(II)+PD(II+1)/2.0);
             SP4(II)=SP2(II)-SP2(II+1);
             PD1(II)=PD1(II)/1000000.0;
  end
  sum=0.0;
  DF=0.0;
  DC=0.0;

    %%%% CALCULATING DC THE AVERAGE DIAMETER OF +50% OF PARTICLES
  for i=2:M-1;
      sum=sum+SP4(i);
      if sum<50;
          SPC(i)=SP4(i);
          PDC(i)=PD1(i);
          DC=DC+(PDC(i)*SPC(i)/50);
          CC=sum;
      else if sum==50;
          SPC(i)=SP4(i);
          PDC(i)=PD1(i);
          DC=DC+(PDC(i)*SPC(i)/50);
              break
          else
              CC=sum;
          SPC(i)=50-CC;
          PDC(i)=PD1(i-1)+(((PD1(i)*sum)-(PD1(i-1)*(sum-
SP4(i))))/(SP4(i)-SP4(i-1)));
          DC=DC+(PDC(i)*SPC(i)/50);
     break
          end
      end
  end

    %%%% CALCULATING DF THE AVERAGE DIAMETER OF -50% OF PARTICLES
    NT=0.0;
    sum=0.0;
  for i=M-1:-1:2;
      NT=NT+1;
      sum=sum+SP4(i);
      if sum<50;
          SPF(NT)=SP4(i);
          PDF(NT)=PD1(i);
          DF=DF+(PDF(NT)*SPF(NT)/50);
          CC=sum;
```

```
      else if sum==50;
          SPF(NT)=SP4(i);
          PDF(NT)=PD1(i);
          DF=DF+(PDF(NT)*SPF(NT)/50);
              break
          else
          SPF(NT)=50-CC;
          PDF(NT)=PD1(i-1)+(((PD1(i)*sum)-(PD1(i-1)*(sum-
SP4(i))))/(SP4(i)-SP4(i-1)));
          DF=DF+(PDF(NT)*SPF(NT)/50);
     break
          end
      end
  end
         D501=0.0;
 for I=1:M-1;
         D50=PD1(I)*SP4(I)/100;
         D50=D501+D50;
         D501=D50;
 end
for I=2:N;
           if SP2(I)<50;
               J=I-1;
               break
           end
end
           DPC=PD(J)-((SP2(J)-50)*(PD(J)-PD(I))/(SP2(J)-SP2(I)));
           DMD=DPC/1000000.0;
%%%%%%%%%%   PRESSURE DROP %%%%%%%
CT=CV;
AK=0.00002;
P=0.026*((AK/D).^0.225)+0.133*AK/D;  %%% unitless
Q=22.0*((AK/D).^0.44);  %%% unitless
R=1.62*((AK/D).^0.136);   %%% unitless
REE=(ROL*V*D)/AMUL;   %%% unitless
AFA=P+Q*(1./(REE.^R));  %%% unitless
WPL=2.0*AFA*(V.^2.0)/(9.81*D);  %%% unitless
CF=CFC*CT;
AMUF=AMUL*(1.0+2.5*CF+10.5*(CF.^2.0));
ROF=(ROL*(1.0-CT)+ROS*CF)/(1.0-CT+CF);
CRC=1+6.88*CV; %%%%%%%%%%% 945
VINF=(9.81*(D50.^2.0)*(ROS-ROF))/(18.0*AMUF)/CRC;
R8=(VINF*D50*ROF)/AMUF;     %%% Settling Reynolds Number
for K=1:100000;
if R8<1
    break
end
XP=4.0*9.81*(D50.^1.625)*(ROS-ROF)/90.0;
    X11=(ROF.^0.375)*(AMUF.^0.625);
    X22=XP/X11;
    VINF=(X22.^0.727)/CRC;

    R8=VINF*D50*ROF/AMUF;
    if R8>1000;
        VINF=sqrt((4.0*9.81*D50*(ROS-ROF))/(3.0*0.10*ROF))/CRC;
    end
```

```
    R8=VINF*D50*ROF/AMUF;
end

%%%%%%%%%%%%%%%%%%%%%%% MLAYER CONCENTRATION DISTRIBUTION  %%%%%%%
AMUFM=AMUL*(1.0+(2.5*CT)+10.5*(CT.^2.0));
ROM=ROS*CT+(1.-CT)*ROL;
REM=ROM*V*D/AMUFM;
 if REM<2000.0;
F1=16.0/(PRI);
     end
P=0.026*((AK/D).^0.225)+0.133*AK/D;  %%%%%%%%%%340
Q=22.0*((AK/D).^0.44);
R=1.62*((AK/D).^0.136);
F1M=P+Q*(1./(REM.^R));
PRE=(2.0*F1M*(V.^2.0)*(ROM/ROL)/(9.81*D));
USTAR=sqrt(PRE*G*D/4.);

for i=1:N;
    if (YC(i)/D) <= 0.337 && (YC(i)/D)>=0.0;
        GCOF=0.369*USTAR*(YC(i)/R);     %Liquid diffusivity
    else if (YC(i)/D) >= 0.337 && (YC(i)/D)<=0.663
          GCOF=0.0775*R*USTAR;
        else
            GCOF=0.369*R*USTAR*((YC(i)/R)-1)*(2-(YC(i)/R));
        end
    end
    %GITA(i)=GCOF*(1.0+0.12504*exp(4.22054*(CTT(i)/CMAX)));
    %if GITA(i)==0;
     %  GITA(i)=0.01;
    % end
end

  for IIL=1:M-1;
    CJBAR(IIL)=SP3(IIL)*CT/1.0;
    VNF1(IIL)=G*(PD1(IIL).^2.0)*(ROS-ROF)/(18.0*AMUF);
    R18=VNF1(IIL)*PD1(IIL)*ROF/AMUF;
    Z=(4.35+17.5*(PD1(IIL)/D))*((R18).^(-0.03));
    CD=24*((R18).^(-1));
    for RR=1:1000000;
        if R18<1;
            break
        end
        XX=((G*(ROS-ROF)/ROF).^0.72)*(PD1(IIL).^1.18);
        XX1=((AMUF/ROF).^0.45);
        VNF1(IIL)=0.2*XX/XX1;
        R18=VNF1(IIL)*PD1(IIL)*ROF/AMUF;
        Z=4.45*((R18).^(-0.1));
        CD=(24/R18)*(1+(0.15*(R18).^0.687));
        if R18>1 && R18<1000.0;
            break
        end
            VNF1(IIL)=sqrt((4.0*G*PD1(IIL)*(ROS-ROF)/(3.0*0.44*ROF)));
            Z=2.39;
            CD=0.44;
       if R18>1000 && R18<200000.0;
            break
```

```
      end
       VNF1(IIL)=sqrt((4.0*G*PD1(IIL)*(ROS-ROF)/(3.0*0.1*ROF)));
        Z=2.39;
   end
 end
 for IIL=1:M-1;
   for IN=1:N;
       VINF1(IIL,IN)=VNF1(IIL)*(1.0-CTT(IN).^Z);
   end
 end

   for IJI=1:N;
  YR(IJI)=IJI*(2/(N-1))-(1+(2/(N-1)));
   YD(IJI)=(YR(IJI)+1.0)/2.0;
   if YD(IJI)<0.33 || YD(IJI)>0.66
      if YD(IJI)<0.33
          YYD=YD(IJI)*D;
      else
          YYD=D*(1.-YD(IJI));
      end
      GCOF=0.369*(1.-2*YYD/D)*YYD*(2/D);
        if GCOF<0.0775
          GCOF=0.0775;
        end
   else
          GCOF=0.0775;
   end

    GITA(IJI)=GCOF*(1.0+0.13*exp(4.6513*(CTT(IJI)/CMAX)));
    if GITA(IJI)==0;
        GITA(IJI)=0.01;
    end
    end

for III=1:M-1;
   for IM=1:N;
       AKJ(III,IM)=VINF1(III,IM)/(USTAR*GITA(IM));
      for ITH=1:180;
          PI=22/7;
          TH=(ITH)*PI/180;
          FT(ITH)=exp(-AKJ(III,IM)*cos(TH)*sin(TH)*sin(TH));
      end
      DSUM=0.0;
      for IE=2:2:178;
          DSUM=DSUM+FT(IE);
      end
      DSUM1=0.0;
      for IO=3:2:179;
          DSUM1=DSUM1+FT(IO);
      end
      EKJ(III,IM)=(2/180)*(FT(1)+FT(180)+(2*DSUM1)+(4*DSUM))/3;
      VJB(III)=CJBAR(III)/(1-CT);
   end
end
   for IJK=1:M-1;
   for IJI=1:N;
```

```
        YR(IJI)=IJI*(2/(N-1))-(1+(2/(N-1)));
        YD(IJI)=(YR(IJI)+1)/2;
        COF(IJK,IJI)=(VJB(IJK)/EKJ(IJK,IJI))*exp((-
AKJ(IJK,IJI)*YR(IJI)));
    end
end
    for KII=1:N;
    ECOFJ=0.0;
    for KI=1:M-1;
        ECOF(KII)=COF(KI,KII)+ECOFJ;
        ECOFJ=ECOF(KII);
    end
    end
   CLIM=CMAX-0.074*((V/VINF).^0.44)*((1-CR).^0.189)*(CMAX-CR);
for KFI=1:M-1;
    for KFII=1:N;
        C(KFI,KFII)=COF(KFI,KFII)/(1.0+ECOF(KFII));
        CAB1(KFI,KFII)=C(KFI,KFII)*CJBAR(KFI);
    end
end
CNET=zeros(1,N-6);
    for i=1:N-6;
        sum=0.0;
        for j=1:M-1;
            sum=sum+C(j,i+3);
        end
            CNET(i)=sum;
    end
CLIMY=0.0;
for I=1:N;
    L=C(:,I);
    SUM=0.0;
    for J=1:M-1;
        SUM=SUM+L(J);
    end
    CL(I)=SUM;
    if abs(CL(I)-CLIM)<=0.01;
        CLIMY=I/N;
    end
end
sum2=0.0;
for i=1:N;
  sum2=sum2+CL(i);
end
CLA=sum2/N;
```